THE UNIVERSITY
of EDINBURGH

Crowd Sourced Self Beacon Mapping with Isolated Signal Aware Bluetooth Low Energy Positioning

Arief Affendi Bin Juri

THE UNIVERSITY *of* EDINBURGH

Thesis submitted for the degree of

Doctor of Philosophy

University of Edinburgh

School of Engineering

Year of Submission 2018

Declaration

I declare that this thesis has been composed solely by myself and that it has not been submitted, in whole or in part, in any previous application for a degree. Except where states otherwise by reference or acknowledgment, the work presented is entirely my own.

Arief Juri

Abstract

In the past few decades, there has been an increase in the demand for positioning and navigation systems in various fields. Location-based service (LBS) usage covers a range of different variations from advertising and navigation to social media. Positioning based on a global navigation satellite system (GNSS) is the commonly used technology for positioning nowadays. However, the GNSS has a limitation of needing the satellites to be in line-of-sight (LOS) to provide an accurate position. Given this limitation, several different approaches are employed for indoor positioning needs.

Bluetooth low energy (BLE) is one of the wireless technologies used for indoor positioning. However, BLE is well-known for having unstable signals, which will affect an estimated distance. Moreover, unlike Wi-Fi, BLE is not commonly and widely used, and BLE beacons must thus be placed to enable a venue with BLE positioning. The need to deploy the beacons results in a lengthy process to place and record the position of each placed beacon.

This thesis proposes several solutions to solve these problems. A filter based on a Fourier transform is proposed to stabilise a BLE signal to obtain a more reliable reading. This allows the BLE signals to be less affected by internal variation than unfiltered signal. An obstruction-aware algorithm is also proposed using a statistical approach, which allows for the detection of non-line-of-sight (NLOS). These proposed solutions allow for a more stable BLE signal, which will result in a more reliable estimation of distance using the signal. The proposed solutions will enable accurate distance estimation, which will translate into improved positioning accuracy. An improvement in 88% of the test points is demonstrated by implementing the proposed solutions.

Furthermore, to reduce the calibration needed when deploying the BLE beacons, a beacon-mapping algorithm is proposed that can be used to determine the position of BLE beacons. The proposed algorithm is based on trilateration with added information about direction. It uses the received signal strength (RSS) and the estimated distance to determine the error range, and a direction line is drawn based on the estimated error range.

Finally, to further reduce the calibration needed, a crowdsource approach is proposed. This approach is proposed alongside a complete system to map the location of unknown beacons. The proposed system uses three phases to determine the user location, determine the beacons' position, and recalculate BLE scans that have insufficient number of known BLE beacons. Each beacon and user's position determined is assigned a weight to represent the reliability of that position. This is important to ensure that the position generated from a more reliable source will be emphasised. The proposed system demonstrates that the beacon-mapping system can map beacons with a root mean squared error (RMSE) of 4.64 m and a mean of absolute error (MAE) of 4.28 m.

Lay Summary of Thesis

The lay summary is a brief summary intended to facilitate knowledge transfer and enhance accessibility, therefore the language used should be non-technical and suitable for a general audience. Guidance on the lay summary in a thesis. (See the Degree Regulations and Programmes of Study, General Postgraduate Degree Programme Regulations. These regulations are available via: www.drps.ed.ac.uk.)

Name of student:	Arief Affendi Bin Juri	UUN	S1271728
University email:	A.Juri@ed.ac.uk		
Degree sought:	Doctor of Philosophy	No. of words in the main text of thesis:	18637
Title of thesis:	Crowd Sourced Self Beacon Mapping with Isolated Signal Aware Bluetooth Low Energy Positioning		

Insert the lay summary text here - the space will expand as you type.

The main project in this thesis described a system to map the location of unknown beacons using a lesser number of known beacons. The aim of this thesis is to reduce the calibration required to map beacons location inside a venue.

The thesis proposes a new filter to reduce the effect of advertisement channels hopping which relates to Bluetooth low energy (BLE) signal variations. This filter works by analysing the signal and try to roughly differentiate the three channels from the signals. After differentiating the channels, the remaining process can be done from only the selected channel to ensure consistency in the RSS readings.

This thesis also proposes a new implementation that can reduce the calibration process by proposing an algorithm to detect a beacon's location. It works by using the same trilateration principle to locate the beacon location using any other positioning technique. The initial positioning can be determined from several initial beacons with known location for trilateration, or any other positioning technique with varying accuracy. The trilateration will give an area based on distance overlap of where the beacon is possibly located, and the thesis proposes an additional parameter to further reduce the estimated area size. The additional parameter is direction which is the estimated direction of the beacon from the reference location.

This thesis also proposes a complete system to map unknown beacons location using crowd sourced approach. The proposes system uses three phases to determine the user location, determine beacons' position and recalculating BLE scans that have insufficient known BLE beacons. Each beacon and user's position determined is given a weight to represent the reliability of the position determine. This is important to make sure the position generated from a more reliable source will be emphasized.

Acknowledgement

Firstly, I would like to express my gratitude to my supervisor, Professor Tughrul Arslan for his continuous support throughout this study and research and for his guidance, motivation and advice.

I would also like to thank the team members at Embedded Mobile, Wireless, and Wearable Sensor Systems (EWireless) research group for their support. My sincere thanks also goes to my college, Xiaoyue Hou and Yichen Du. Without their precious support it would not be possible to conduct this research.

I would also like to express my gratitude to the team at sensewhere Limited for providing opportunity for a valuable experience and knowledge.

I would also like to thank my wife and kids for being a great support when facing the hardship when completing the study.

Finally, I would like to thank my parents, siblings, and friends for their support and encouragement. I dedicate this thesis to their love, patience and belief in my capabilities.

List of figures

List of tables

List of equation

Content

1. Introduction

1.1. Evolution of localisation and navigation

Knowing own's position is important information that humans have been striving to determine for centuries. It allows people to locate themselves and landmarks within the environment, and it helps them to navigate to another location without getting lost. Previous navigation and positioning processes were purely based on the sight of landmarks or land characteristics. With the help of primitive compass directions, which are based on the observation of celestial objects such as the sun and stars, navigation has become more reliable and has allowed humans to navigate even further. Localisation based on celestial observation has been further improved with the invention of some tools to accurately observe celestial objects such as a tool is the astrolabe, an elaborate inclinometer that was historically used by astronomers and navigators to measure the altitude above the horizon of a celestial body. As the astrolabe requires the observation of celestial objects, its usage is greatly hindered in an overcast sky. This issue was solved with the invention of the compass, which enables localisation and navigation without sky visibility.

Modern positioning marks a significant advancement in positioning technology. Radios began to appear on ships at sea in 1891 [1]. They were initially used as wireless communication devices to request assistance at sea. In 1906, they were later expanded to be used for determining direction [2]. Before the introduction of a global navigation satellite system (GNSS), long-range navigation (LORAN) was used; LORAN is a pulsed hyperbolic radio aid to navigation that was developed by the US during World War II [3]. It can achieve an accuracy of 5 miles in a range of 1,500 miles. A further leap in modern positioning history saw the introduction of global positioning systems (GPSs) in 1980 [4]. With superior

availability, accuracy, and reliability, the GPS is fast becoming the positioning technique adopted worldwide. The advantages of GPS piqued the interest of other countries to adopt the same positioning technique, which consequently saw the introduction of other GNSS such as GLONASS, Galileo, and BeiDou. The successful commercialisation of GNSS demonstrates a mass-market demand for location-based services (LBSs). The technology, which was previously only used by surveyors because of cost constraints, is now also available for personal civilian use.

The demand for LBSs is further increasing with the introduction of smartphones, which have the performance capabilities of a computer. Smartphones are equipped with several sensors and receivers, with a GPS sensor being one of them. This allows for a more complex use of positioning, such as location sharing, emergency assistance, and even gaming, to be accessible to a wider population. Even with all the advantages of GNSS, there are unfortunately still locations that are not accessible by GNSS, such as indoor areas. Similarly to navigation using celestial object observation, GNSS requires line-of-sight (LOS) to the reference objects – in this case, the satellites [5]. For indoor positioning, most if not all of the satellites are blocked by roofs or walls, and their signals are unable to penetrate the obstruction, thereby leading to losses in the GNSS signals. Even if the signals are visible, signal degradation because of multipath causes misinterpretation of the data, which ultimately results in a large error in positioning displacement. Given this challenge, other means of positioning are preferred for indoor positioning.

Several technology classifications have been proposed, as discussed in [6], based on different criteria such as the hardware required and the existence of a network, among others. The classification that would clearly highlight the different technologies used for indoor positioning system (IPS) is based on the main medium used to determine position, as

proposed by [7]. The technology categories are as follows: vision-based, radio frequency (RF), magnetic, and audible and ultrasound technologies.

Vision-based positioning previously only appealed to those who worked in robotics. However, because of improvements in camera lenses, computing capabilities, and its availability in many mobile devices, this type of positioning has begun to gain popularity for human positioning and navigation [8].

Magnetic positioning is an increasingly popular positioning technique that is based on magnetic reading. In most cases, magnetic positioning will be based on scene analysis, also known as the fingerprint technique. When a user attempts to locate his or her position, the magnetic reading will be compared with a reading pre-recorded in the database. The user's position will be returned as the location with a similar pre-recorded reading from the database.

Audible and ultrasound positioning utilises the same principle as echo localisation for dolphins, for example as proposed in [9]. This type of positioning is currently not actively used for mobile device positioning.

Radio frequency positioning is a widely accepted positioning technology for indoor positioning, and a number of different radio technologies are available. Radio frequency positioning ranges from GSM and Wi-Fi to Bluetooth. The introduction of Bluetooth 4.0 with the Bluetooth low energy (BLE) standard allows for more opportunities for positioning using Bluetooth. Positioning using Bluetooth is usually done using BLE beacons, which can be deploy as needed. The advantages of these beacons are low operation power consumption and low hardware costs. However, to obtain the best accuracy from BLE positioning, the location of the beacons must be accurately recorded, which can be a laborious task.

1.2. Problem statement

Positioning using BLE beacons can be done in two ways: fingerprint or trilateration. The fingerprint technique requires a BLE radio map created by pre-recording BLE signals at predetermined locations. This step is known as the offline or calibration phase. The more pre-recorded data gathered, the more accurate the positioning will be. In this online or positioning phase, the user will receive the BLE readings, and the current reading will be compared with the radio map database; the most identical result will then be used as the user's location. In the trilateration technique, the user's location is determined by estimating the distance overlap of three or more beacons. With this technique, it is important to know the initial location of the beacons.

Both techniques are laborious in either collecting the data for the radio map or mapping the exact locations of the beacons to the systems. However, the mapping of the beacons' locations is less time consuming than preparing the data for the radio map, and further reducing the requirement to map the beacons' locations through a manual process will further reduce the calibration tasks.

Both techniques generally make use of the received signal strength (RSS). Other techniques, such as the angle of arrival (AoA) or the time of arrival (ToA), are also available; however, these techniques require specific and additional hardware, compared to RSS, which can be used with the current receiver in most mobile devices with Bluetooth capability. With RSS, the signal's power decays as the signal travels; therefore, the RSS can be an indicator of the distance travelled. However, it can fluctuate because of shadowing and multipath, which can be caused by the environment and can be dependent on each environment and location. Moreover, with the BLE standard that introduced three separate channels for advertisement,

an additional signal variation can be seen because of channel hopping across the three channels.

1.3. Contribution

The main project in this thesis describes a system to map the location of unknown beacons using a small number of known beacons. The aim of this thesis is to reduce the calibration required to map beacon location inside a venue.

The thesis also proposes a new filter to reduce the effect of advertisement channel hopping, which relates to BLE signal variations. This filter works by analysing the signal and attempting to roughly differentiate the three channels from the signals. After this differentiation, the remaining process can be done using only the selected channel to ensure consistency in the RSS readings.

Furthermore, this thesis proposes a new type of implementation that can reduce the calibration process by utilising an algorithm to detect a beacon's location. It works by employing the same trilateration principle to locate a beacon using any other positioning technique. The initial positioning can be determined from several initial beacons with known locations for trilateration or through any other positioning technique with varying accuracy. The trilateration will yield an area where the beacon is possibly located based on a distance overlap, and to further reduce the estimated area size, the thesis proposes an additional parameter namely direction, which is the estimated direction of the beacon from the reference location.

Finally, this thesis suggests a complete system to map the location of unknown beacons using a crowdsourced approach. The proposed system utilises three phases to determine the user location, determine beacons' positions, and recalculate BLE scans that have an

insufficient number of known BLE beacons. Each beacon and user's position determined is assigned a weight to represent the reliability of that position. This is important to ensure that the position generated from a more reliable source will be emphasised.

1.4. Thesis Structure

The rest of the thesis is organised as follows:

In Chapter 2, the background about indoor positioning is provided, and the techniques and technologies used in this thesis are discussed in detail.

Chapter 3 proposes a novel channel selection filter to reduce the effect of channel hopping across the BLE advertisement channel. Then, the implementation of the proposed filter is performed, and the result is compared against positioning using a mean value.

Thereafter, Chapter 4 proposes another novel filter to further reduce the instability in BLE signals. This filter tries to detect an isolated beacon; by doing so, the distance estimation can be adjusted to accurately predict the correct distance. The proposed filter is implemented and compared to another state-of-the-art filter algorithm.

In Chapter 5, a beacon-mapping algorithm is proposed that adds extra information that can be used to determine the location of a beacon. This added information is the estimated direction of the beacon.

Chapter 6 proposes a complete system to map the location of unknown beacons using a crowdsourced approach. The proposed system uses three phases to determine the user location, determine beacons' positions, and recalculate BLE scans that have an insufficient number of known BLE beacons.

Finally, Chapter 7 concludes the work presented in the thesis and suggests further works that can be done to improve the current proposed system.

2. Indoor positioning

2.1. Introduction

The previous chapter provided a brief introduction to indoor positioning. Achieving an accurate position is important for indoor positioning, as an indoor area tends to have a small boundary. A low accuracy in localisation could point a user to a different room or, in the worst case, a different building altogether.

This chapter discusses indoor positioning techniques. The challenges and solutions for these techniques are reviewed to determine the current solution and remaining challenges. Then, the technologies used for indoor positioning are reviewed to identify the similarities and differences between them.

2.2. Classification of indoor positioning techniques

Several techniques can be adopted for indoor positioning. Even though many solutions are available for positioning, most of them relate back to the common techniques, and most are an expansion thereof. These techniques are not specifically for indoor positioning; nevertheless, those used widely in indoor positioning are highlighted. As the techniques are not specifically for indoor positioning, some solutions to the challenges developed for outdoor positioning might also work in indoor areas.

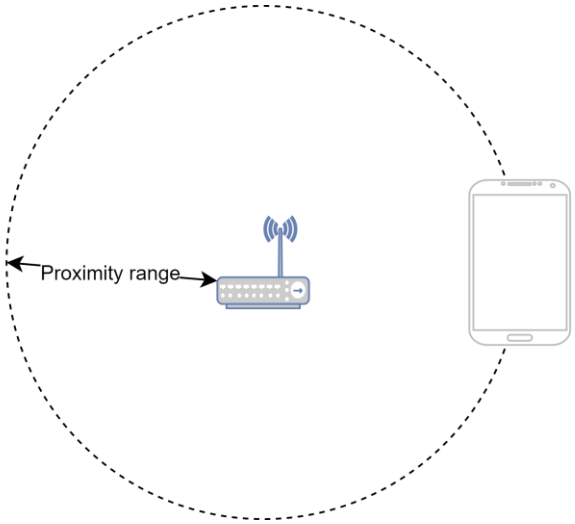

Figure 2.1. A schematic diagram of the proximity technique. The area within the proximity range is detected as being in proximity

2.2.1. Proximity

Proximity techniques determine the position of a receiver based on the range of a transmitter. The proximity range can be based on the maximum range of the transmitter or signal strength within a pre-set threshold value [10], as illustrated in Figure 2.1. This technique is generally only used for a fenced area rather than for absolute distance estimation. A well-known implementation of this technique is the iBeacon, a specification for the BLE beacon released by Apple [11]. The proximity technique implemented in iBeacon is based on predetermined threshold values that allow for the detection of three proximity stages: far, near, and immediate. The simplicity if this technique makes it an ideal solution to tag an area of interest; however, this same reason became the technique's drawback, as it is not usable to obtain the absolute position of a receiver. Chawathe [12] has proposed a positioning algorithm, which is also based on proximity, using the visibility of a set of beacons. It relies on the availability of a combination of beacons to know the exact position of the user. However, it requires complete information of the area covered by each beacon to determine

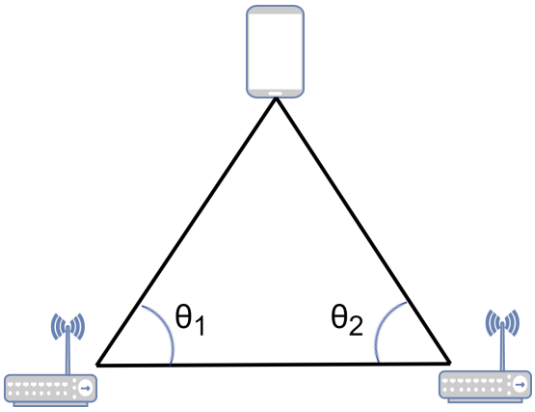

Figure 2.2. A schematic diagram of angulation technique. Directional antenna is required in either the transmitter or receiver, to detect the direction of the signal

the area that is visible only for a certain set of beacons. Bouchard et al. [13] attempted to improve proximity-based localisation by adding a set of features to each of the recorded beacons, but the drawback of a proximity technique remains. The proposed algorithm returns the position of the closest proximity beacon, and the position is thus limited to the deployment of that beacon.

2.2.2. Angulation

The angulation technique uses direction information, or angles, to estimate the position of a receiver. The measured angles are the angles of the receiver to a reference point (RP) with a known location [14]. The measured angle is called the AoA, and the location of the receiver can be deduced using the AoA from multiple transmitters by applying a trigonometry calculation, as illustrated in Figure 2.2. However, this technique has several issues. For example, it requires a specific antenna in the transmitter or receiver to allow for the detection of the angles. This would require a device that is specifically manufactured for use with this technique.

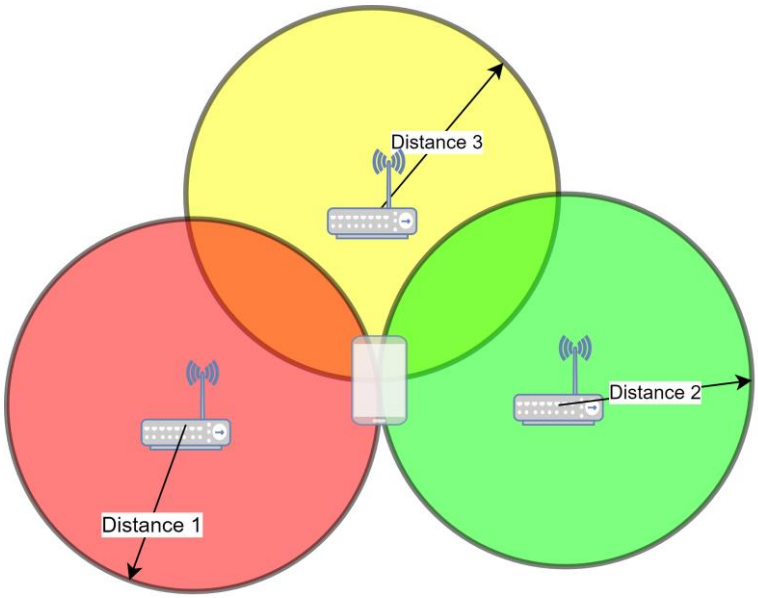

Figure 2.4. A schematic diagram of the lateration technique. The ideal situation with accurate distance will point to the location of the device

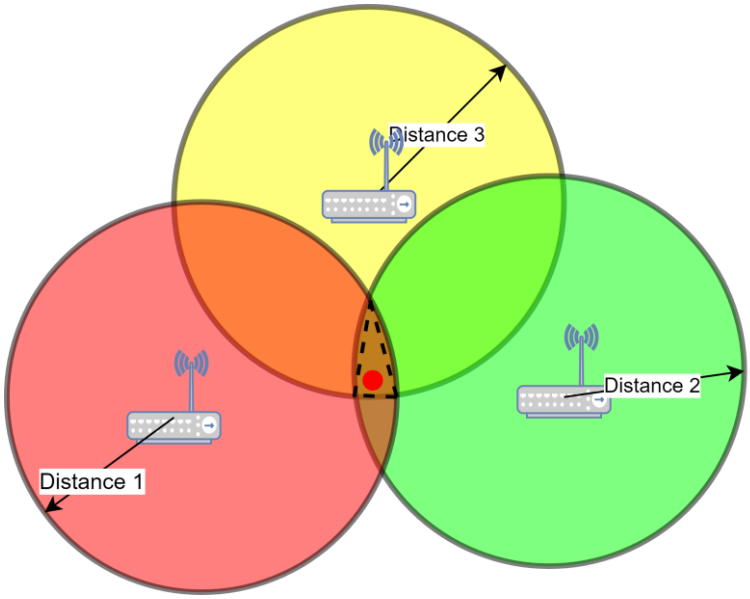

Figure 2.3. A schematic diagram of the lateration technique with a centroid. In real-world implementation, errors in estimated distance will provide an area of a possible position rather than the exact location

2.2.3. Lateration

Lateration is a technique to determine the position of a transmitter based on the distance between the transmitter and the receiver [15]. Using a single transmitter with a known

location and distance allows for an accurate proximity estimation, as discussed in Section 2.2.1. With multiple transmitters, the actual position of the receiver can be determined. Each of the transmitters creates its own circle with the distance as the radii centred at the transmitter's location. The point at which these circles overlap is the location of the receiver, as depicted in Figure 2.4. However, in real-world implementation, instead of overlapping at a single point, an overlapping area will be established, as illustrated in Figure 2.3. Therefore, a minimum of three beacons is required to properly locate a position using a lateration technique. The receiver's location with the overlapped area can be estimated using a centroid.

To reduce the complexity of the problem into a single problem of determining the intersection point of several planes, linearisation is applied [16]. This also simplifies the problem when determining the intersection point when the number of transmitters is more than three. The basic equation of a sphere with a distance radius of d is

$$(x - x_i)^2 + (y - y_i)^2 + (z - z_i)^2 = d_i^2 \quad (i = 1,2 \dots n, n \geq 4) \tag{2.1}$$

where d denotes the distance between a transmitter and a receiver with a total of n transmitters, and x, y, and z denote the position of the receiver to be located. To linearise (2.1), a reference node or transmitter is needed. The selection of the reference node does not matter, because the same reference node is used throughout the calculation. For this, the first reference node is used.

The linearisation process starts by subtracting the reference node with the ith transmitter.

$$[(x - x_1)^2 + (y - y_1)^2 + (z - z_1)^2] - [(x - x_i)^2 + (y - y_i)^2 + (z - z_i)^2] \tag{2.2}$$

$$= d_1^2 - d_i^2 \qquad (i = 2, 3 \dots n, n \geq 4)$$

Expanding the equation in parentheses results in

$$[x^2 - 2xx_1 + x_1^2 + y^2 - 2yy_1 + y_1^2 + z^2 - 2zz_1 + z_1^2] - \tag{2.3}$$
$$[x^2 - 2xx_i + x_i^2 + y^2 - 2yy_i + y_i^2 + z^2 - 2zz_i + z_i^2]$$
$$= d_1^2 - d_i^2 \qquad (i = 2, 3 \dots n, n \geq 4)$$

Further expanding the equation results in

$$x^2 - 2xx_1 + x_1^2 + y^2 - 2yy_1 + y_1^2 + z^2 - 2zz_1 + z_1^2 - \tag{2.4}$$
$$x^2 + 2xx_i - x_i^2 - y^2 + 2yy_i - y_i^2 - z^2 + 2zz_i - z_i^2$$
$$= d_1^2 - d_i^2 \qquad (i = 2, 3 \dots n, n > 3)$$

This can be solved to

$$-2xx_1 + x_1^2 - 2yy_1 + y_1^2 - 2zz_1 + z_1^2 + \tag{2.5}$$
$$2xx_i - x_i^2 + 2yy_i - y_i^2 + 2zz_i - z_i^2$$
$$= d_1^2 - d_i^2 \qquad (i = 2, 3 \dots n, n \geq 4)$$

Extracting the unknown position of the receiver and rearranging the equation yields

$$2x(x_i - x_1) - 2y(y_i - y_1) + 2z(z_i - z_1) \tag{2.6}$$
$$= d_1^2 - d_i^2 - x_1^2 - y_1^2 - z_1^2 + x_i^2 + y_i^2 + z_i^2 \qquad (i = 2, 3 \dots n, n \geq 4)$$

given

$$k_i = x_i^2 + y_i^2 + z_i^2 \tag{2.7}$$

Using (2.7), (2.6) can be written in a more concise form:

$$2x(x_i - x_1) - 2y(y_i - y_1) + 2z(z_i - z_1) = d_1^2 - d_i^2 - k_1 + k_i \tag{2.8}$$
$$(i = 2, 3 \dots n, n \geq 4)$$

The equation can then be rewritten in matrix form to

$$2\begin{pmatrix} x_i - x_1 & y_i - y_1 & z_i - z_1 \\ x_{i+1} - x_1 & y_{i+1} - y_1 & z_{i+1} - z_1 \\ \dots & \dots & \dots \\ x_n - x_1 & y_n - y_1 & z_n - z_1 \end{pmatrix}\begin{pmatrix} x \\ y \\ z \end{pmatrix} = \begin{pmatrix} d_1^2 - d_i^2 - k_1 + k_i \\ d_1^2 - d_{i+1}^2 - k_1 + k_{i+1} \\ \dots \\ d_1^2 - d_n^2 - k_1 + k_n \end{pmatrix} \quad (2.9)$$

$$(i = 2, 3 \dots n, n \geq 4)$$

which corresponds to

$$A\vec{x} = \vec{b} \quad (2.10)$$

with

$$A = \begin{pmatrix} 2(x_i - x_1) & 2(y_i - y_1) & 2(z_i - z_1) \\ 2(x_{i+1} - x_1) & 2(y_{i+1} - y_1) & 2(z_{i+1} - z_1) \\ \dots & \dots & \dots \\ 2(x_n - x_1) & 2(y_n - y_1) & 2(z_n - z_1) \end{pmatrix}, \vec{x} = \begin{pmatrix} x \\ y \\ z \end{pmatrix}, \quad (2.11)$$

$$\vec{b} = \begin{pmatrix} d_1^2 - d_i^2 - k_1 + k_i \\ d_1^2 - d_{i+1}^2 - k_1 + k_{i+1} \\ \dots \\ d_1^2 - d_n^2 - k_1 + k_n \end{pmatrix}$$

$$(i = 2, 3 \dots n, n \geq 4)$$

The value of $\vec{x}$ can be computed by solving (2.10) using

$$\vec{x} = (A^T A)^{-1} A^T \vec{b} \quad (2.12)$$

It must be noted that the given equation is for solving lateration in a 3D plane. To solve lateration in a 2D plane, the equation of $A, \vec{x}$ and $\vec{b}$ can be changed to the following:

$$A = \begin{pmatrix} 2(x_i - x_1) & 2(y_i - y_1) \\ 2(x_{i+1} - x_1) & 2(y_{i+1} - y_1) \\ \dots & \dots \\ 2(x_n - x_1) & 2(y_n - y_1) \end{pmatrix}, \vec{x} = \begin{pmatrix} x \\ y \end{pmatrix}, \quad (2.13)$$

$$\vec{b} = \begin{pmatrix} d_1^2 - d_i^2 - k_1 + k_i \\ d_1^2 - d_{i+1}^2 - k_1 + k_{i+1} \\ \dots \\ d_1^2 - d_n^2 - k_1 + k_n \end{pmatrix}$$

$$(i = 2, 3 \dots n, n \geq 3)$$

with

$$k_i = x_i^2 + y_i^2 \tag{2.14}$$

Furthermore, the minimum number of transmitters, n, corresponds to the number of unknowns to be solved: four for the 3D plane and three for the 2D plane. For n with more than the minimum number of transmitters needed, a solution based on a least square can be used.

This technique is widely used because of its simplicity and independence from any specific technology or hardware. It can be used with any distance estimator technology and algorithm. However, the trilateration technique is highly dependent on the accuracy of the estimated distance.

2.2.4. Scene Analysis

A scene analysis technique is a positioning technique that compares a scanned signal with a pre-recorded signal at a previously visited position. This technique, which also called the

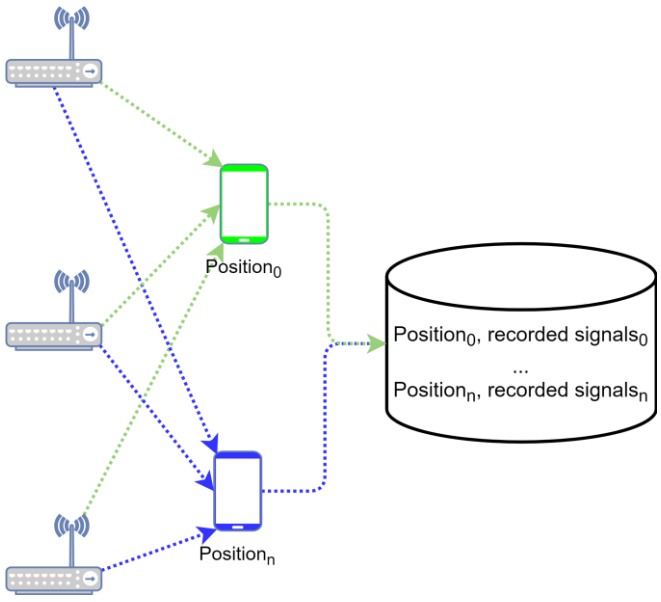

Figure 2.5. A schematic diagram of the scene analysis calibration phase. Radio signals are recorded and sent to the database along with the position where the signal is recorded. The information from a different device can also be sent to the same database; this will allow for a faster and more complete radio map

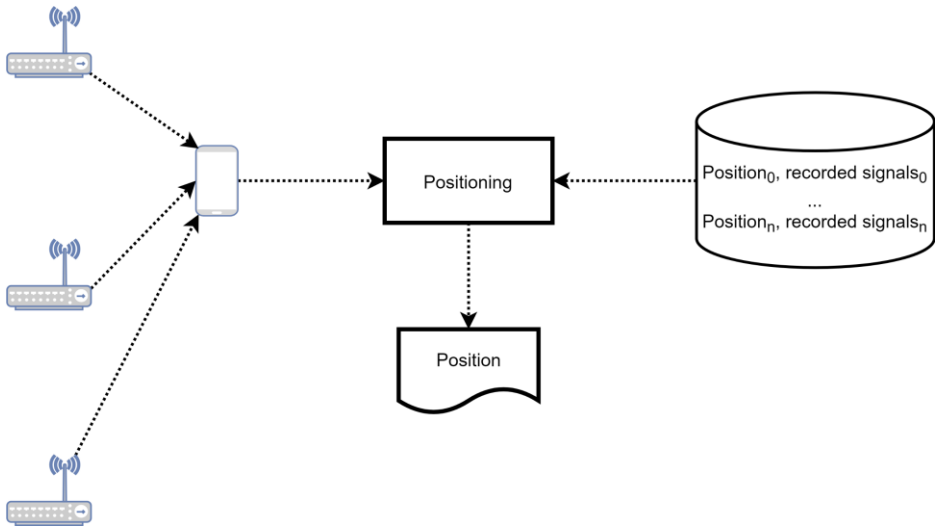

Figure 2.6. A schematic diagram of the scene analysis positioning phase. A device records the radio signals, and the information is compared against the database created in the calibration process. The position of the matching signals is returned as the position of the device

fingerprint technique, is based on the idea that the pre-recorded signal is a digital signature for the location, and it requires a database to be built before any positioning can be done. In the case of the fingerprint technique using wireless signals, the pre-recorded signal or the database is the source of information of the signal to be used. The information can be the RSS, the ToA, the AoA, or any other information that changes because of a position or distance change.

As a fingerprint technique requires a built database for positioning, it is usually separated into two phases: a calibration phase and a positioning phase. The calibration phase involves recording and tagging the signals at a number of predetermined positions. These points are known as calibration points. The calibration process is depicted in Figure 2.5.

The positioning phase is the process to determine a specific position. When a position is requested, the scanned signal is sent along with the request. The positioning phase makes use of the database generated in the calibration phase by comparing the scanned signal with

the recorded signals in the database. The recorded position of the matched signals will be returned as the position of the requested location.

The scene analysis technique is widely used, including in the indoor positioning industry, because of its robustness against attenuation and multipath. Any attenuation and multipath are captured alongside the signal when it is recorded in the database. However, a laborious calibration phase is required to build the radio map before the positioning can take place.

2.3. Distance Estimator

A distance estimator is important for several distance estimation techniques, especially for those based on the lateration technique. Since distance is the main information used in lateration, any errors in the estimated distance will cause errors in the calculated position.

2.3.1. Time of Arrival

A distance estimator based on the ToA is obtained using the time taken for a signal to travel from the transmitter to the receiver, as illustrated in Figure 2.7. It is calculated by dividing the time travelled by the speed propagation of the medium. The ToA is modelled as a Gaussian random variable:

$$T = \frac{d}{v_p} + Z_T \qquad (2.15)$$

where d is the distance travelled, v_p represents the propagation speed of the medium, and Z_T represents a zero mean Gaussian noise. The main drawback of this solution is that it requires specific hardware to obtain a precise time stamp. Furthermore, the time between the transmitter and the receiver needs to be synchronised.

2.3.2. Time Difference of Arrival (TDoA)

The time difference of arrival (TDoA) uses the same principle as the ToA; however, it measures the time delays between multiple transmitters, and the relative measurements are used to estimate the distance. The advantage of this technique is that it does not need to maintain a precise synchronisation between the transmitter and the receiver. The main drawback of this approach is that it still requires time stamping with the signal, which is not supported in a number of wireless protocols.

2.3.3. Received Signal Strength (RSS)

In distance estimated using RSS, a transmitter transmits a signal with a set transmit power, and a receiver receives the attenuated signal. The distance is estimated based on the power difference of the transmitted signal and the received signal. The relation between the power and the distance is described by a radio propagation model used.

The advantage of a distance estimator based on RSS is the availability of information to be used for estimating the distance. Received signal strength is common information

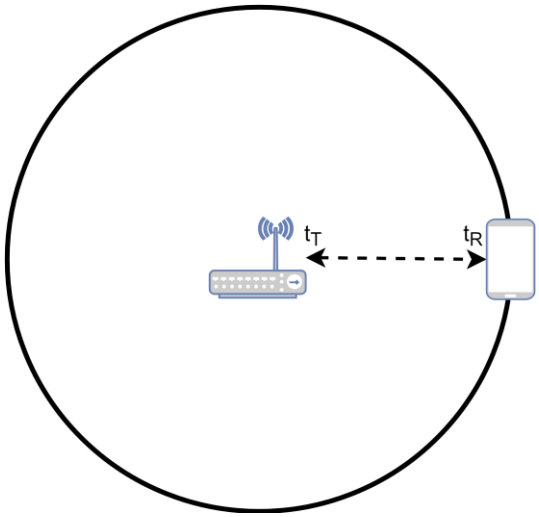

Figure 2.7. A schematic diagram of time of arrival. Distance is estimated by measuring the time taken for a signal to travel from a transmitter to a receiver

obtained when receiving a signal. Most applications and devices can thus use this distance estimator without any specific hardware required. However, the RSS can be affected by a number of factors, and it thus tends to be unstable, depending on the technology and frequency used.

2.4. Propagation Model for RSS-based distance estimator

The RSS provides information about the power of a received signal. By itself, it is simply a measure of the degree to which the signal was attenuated before it reached the receiver. To relate the attenuation to the signal distance travelled, a correct propagation model must be used. A radio propagation model is a mathematical representation of propagation characteristics as a function of the frequency of the radio wave and the distance between the transmitter and receiver [17]. Accurately predicting the radio propagation behaviour for a wireless communication system is important to estimate the signal coverage. Site measurement would provide an accurate representation of a signal characteristic; however, doing so is costly. A radio propagation model was designed to allow a representation of radio characteristic to be adequately estimated. Using the same model, the relation between a signal loss from a transmitter and a receiver can be estimated.

A radio propagation model can be divided into three types: deterministic, empirical, and physical [18] or stochastic [19] models. Deterministic models make use of the laws governing electromagnetic wave propagation to determine the received signal power at a particular location [19]. An example of a deterministic model is a ray-tracing model [20]. Empirical models are based on observations and measurements. The COST 231 Hata model implemented in [21] is a well-known example of an empirical model. Physical or stochastic models, on the other hand, model the environment as a series of random variables. These models are the least accurate of the three types but require the least amount of information

about the environment and use much less processing power than the other two models to generate predictions.

Two path-loss models are widely used for Wi-Fi radio signals in indoor environments: the log-distance path-loss model and the International Telecommunication Union (ITU) indoor path-loss model.

2.4.1. Log-distance path-loss model

The log-distance path-loss model is the most commonly used model in an indoor radio propagation model, as it require less specific details than other models, as employed in [22]. The relation between the power and the distance is described by a log-distance path-loss model

$$P = P_0 + 10nlog\left(\frac{d}{d_0}\right) + X_g \quad (2.16)$$

where P_0 is the RSS measured at a reference distance d_0, with a distance of 1 m chosen to simplify the equation. Moreover, n is the path-loss exponent, and X_g is the zero-mean Gaussian noise.

2.4.2. International Telecommunication Union indoor path-loss model

The ITU indoor path-loss model is derived from the Wall and Floor factor model [23]. The mathematical representation of this factor model, with a fixed exponent of 2 (as in free space) and additional loss factors relating to the number of floors n_f and walls n_w, intersected by the straight-line distance r between terminals, is represented as follows:

$$L = L_1 + 20\log r + n_f a_f + n_w a_w \quad (2.17)$$

where L is the total path loss, L_1 is the path loss at 1 m, a_f is the floor attenuation factor, and a_w is the wall attenuation factor.

The ITU indoor path-loss model uses a similar approach, except that only floor loss is explicitly accounted for, and the loss between points on the same floor is included implicitly by changing the path-loss exponent [23]. It is given by (2.18):

$$L = 20\log_{10} f + 10n\log_{10} d + L_f(n_f) - 28 \qquad (2.18)$$

where

L is the total path loss in decibel (dB);

f is the transmission frequency in megahertz (MHz);

d is the distance in metres;

n is the distance power loss coefficient;

n_f is the number of floors between the transmitter and receiver; and

$L_f(n)$ is the floor-loss penetration factor.

2.5. Indoor positioning technology classification

Several technologies can be used for indoor positioning, and various technology classifications have been proposed, as discussed in [6]. These classifications are based on numerous criteria, such as the hardware required and the existence of a network, among others. The classification that would clearly demonstrate the different technologies used for IPS is based on the main medium utilised to determine position, as proposed by [7]. The categories are divided into optical, magnetic, audible and ultrasound, and RF positioning technologies.

2.5.1. Optical

Optical-based positioning technology was previously employed predominantly by those working in robotics, as this technology requires a database and considerable processing power to process images, depending on their resolution. However, current smartphones contain high processing power and accurate lenses, which can be used to calculate and perform a better analysis using an accurate image.

The algorithm in [24] attempted to map the unique features in a corridor area, which contains many wall edges and intersections to be used to determine its location and direction. Meanwhile, [25] and [26] attempted to locate a user's position by comparing the captured image with the floor plan, using the wall edges of corridors and rooms as the unique features. The author in [27] has proposed an optical positioning technique by comparing the unique features of a captured image to the database rather than the area floor plan. These algorithms target small indoor areas, such as corridors, because of the limitation in vision-based indoor positioning. To overcome this limitation, the author in [28] has proposed a solution that makes use of static objects such as doors and windows. The system targeted monocular photography by integrating computer vision and a deep learning algorithm. To ensure a precise comparison of an image with the images in the database, [29] and [30] have proposed a key graph or a specific landmark, which is assigned at a certain location. This approach would allow for a more accurate detection but with the cost of a higher calibration process.

More recent optical positioning also demonstrates the interest in the inclusion of a 3D map to the algorithm, for example as adopted by [31] and [5]. A mobile device released by Google and equipped with RGB-D sensors has further raised interest in this area, such as in [32]. The author in [33] has proposed a simultaneous localisation and mapping (SLAM)

solution by making use of an RGB-D camera. The proposed algorithm focuses on a dynamic environment to overcome the limitation of most state-of-the-art SLAMs, which assume no moving object in the environment [33].

The author in [34] has proposed a camera-based indoor positioning system that uses visible light communication rather than environmental features of a captured or live image. The proposed algorithm requires reference LEDs transmitting their unique co-ordinate information to be deployed.

Several researchers have also proposed hybrid techniques that make use of optical positioning. A recent system has been proposed in [35] to perform a distance measurement using a hybrid system based on optical camera communication and the TDoA. The system requires a unit that receives optical and audible signals and sends back another optical signal. A system suggested in [36], on the other hand, proposes a hybrid system alongside integrated sensors, making use of a pedestrian dead reckoning (PDR) solution. It uses optical camera communication alongside digital zoom to calibrate and remove errors caused by PDR.

However, optical positioning still requires the user to capture the image, and there is sometimes a limitation in terms of what image is being captured for the technology to work properly.

2.5.2. Magnetic

Interest in magnetic positioning has been increasing because of the idea of positioning without the need to deploy anything. Earth is known to have its own geomagnetic field, and this field can be used to determine a user's position, as proposed by [37]. However, in an indoor area, the ambient magnetic field tends to be affected by surrounding objects, including building materials, and this can cause signal irregularities or anomalies in the

magnetic field. These magnetic field anomalies can be used as unique references for fingerprinting, as proposed by [38] and [39]. However, magnetic positioning demonstrates much uncertainty because of the limited number of elements for fingerprinting. Moreover, the changes in a magnetic field can be rapid, thereby making the calibration process a laborious task [40].

2.5.3. Audible and ultrasound technologies

Acoustic positioning is well known because it is a unique positioning technique adopted by animals, such as dolphins. It can be used not only with methods such as radar systems but also with fingerprint [41][42] and trilateration methods [43]. Nowadays, acoustic positioning can also be utilised with a smartphones, such as in [44]. The advantage of acoustic positioning is that it can achieve sub-centimetre levels of accuracy without the need for any additional infrastructure or devices apart from what is already available nowadays. However, the deployment of acoustic positioning might be limited, as this technology poses a significant challenge in terms of diverse noise sources, synchronisation, and strong interference of the audible band [43].

2.5.4. Radio Frequency

Indoor positioning based on RF is the choice of technology for many, as it is easily accessible with modern mobile devices and because of the high accuracy it can achieve. In some cases, small or no additional infrastructure is required to employ this positioning technology, since the signals are already available throughout the indoor area [45].

2.5.4.1. Radio frequency identification

Radio frequency identification (RFID) systems make use of a network of radio beacons and tags. Using this technology would allow for high accuracy and reliability in positioning. The

unique identification of different objects in an indoor area makes the technology a promising option for accurate positioning with a sub-meter level of accuracy [46]. The author in [47] has proposed indoor positioning using active RFID tags with a trilateration approach. However, this algorithm requires a large number of RFID tags to be deployed with up to one tag per 1 m^2 area. Zou et al. [46] attempted to lower the deployment cost of the algorithm in [47] by reducing the number of RFID readers and replacing them with RFID sensors instead. Furthermore, the author in [48] attempted to combine RFID positioning with a GPS to allow for automatic switching between indoor and outdoor positioning. However, the algorithm for RFID itself remains the same as the one used in [47].

2.5.4.2. Wi-Fi

Radio frequency signal positioning based on Wi-Fi is increasingly common nowadays. Unlike RFID positioning, no additional Wi-Fi access points (APs) are needed apart from what is already available in the area. In most buildings, the Wi-Fi signal covers the whole indoor area, and this signal can be used to locate a user's position. As with the previous algorithm, Wi-Fi positioning can be used with fingerprint [49][50][51] or trilateration [52][53][54]. The Wi-Fi signal is highly affected by attenuation and multipath; therefore, it is challenging to apply the appropriate estimation of the path-loss model for the signal. Furthermore, the placement of an AP is based on the widest coverage rather than on the optimal dilution of position (DOP) for positioning. The AP itself requires high power consumption; it thus needs to be deployed in an area with an accessible power supply. These problems can affect the Wi-Fi positioning accuracy,, which can be up to 3–5 m [55].

2.5.4.3. Bluetooth

Bluetooth has become a widely used technology for indoor positioning in recent years. It utilises the same 2.4 GHz signal as Wi-Fi, and most of the positioning algorithms developed

for Wi-Fi can thus be adopted with Bluetooth. Moreover, the introduction of Bluetooth 4.0 with a BLE sub-module has further gained the interest of researchers in terms of the use of Bluetooth technology for indoor positioning. Unlike APs, BLE beacons can be powered up using a battery, and they can last for years using only a coin-operated battery. For these reasons, a BLE beacon can be deployed in the best possible DOP for the best accuracy of positioning. Moreover, the low-cost factor of BLE enables an affordable deployment of a number of these beacons in the area to be localised.

With the release of two advertisement protocols for BLE beacons, namely iBeacon [11] and Eddystone [56], the demand for Bluetooth positioning has further increased. The new advertisement protocol allows for a more unique classification among each beacon and a more accurate distance estimation, even among different beacon manufacturers. Furthermore, the new protocol also enables additional information to be advertised, such as the identification of the following: code that allows for interaction from an application, a beacon's telemetry information, and the URL for beacon use without any specific application [57].

Faragher et al. [58] and King et al. [59] have proposed the use of Bluetooth positioning using the fingerprint approach. A Bluetooth fingerprint can also be used alongside a Wi-Fi fingerprint to improve the accuracy of Wi-Fi positioning in an area with low Wi-Fi positioning accuracy, as was done in [60], [61], and [62]. As with any other fingerprint technique, this approach requires a large number of RPs through calibration. A trilateration approach using Bluetooth has been proposed in [63], [64], and [65]. In general, only the beacons' locations and their RSS are required to perform the trilateration. Since less calibration is required, many researchers have also studied Bluetooth positioning using this approach.

2.6. Conclusion

This chapter described the background of various techniques and technologies used in indoor positioning. A summary of the indoor positioning techniques is presented in Table 2.1. Lateration and scene analysis techniques are widely used because of their low-complexity implementation. These techniques are used in this research because of their low dependency on specific hardware and because they can be easily implemented with widely available consumer devices. Table 2.2 contains a summary of the distance estimators that are widely adopted in conjunction with the lateration technique. The most popular selection of distance estimators is based on RSS because of the availability of the device and protocol. Received signal strength is chosen as the distance estimator, as it does not require any specific antenna for both transmitter and receiver. The summary of indoor positioning technologies is presented in Table 2.3. The RF technology is chosen as the technology for this research because it requires little to no additional infrastructure while still maintaining high positional accuracy. An analysis of RF is consequently performed and summarised in Table 2.4. Wi-Fi tends to be the radio technology choice for most because of its widespread availability;

Table 2.1. Analysis summary of indoor positioning techniques

Indoor Positioning Technique	**Advantages**	**Disadvantages**
Proximity	• Easy to implement	• Limited or no absolute positioning
Angulation	• Accurate	• Requires a specific antenna
Lateration	• Only requires distance, which can be estimated using RSS	• Highly dependent on the accuracy of the estimated distance
Scene Analysis (Fingerprint)	• Robust against attenuation and multipath	• Laborious calibration phase

however, the introduction of BLE as well as the protocols specifically meant for positioning brings BLE to the attention of many researchers. This research focuses on BLE because of its low cost and low power consumption. This allows accurate positioning to be implemented in areas with limited access to other RF technologies.

Table 2.2. Analysis summary of distance estimators

Distance Estimator	**Advantages**	**Disadvantages**
Time of Arrival (ToA)	• Accurate	• Requires specific hardware to obtain a precise time stamp • Transmitter and receiver need to be synchronised
Time Difference of Arrival (TDoA)	• Does not require precise synchronisation	• Requires specific hardware to obtain a precise time stamp
Received Signal Strength (RSS)	• Commonly available	• Can be unstable depending on the RF technology and frequency used

Table 2.3. Analysis summary of indoor positioning technologies

Indoor Positioning Technology	**Advantages**	**Disadvantages**
Optical	• No additional infrastructure • Accurate even with 3D positioning	• Requires large database • Requires considerable processing power • Requires a specific lens for accurate positioning
Magnetic	• No additional infrastructure	• Can be unreliable because of interference • Limited indoor positioning technique can be apply
Audio	• No additional infrastructure • Can achieve sub-centimetre accuracy	• Limited application as a result of diverse noise sources • Synchronisation
Radio Frequency	• Small or no additional infrastructure • High accuracy	• May require additional infrastructure • Susceptible to multipath

Table 2.4. Analysis summary of radio frequency technologies used for indoor positioning

Radio Frequency Technology	**Advantages**	**Disadvantages**
Radio frequency identification (RFID)	• High accuracy • High reliability	• Requires additional infrastructure • Requires a large number of RFID tags to be deployed
Wi-Fi	• Readily available • High coverage	• Susceptible to attenuation and multipath • Access point (AP) placement is usually not optimal for positioning
Bluetooth	• Low cost • Low power consumption	• Susceptible to attenuation and multipath • Requires additional infrastructure

3. Channel Selection Filter

3.1. Introduction

The previous chapter discussed positioning techniques and their challenges. One of the widely used proximity or distance estimation techniques is based on RSS. As discussed, this approach suffers from unreliable signals as a result of the uncertainty of the signals. This uncertainty can be caused by multiple sources: external or internal.

This chapter discusses the challenges of estimating distance using RSS values. Previous studies that have attempted to find the best distance estimation based on RSS are reviewed. A new filter algorithm is then proposed; it allows for the use of a more stable and thus reliable signal. Finally, the proposed filter algorithm is analysed to study the impact when implemented for positioning.

3.2. Bluetooth Low-energy Signal Advertisement Channel

A BLE signal uses the same 2.4 GHz signal as Wi-Fi and is a subset of Bluetooth 4.0, which was adopted on 30 June, 2010. Since it uses the same 2.4 GHz as the previous version of Bluetooth, it also has the same signal characteristics, meaning that it is susceptible to signal degradation via attenuation and multipath. There is already some research aimed at minimising these effects [66][67]. However, the approaches therein only target the variation resulting from external causes, which are mainly affected by the environment.

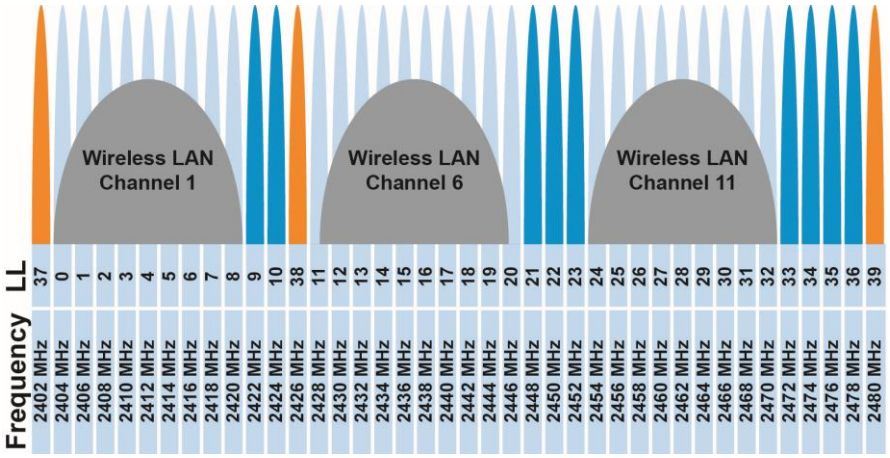

Figure 3.1: Bluetooth low energy 2.4 GHz band channels. Orange represents the three advertisement channels located in the middle and at both ends of the spectrum [95]

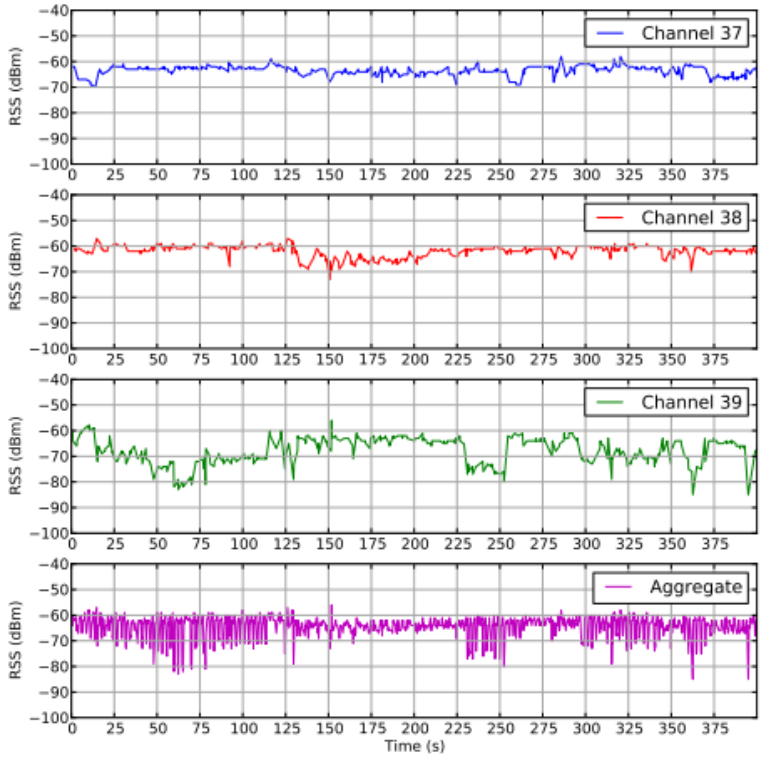

Figure 3.2: Channel variation RSS. Channels 37 and 38 have similar signals compared to channel 39 [58]

The instability in a BLE signal is caused not only by degradation and multipath but also by the protocol design, as highlighted in [68]. By design, the advertisement channel consists of three channels – 37, 38, and 39 [69]. These three channels are selected to avoid overlapping in order to allow the least interference in the signal.

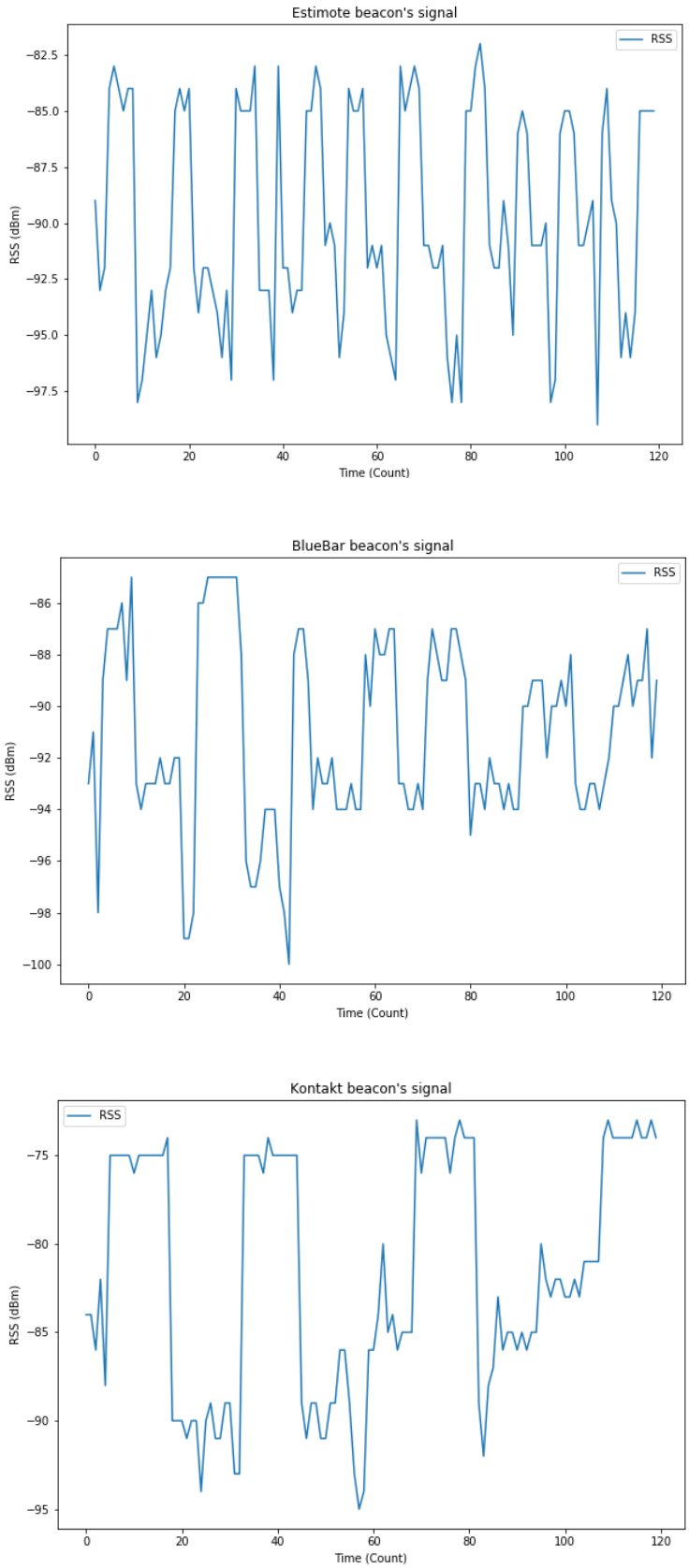

Figure 3.3: One-minute signal variation from three different manufacturers.

As the BLE uses the same 2.4 GHz signal as used by Wi-Fi, the signal will also be affected by Wi-Fi. Therefore, the three BLE advertisement channels are chosen based on the frequency that is least affected by the following three common Wi-Fi channels: 1, 6, and 11. This also causes the three channels to be located far from one another in the 2.4 GHz channel band, as illustrated in Figure 3.1. The figure also depicts the distance between channels 37 and 39, which are located at the opposite ends of the 2.4 GHz band. The far distance between each channel causes the signals of these channels to be significantly different, as seen in Figure 3.2 [56, Fig. 2]. Comparing the channel location illustrated in Figure 3.1 against the RSS variation in Figure 3.2, channel 37 and channel 38 have similar RSS values and variation within the range of a 1–5 dBm difference, compared to channel 39, which differs greatly with up to a 25 dBm difference. This is because channels 37 and 38 are much closer to each other compared to channel 39. The aggregated result demonstrates the effect of the largely different signal variation.

Figure 3.3 illustrates the signal variation of three different beacon manufacturers. The signals were recorded for 1 min, and all the beacons' settings were set to default. The Estimote beacon's advertisement interval was set at 300 ms, the BlueBar beacon was set at 750 ms, and the Kontakt beacon was set at 350 ms. The default settings were chosen instead of specific intervals because this configuration was expected to be used by the majority of BLE beacon users. A similar pattern can be seen from the graph. The signal can be clustered into two or three groups, corresponding to the three advertisement channels. Two of the clustered groups will resemble each other, and another group will have a significantly different value. This aligned with the fact that the positions of channels 37 and 38 are close to each other, while channel 39 is at the other end of the 2.4 GHz band. The graph pattern is also similar to the pattern in Figure 3.2. This confirms that channel hopping affected the

signals read by the mobile device, and the hopping corresponds to the three advertisement channels.

As with any other signals, the BLE signal also contains Gaussian noise, which can be differentiated by only a small change in the RSS of around 1–5 dBm, as opposed to large changes in the RSS as a result of channel hopping with changes up to 15 dBm. The large changes in the RSS might also be affected by the environment, such as obstruction and multipath.

3.3. Channel Selection Filter

Multiple filters are used to aggregate and find the true value of varied signals. Some researcher record the mean signal but records it with variance to keep the signal variation information as done by [70]. This approach is mainly to record the important information while minimising the size of data that needs to be recorded. Another researcher designed a tailor-made smoothing algorithm with a proposed value of window width and stage [71]. The smoothing filter ignores the channel hoping and process the data indiscriminately. This produce a smooth signal but channel hoping greatly affect the resulting signal.

Based on the knowledge of the channel hopping condition, a channel selection filter is designed to reduce the effect of advertisement channel hopping. Using the same channel to analyse the signal for positioning can improve distance estimation. It would also enhance the fingerprint algorithm by ensuring that only the same advertisement channel is being compared to guarantee that the correct signal is being recorded and compared. For these filters, it is important to have a complete signal that contains the values for all three channels. From our observation, a minimum of 15 s is needed to ensure the signals from all three channels are read.

3.3.1. High-pass Fourier transform filter

The Fourier series is a periodic function in time that can be decomposed into the sum of a constant and a series of sinusoids. The sinusoidal signals are defined by the individual frequency of sine and cosine. The Fourier series is written as (3.1).

$$f(t) = \frac{1}{2}a_0 + \sum_{k=1}^{\infty}(a_k cos2\pi kt + b_k sin2\pi kt) \quad (3.1)$$

A Fourier transform is used to analyse the signal in a different domain – in this case, a frequency domain. In relation to the Fourier series, it is used to calculate the coefficient (a_k and b_k), also known as the correlation of the sinusoids. To do this, the function is multiplied by the analysing function, which is written as (3.2):

$$X(F) = \int_{-\infty}^{\infty} x(t)e^{-j2\pi Ft}dt \quad (3.2)$$

Since the BLE signals are recorded as a set of discrete points, a solution based on a discrete Fourier transform (DFT) is employed instead. To convert the Fourier transform from continuous to discrete, the function related to time needs to be modified to make it based on sampling rate and sampling number instead.

$$F \widehat{=} \frac{k}{N} \quad (3.3)$$

$$t \widehat{=} n \quad (3.4)$$

Using (3.3) and (3.4) in (3.2) would result in a DFT equation, which is written as (3.5):

$$X_k = \sum_{n=0}^{N-1} x_n \, e^{-\frac{j2\pi kn}{N}} \tag{3.5}$$

This change allows the evaluation to change from ∞ to $-\infty$ and from $n = 0$ to $N - 1$, which correspond to the finite discrete sampling. This change also causes the evaluated frequency to be restricted by the sample frequency and the number of samples used.

Euler's formula is used to establish a relationship between the trigonometric functions and the complex exponential function in complex analysis. This formula is written as (3.6):

$$e^{jx} = \cos x + j \ \sin x \tag{3.6}$$

Applying (3.6) to (3.5) would result in (3.7):

$$X_k = \sum_{n=0}^{N-1} x_n (\cos(-\frac{2\pi kn}{N}) + j \sin(-\frac{2\pi kn}{N})) \tag{3.7}$$

Furthermore, simplifying (3.7) would result in (3.8):

$$X_k = A_k + B_k j \tag{3.8}$$

Based on the decomposed signal, it is possible to select only the required signal and filter out other signals. A high-pass Fourier transform filter is performed by filtering the signal in the frequency domain. Applying a high-pass filter to the signal will smoothen out the signal by removing the noise in the signal. This will allow for a cleaner signal, which makes the identification of changes in the signal easier. For the proposed implementation, only the highest frequency was chosen.

As a Fourier transform generates a sinusoidal signal, only the positive values are kept, and values lower than zero are limited to zero. This will make the filtered signal focus only on the stronger signal, which, in most cases, is the more reliable signal. The use of only

positive values can also reduce the effect of a large signal drop to the overall or the mean values. The mean of the resulting Fourier transformed signal is used as the final value for positioning.

Figure 3.4 illustrates the resulting high-pass Fourier transform filter over the measured signal. It maintains the values in the middle advertisement signal, which can be seen from the thick blue line. The effects of large variations of low signal value are reduced, as seen from the graph. The green line depicts a moving average of 15 s data, and it closely resembles the shape of a high-pass Fourier filter but with a lower signal value.

It is important to take into consideration that these algorithms are not meant to determine the variation originating from signal degradation or multipath. However, the analysis of signal degradation and multipath can be performed on the selected signal to ensure that signal changes are not related to advertisement channel hopping.

3.3.1.1. Distance Effect

A further analysis was performed to study the effect of distance on channel hopping and the reliability of the high-pass Fourier transform filter. The further the signal is from the beacon, the lower the BLE signal variation will be; this is because the signal strength is based on a logarithmic model rather than a linear model. The signals for the three advertisement channels are consequently still discernible.

Figure 3.5 illustrates the result of the BLE beacon's signal taken at a 1 m distance for a period of 8 minutes. The effect of channel hopping is not as clearly visible when looking at the large result. However, if the result is seen with a smaller set of data, with sufficient size to capture the changes in the signal, then the effect of signal hopping can be clearly seen, as demonstrated in Figure 3.6.

From the figures, the red lines denote the result of the proposed high-pass Fourier transform filter, and the green dashed lines represent a moving average filter. Both algorithms were calculated using a window size of 15 s, disregarding the number of scans contained within. The figures demonstrate that the result using the proposed filter follows the middle step of the signal as opposed to a moving average filter, which attempts to obtain a balance between the maximum and minimum values.

A similar finding can be seen in Figure 3.7, which illustrates the result of a BLE beacon's signal taken at a 3 m distance for a period of 8 min. The result of the signal with a

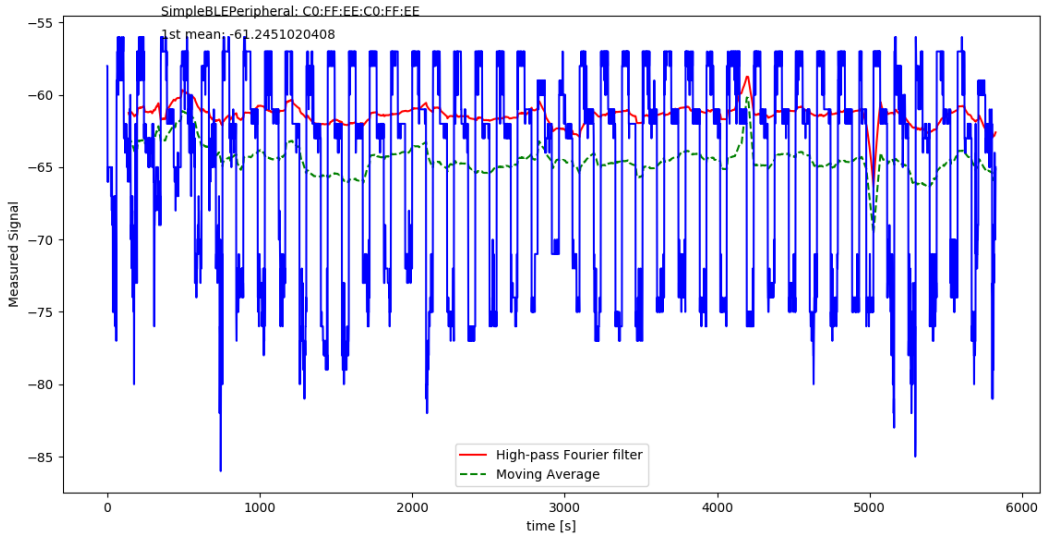

Figure 3.4: Bluetooth low-energy signals and the resulting signals when filters are applied. The high-pass Fourier transform filter result is depicted in red, and green indicates the moving average filter

smaller set of data is depicted in Figure 3.8. The signal taken at 3 m also demonstrates the same three different steps for the signal, which represent the three different advertisement channels. This is further confirmed by the result presented in Figure 3.9 and Figure 3.10, which display the result of a BLE beacon's signal taken at a 5 m distance.

A similar finding can also be seen from the results taken at multiple distances. Furthermore, the proposed filter algorithm closely matches the middle signal, which would be the chosen signal to be used. By using the signal from the same advertisement channel, a more consistent signal reading and distance estimation can be expected.

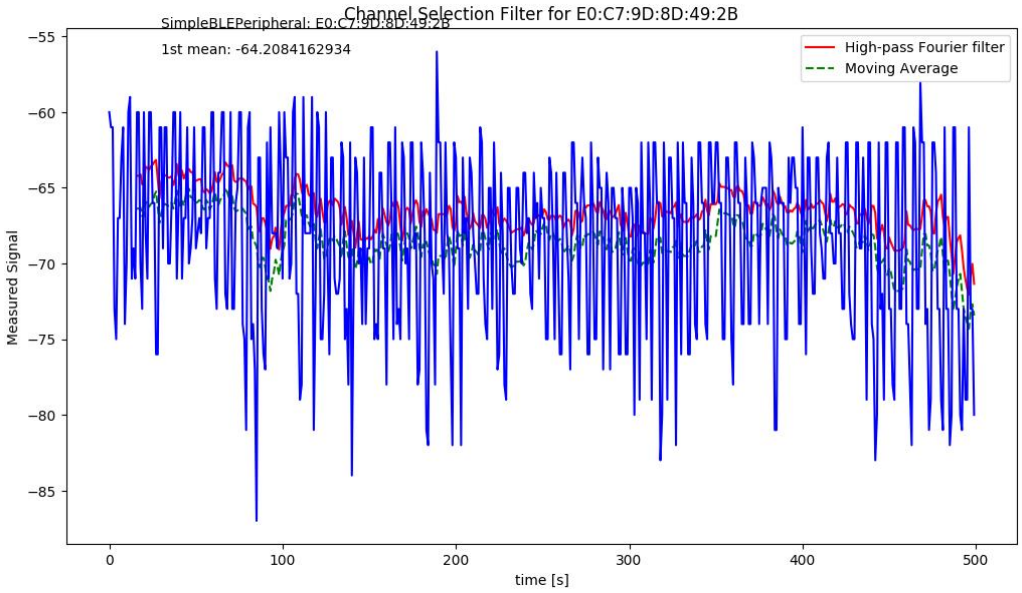

Figure 3.5: Bluetooth low-energy signals at a 1 m distance: comparison among original signal, high-pass Fourier, and moving average filter results

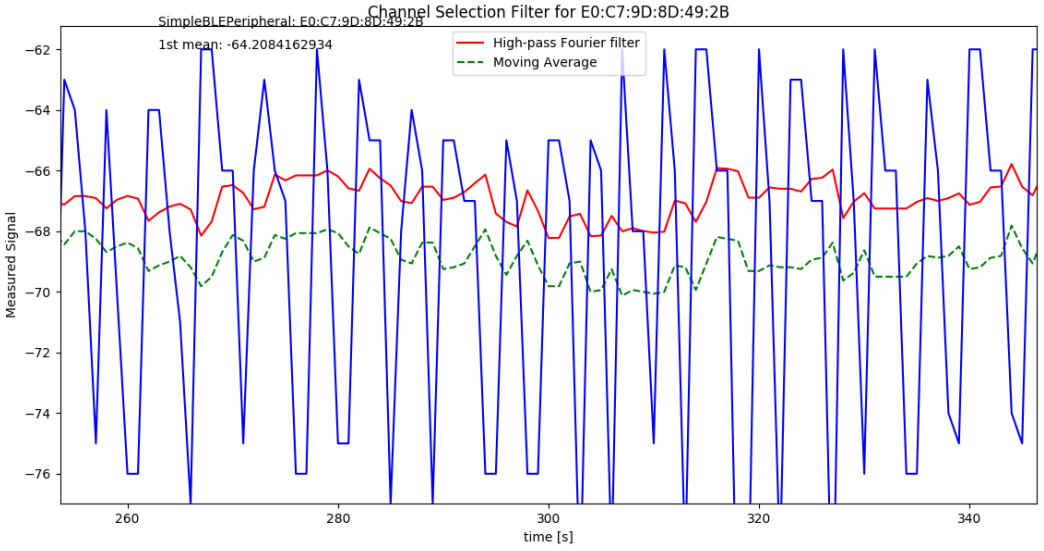

Figure 3.6: Bluetooth low-energy signals at a 1 m distance: comparison among original signal, high-pass Fourier, and moving average filter results (zoomed in)

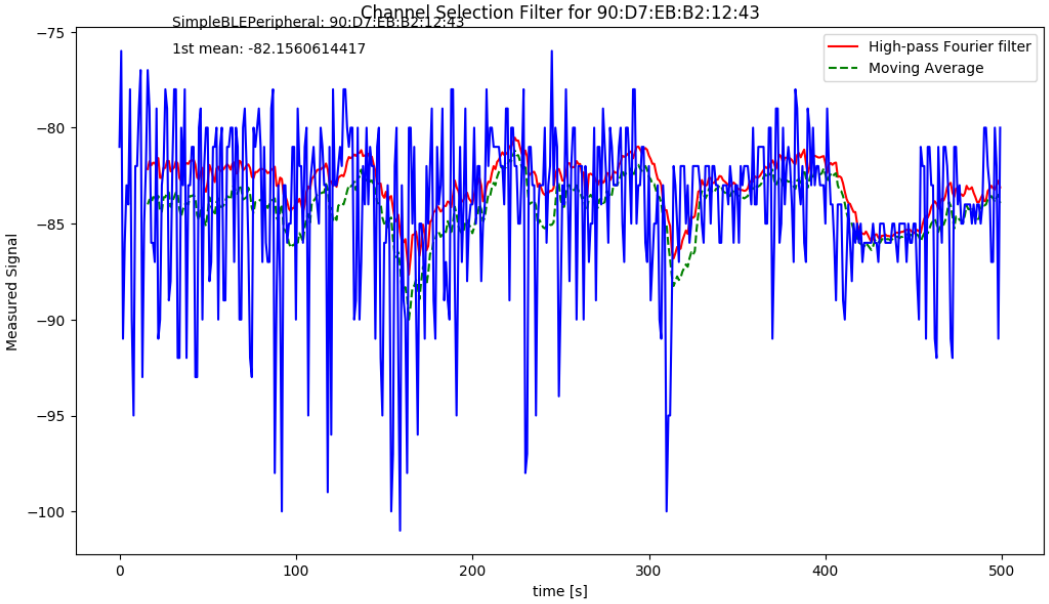

Figure 3.7: Bluetooth low-energy signals at a 3 m distance: comparison among original signal, high-pass Fourier, and moving average filter results

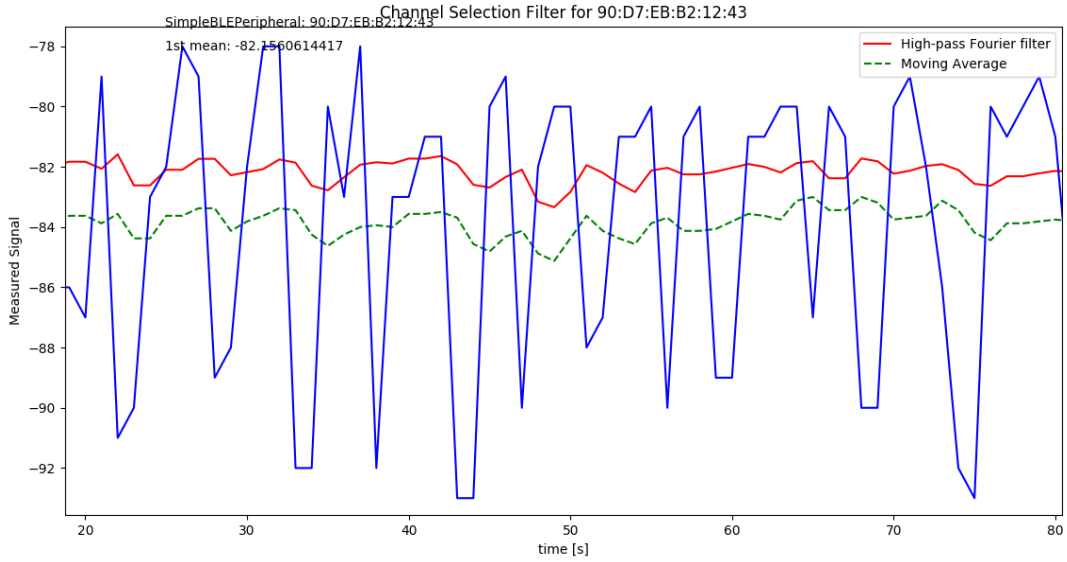

Figure 3.8: Bluetooth low-energy signals at a 3 m distance: comparison among original signal, high-pass Fourier, and moving average filter results (zoomed in)

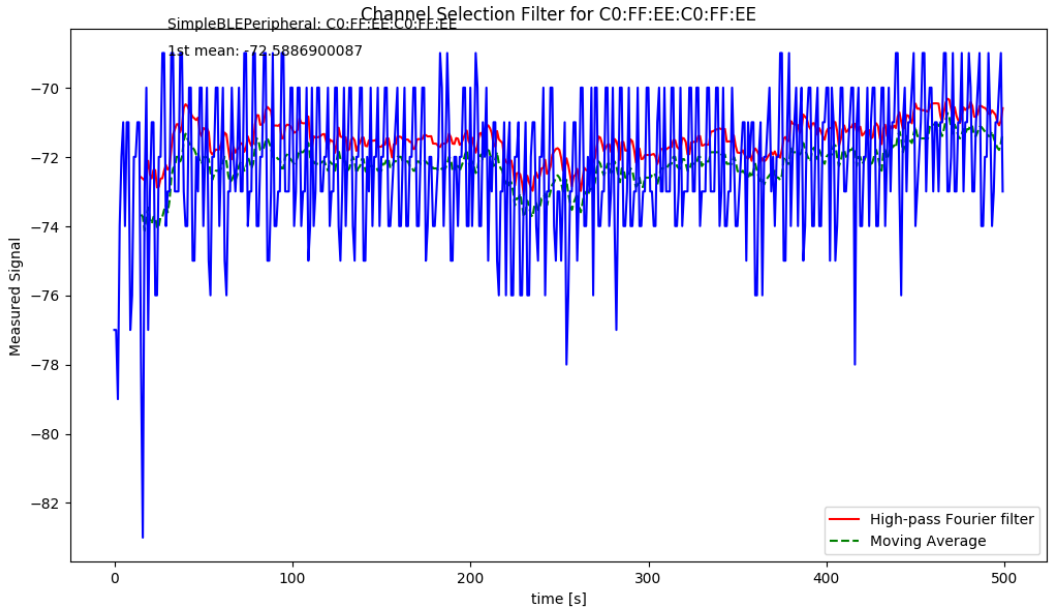

Figure 3.9: Bluetooth low-energy signals at a 5 m distance: comparison among original signal, high-pass Fourier, and moving average filter results

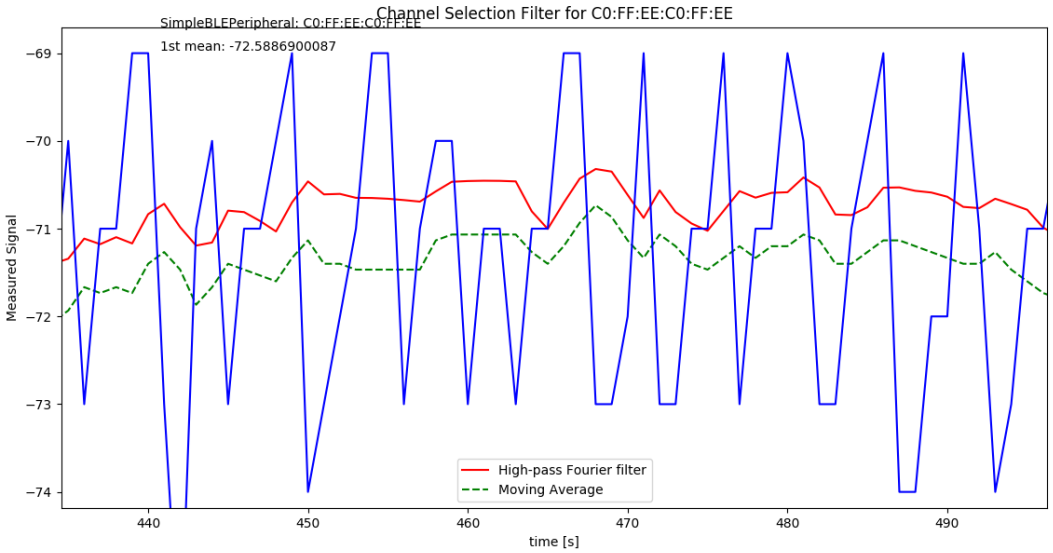

Figure 3.10: Bluetooth low-energy signals at a 5 m distance: comparison among original signal, high-pass Fourier, and moving average filter results (zoomed in)

3.3.1.2. Obstruction Effect

An experiment was also performed to check the effect of obstruction on the BLE signal. Bluetooth low-energy signals were recorded under LOS and non-line-of-sight (NLOS) conditions. For the NLOS signals, two obstructions were used: soft partition and hard partition. The soft partition is a wall partition made of hollow interior plasterboard, while the hard partition is a brick wall.

Figure 3.11 illustrates the BLE signal blocked by a soft partition. Despite the large variation in RSS values, the signals can still be divided into three categories: minimum, maximum, and middle signals, which could also correlate to the three advertisement channels. For this case, the moving average filter was able to detect the middle value, and the proposed algorithm was able to match the estimation result with a difference less than one dBm.

The result for hard partition obstruction is illustrated in Figure 3.12. Even though the signal is less noisy because of its attenuation, the signal variation resulting from the three different advertisement channels is still visible. In this case, most of the signal will be in the middle signal group, and similarly to the result of soft obstruction, the proposed algorithm will be able to match the result with differences less than 0.5 dBm.

These results confirm that the three advertisement channels are showing even in different cases and environments. Furthermore, the proposed filter was able to find the middle value in all the given cases. This allows for a more streamlined BLE signal reading, which will allow for a more reliable signal reading.

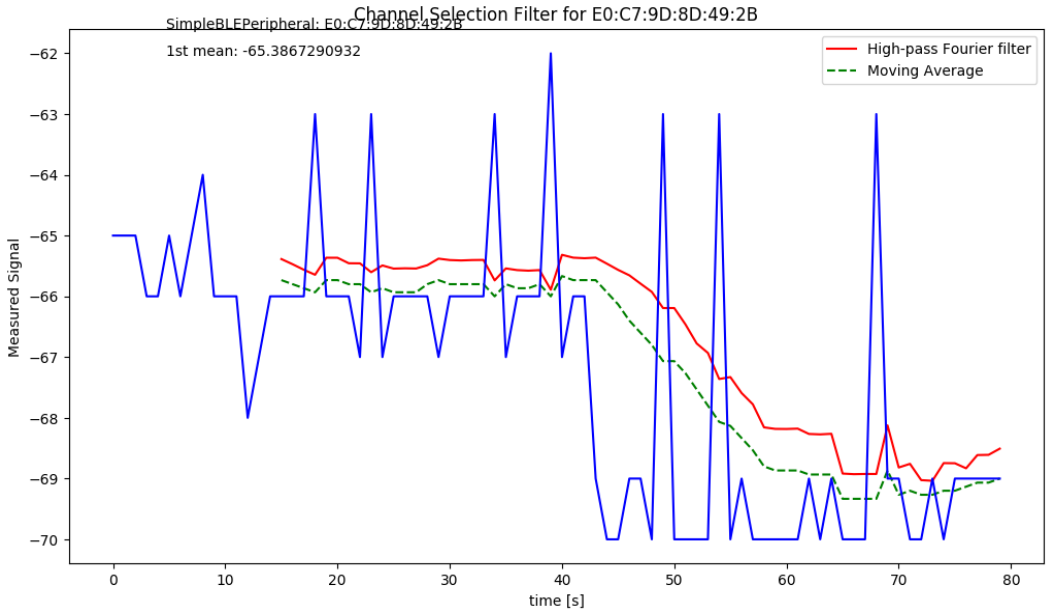

Figure 3.11: Bluetooth low-energy beacon's signal blocked by soft partition

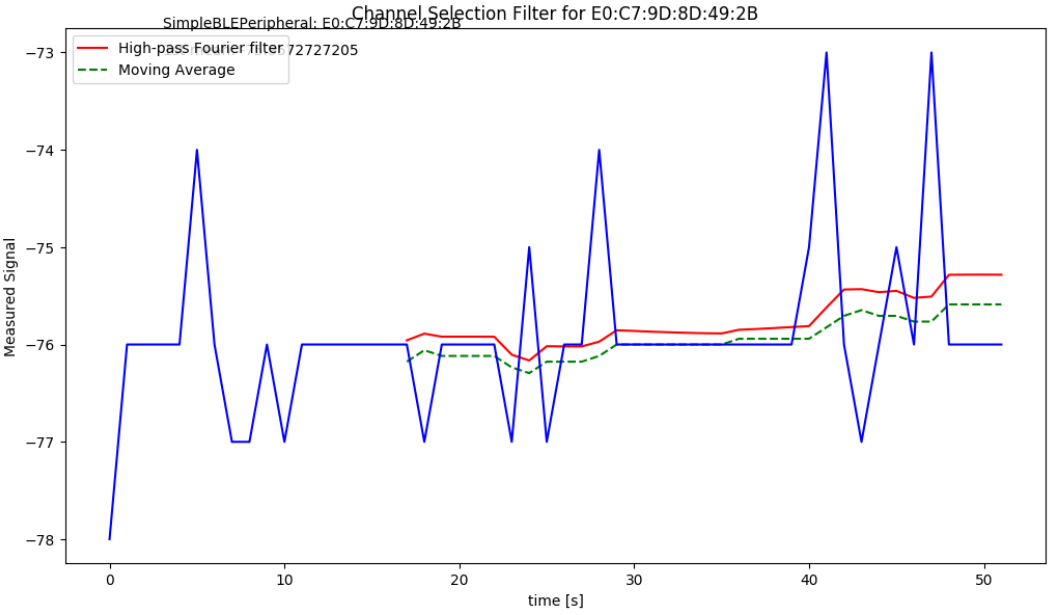

Figure 3.12: Bluetooth low-energy beacon's signal blocked by hard partition

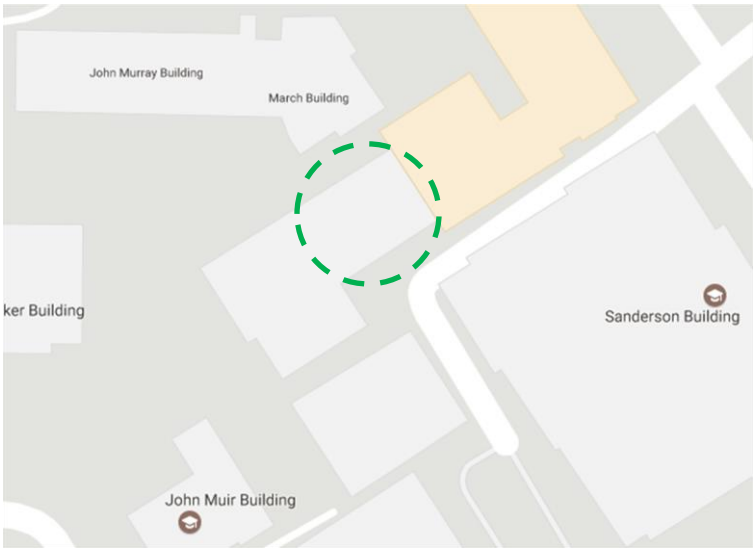

Figure 3.13: The Mary Bruck Building. The area used for the testing is circled

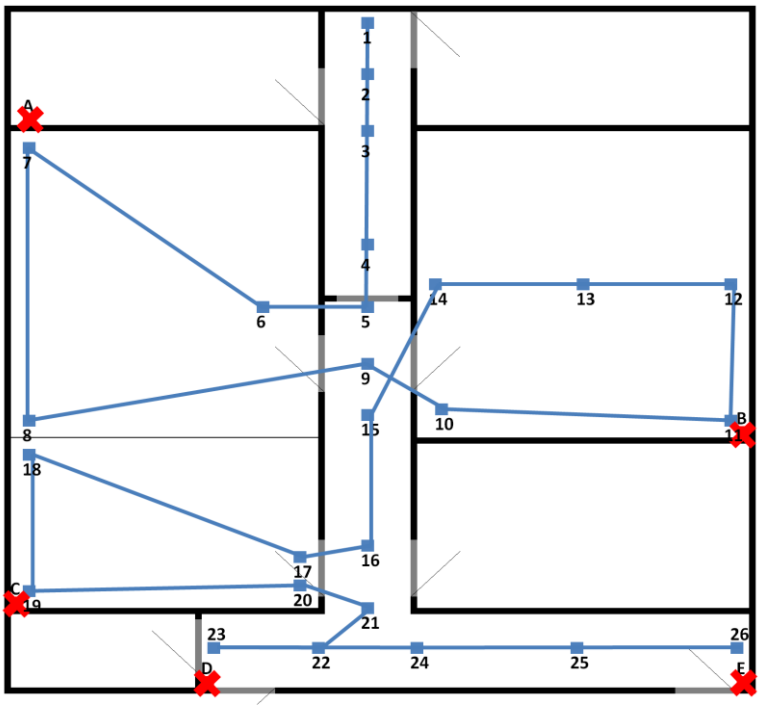

Figure 3.14: Test area floor plan and test layout. Red crosses mark the BLE beacons, while blue squares indicate the points where the signals are recorded, and the blue line is the path taken to reach the points

3.4. Impact on Positioning

It was important to verify the impact of the proposed algorithm on positioning accuracy improvement. Therefore, the algorithm was tested in a part of the Mary Bruck Building at

the University of Edinburgh, as illustrated in Figure 3.13. The floor plan for the test area, with a size of 12m x 12m, and the test point locations are seen in Figure 3.14. The red crosses denote the position of the beacons, and the blue squares mark the test points.

Five beacons were utilised and were of the Estimote and Texas Instrument varieties. A total of 26 test points were employed in the test, which was conducted with the Samsung Galaxy S5 smartphone, and the measurements were recorded for at least 30 seconds. This was to make certain that all three variations were recorded while still permitting additional data to be processed in the case of signal degradation and multipath affecting the signal variation.

The algorithm used to calculate the position was based on trilateration with distance estimation based on a log-distance path-loss model, as in (3.9):

$$RSS(d) = RSS(d_0) + 10nlog\left(\frac{d}{d_0}\right) + X_g \quad (3.9)$$

where $RSS(d_0)$ is the RSS measured at distance d_0, n is the path-loss exponent, and X_g is the zero-mean Gaussian noise.

The implementation results were compared against distance estimations calculated using a smoothing algorithm [71]. 13-point window width and 3-stage smoothing filter is used as suggested by the author. Figure 3.15 illustrates the result tracks for both algorithms. Both results indicate that the estimated positions are centred in the middle of the test area. This is because at most test points, 80% of the utilised beacons are blocked by walls. This would require a higher path-loss exponent to be used to mitigate the effect of obstruction. To mitigate the NLOS effect, a path-loss exponent of 2.6 was used, as suggested by the author

in [72]. However, as demonstrated in Section 3.3.1.2, the proposed filter will work even in the NLOS situation, albeit with less efficiency.

Figure 3.16 portrays the results of each test point against the smoothing algorithm. The error for each test point was determined by comparing the resulting positions with the actual position of the test points. The smoothing algorithm demonstrates that 68% of the results are within a 9.55 m accuracy, and 95% of the results fall within a 12.47 m accuracy. These results slightly improved to 9.28 m for 68% of the results and 12.21 m for 95% of the results by implementing the proposed filter. Furthermore, 88% of test points indicate improvements, with the highest improvement being from test point 22 with an improvement of 1.33 m. Overall, the root mean squared error (RMSE) for the smoothing algorithm improved from 7.23 m to 6.97 m with the proposed filter, and the RMSE can be further improved by deploying it alongside a multipath mitigation technique. It can be seen that the highest error peaks occurred at points 1 and 12, and smaller error peaks appeared at 2, 3, 19, and 26. These error peaks occurred at test points located at the far end of the building, close to the outer wall. This caused the beacon on the other side of the building to affect the position estimation. The proposed filter was able to improve the result; however, it was unable to mitigate the error entirely.

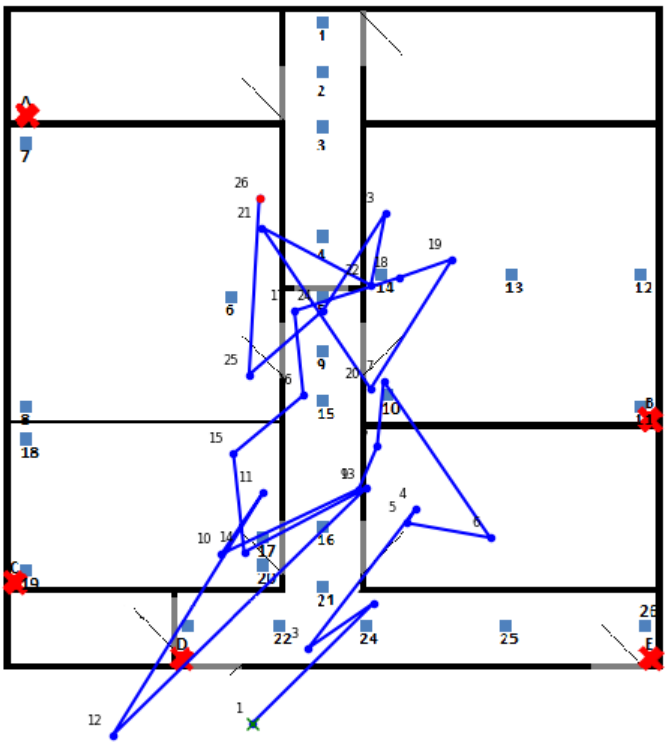

a) Resulting track by Hou et al. [72]

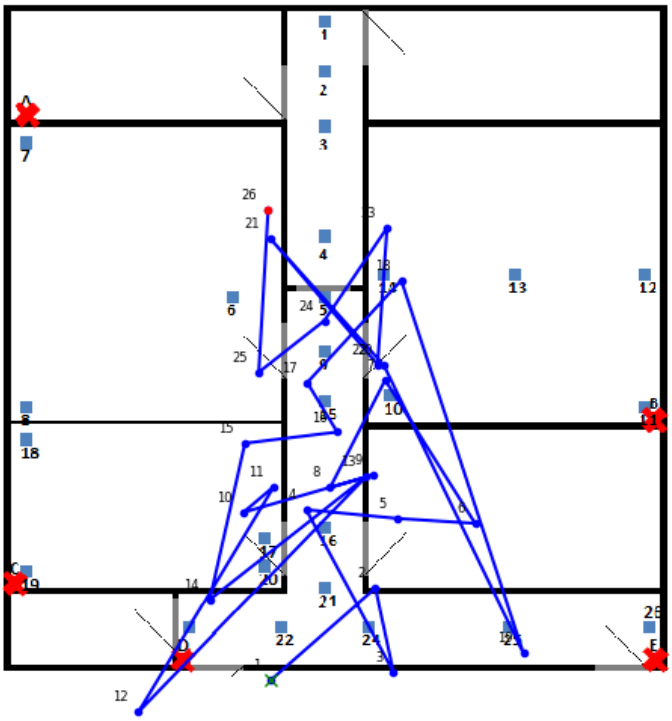

b) Track for proposed algorithm

Figure 3.15: Result tracks. a) Resulting track for Hou et al. [72]. *b) Track for proposed algorithm*

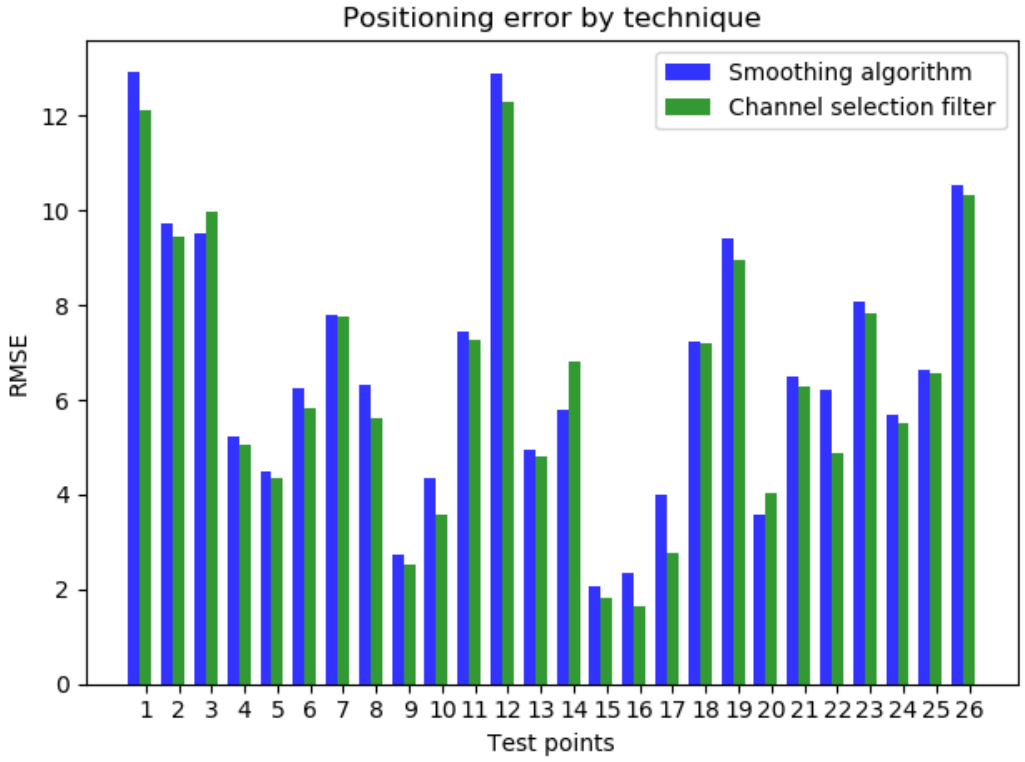

Figure 3.16: Implementation result comparison between Hou et al [71] and proposed algorithm

3.5. Conclusion

In this chapter, first, the BLE signal advertisement channel was introduced. Then, the signals of the three advertisement channels were presented, highlighting channel 39 with a significantly different signal compared to channels 37 and 38. The effect of the three different advertisement channels was demonstrated thereafter by using multiple beacon manufacturers, and the results confirm that the signal variation because of the advertisement channels is not device-specific. With a 2.4 GHz signal known to be highly affected by attenuation and multipath, any additional variation to the signal will have a large impact when estimating the actual signal.

Following this, a new channel selection filter was proposed using a high-pass Fourier filter. First, the concept of this type of filter was introduced, and analyses were performed to study the effect of distance and obstruction. It was demonstrated that the filter works for different distances and obstruction states. The implementation of the filter was also demonstrated to study the impact of the proposed filter on actual positioning. The filter improves the majority of the test points, albeit with low overall RMSE improvement. This confirms the viability of the filter to smoothen the signals, thereby improving the distance estimation and positioning.

4. Isolated Beacon Identification

4.1. Introduction

The previous chapter described the detailed implementation of a proposed filter algorithm to minimise the effect of channel hopping. This chapter presents a solution to another challenge in estimating distance based on RSS values. Signal variations resulting from external disturbance are another cause of BLE signal variation.

Signal attenuation can be affected by materials obstructing the signals. The more the material obstructs the signal, the more it will affect the RSS values. This will affect the distance estimated using those RSS values. To counter this problem, an algorithm is proposed to differentiate the obstructed and unobstructed signals, so a distance estimation can be estimated appropriately.

4.2. Non-line-of-sight and Multipath

Bluetooth low-energy signals use a 2.4 GHz spectrum for operation. This spectrum is known to be highly attenuated by the NLOS condition. Several studies were performed to differentiate and identify NLOS and LOS signals, and multiple different approaches were used, ranging from multiple antennae [73], map stitching [74], channel statistic [75], and probability distribution analysis [67].

The author in [76] has proposed a solution using mean, standard deviation, kurtosis, skewness, Rician K factor, $\chi 2$ goodness of fit, and log-mean. The support vector machine (SVM) algorithm is used to process the features for NLOS detection. Another author in [77] has proposed a similar approach, with mean, standard deviation, skewness, and kurtosis chosen as the features derived from the estimated channel impulse response (CIR). A

different machine learning approach, namely the random forest algorithm, was then applied to tackle the NLOS identification problem.

More recent Wi-Fi APs are equipped with a dual band antenna for 2.4 GHz and 5 GHz bands. The author in [78] has proposed a solution to make use of this by estimating the path-loss difference between the two bands. Given the same distance, the path-loss difference caused by different signal attenuations depends on the path-loss exponent. The idea is that both signals attenuate differently because of the wavelength of the signals.

A different NLOS identification technique proposed in [79] attempted to use a hybrid solution by incorporating PDR data into the algorithm. Pedestrian dead reckoning information is used to initially locate a user's position, and the RSS of the beacon whose NLOS state needs to be identify is estimated. The difference between the measured and estimated values is then used to determine the NLOS identification.

The author in [80] has proposed TDOA-based NLOS identification by making use of multiple base stations. When all base stations are in LOS, the measured distances are close to the true distances. However, if one or more base stations are NLOS, this will cause a large positive bias in the measurement.

The author in [81] has highlighted the relation between an RSS value's standard deviation and the NLOS condition. The author observed a more stable signal in the NLOS condition compared to the LOS condition. A table presented in [82] further confirmed the relationship between standard deviation and the NLOS condition with a standard deviation value of 14.1 dBm in the soft partition office and a standard deviation of 7.0 dBm in the hard partition office. However, no exact value for the LOS condition was given. The same paper has also demonstrated that the standard deviation of the LOS condition in a metalworking factory is

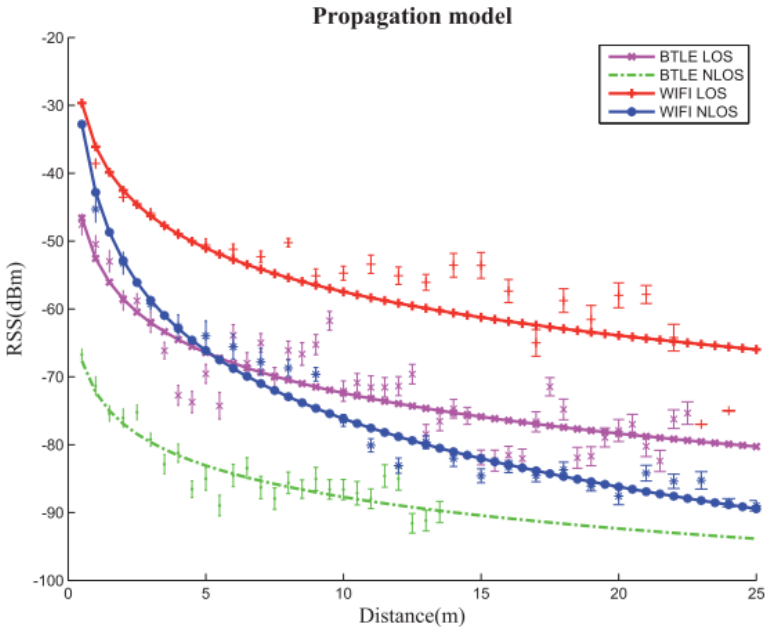

Figure 4.1: Propagation model of wireless signals [55]

5–8 dBm, while the standard deviation for LOS in an obstructed metalworking factory is 6.8 dBm. This is because metal is a highly conductive material and is thus also an optimal reflector. However, this is a unique case when the user is surrounded by metal.

The resulting difference of BLE signals between NLOS and LOS has been demonstrated by [55]. The result is most likely to follow the propagation model in the NLOS condition. From an RSS perspective, a mean RSS value of an LOS condition's signal could relate to distances with a range of more than 10 m and up to 20 m, whereas the same mean RSS value of an NLOS condition's signal could relate to distances with a range of only 5 m. For example, a graph in [53, Fig. 2] illustrated in Figure 4.1 indicates that the distance for LOS at an RSS of approximately -73 to -75 dBm can differ between five metres and 23 m, whereas for NLOS with the same RSS, the range difference is less than five metres.

The difference in range variation is because with the same RSS value, the LOS position is much farther than in the NLOS condition. In this situation, the LOS condition will be susceptible to more variation of signal interference and multipath, which can include destructive and constructive interference, thereby creating a larger variety of RSS values. Furthermore, the use of three widely spaced narrow bands causes the three signals to be affected by multipath and attenuation differently, thus creating three separate variations of RSS readings. These situations are illustrated in Figure 4.3 and Figure 4.3, where (a) is an LOS result at 2 m, (b) is a plasterboard NLOS at 2 m, (c) is a two-plasterboard NLOS at 2 m, and (d) is a concrete NLOS at 0.5 m. The concrete NLOS was chosen at a smaller distance to maintain the average RSS for comparison.

The graphs suggest that there are two or three distinct level sets of variation across the RSS readings. The difference among these variations is clearest in the LOS condition, where we can roughly estimate the upper and lower limits for the graph. The further blocked signal has less clear variation than the less obstructed ones, and as illustrated in Figure 4.3(d), the differences are mixed up and identical to white noise rather than visible change. In addition, these results were taken using an isolated beacon with complete obstruction (separate room) rather than partial obstruction (different side of a junction).

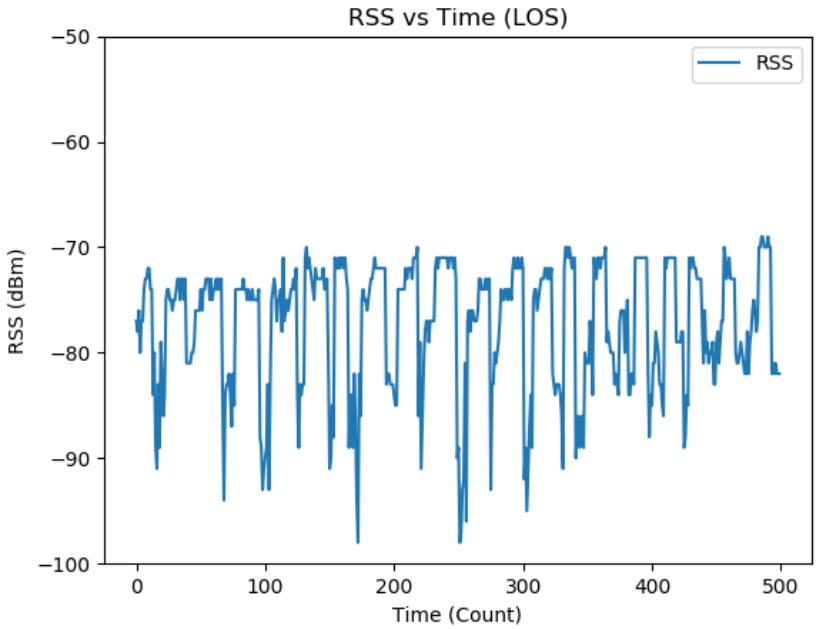

a) The RSS vs time for LOS at a 2 m distance

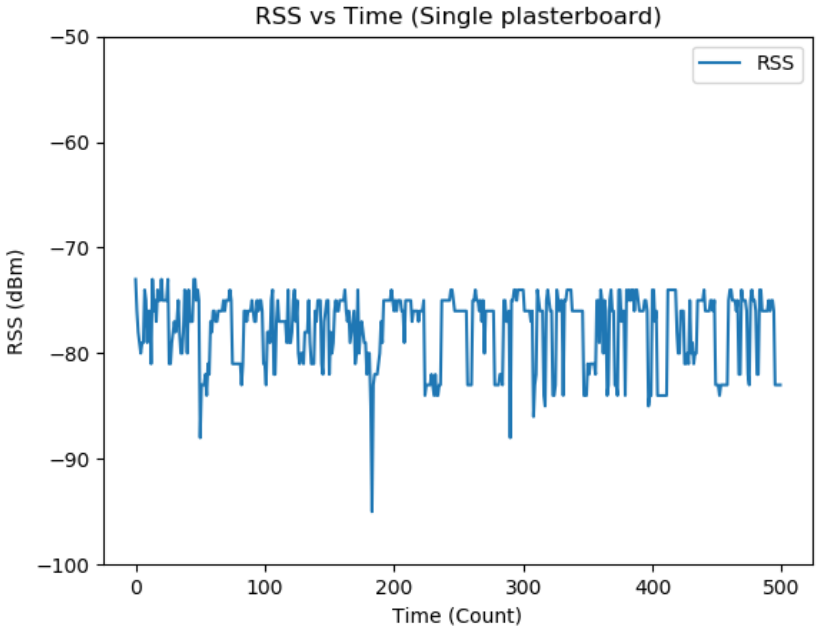

b) The RSS vs time for plasterboard NLOS at a 2 m distance

Figure 4.2: The RSS variation across LOS and single plasterboard conditions

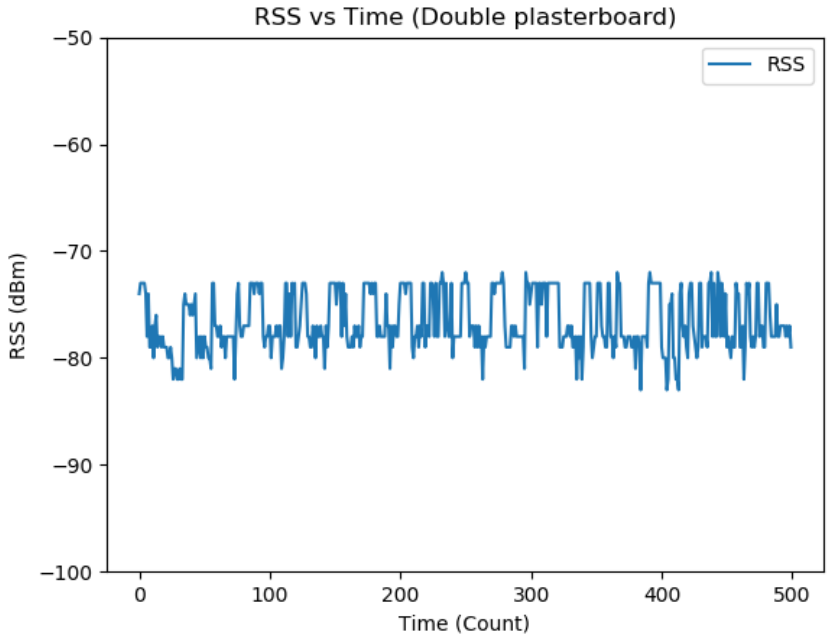

c) The RSS vs time for double plasterboard NLOS at a 2 m distance

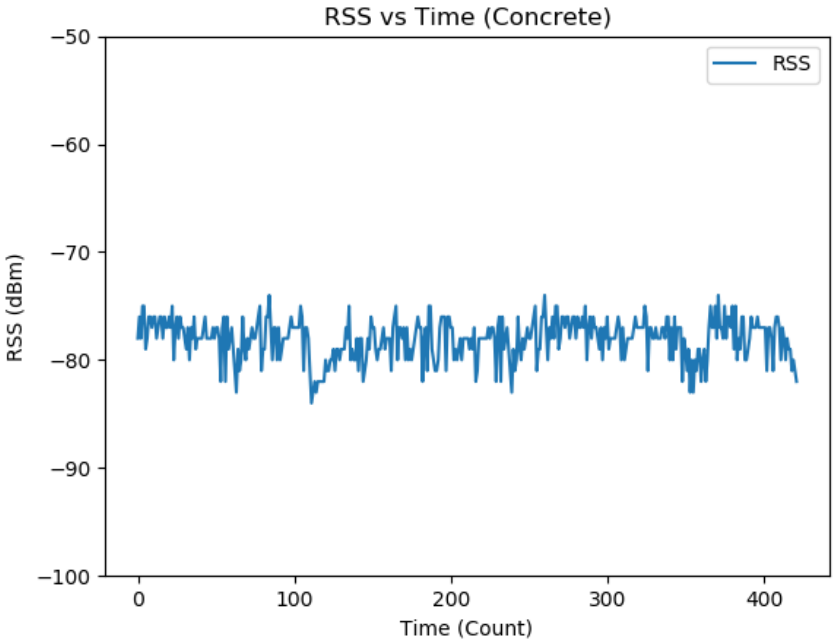

d) The RSS vs time for concrete NLOS at a 0.5 m distance (similar average RSS)

Figure 4.3: The RSS variation across double plasterboard and concrete conditions

4.3. Proposed Algorithm

We performed an experiment to study the relation between the RSS standard deviation and the state of both LOS and NLOS. The experiment was performed using two different beacon manufacturers, namely a Texas Instrument beacon (CC2540DK-MINI) and an Estimote beacon (proximity beacon model), and the RSS readings were recorded using two separate mobile devices: Samsung Galaxy S5 and Samsung K Zoom.

The experiment was performed under three different conditions: LOS, light NLOS obstruction (10 cm plasterboard), and hard NLOS obstruction (26 cm concrete). As this experiment was designed to study the relationship in terms of the RSS, it was important to ensure that the same range of RSS values could be seen from all three conditions. For LOS, the RSS measurements were taken at a distance of 1–7 m. For light NLOS, the distance was from 1–4 m, and for hard NLOS obstruction, the distance was taken from 0.5–2 m.

The RSS measurements were recorded for 10 min, and the readings were divided into groups of 10 RSS readings. These 10 RSS values were used to calculate the standard deviation of the group. The standard deviation results were then further divided into groups of 10 standard deviations to study the distribution of the standard deviation results.

The relation between RSS and the standard deviation for LOS is illustrated in Figure 4.4. The same result for the NLOS counterpart is depicted in Figure 4.5. The standard deviation is plotted against RSS because, as demonstrated by Figure 4.1, Figure 4.2 and Figure 4.3, the LOS-NLOS state relates not only to the standard deviation but also to the corresponding RSS values. The results reveal that for NLOS, the majority of the results have a low standard deviation value that gradually increases when the RSS decreases, as illustrated in Figure 4.5 and Figure 4.6 and is evident in Figure 4.7. The pattern is clearly visible in the hard NLOS condition because this condition obstructs the most signal, thereby causing the most power

loss. On the other hand, the standard deviations of the LOS results are more randomly distributed across the graph. In addition, the chart is drawn relative to the mean RSS, and disregarding the actual distance as in the actual positioning, only the information of the RSS

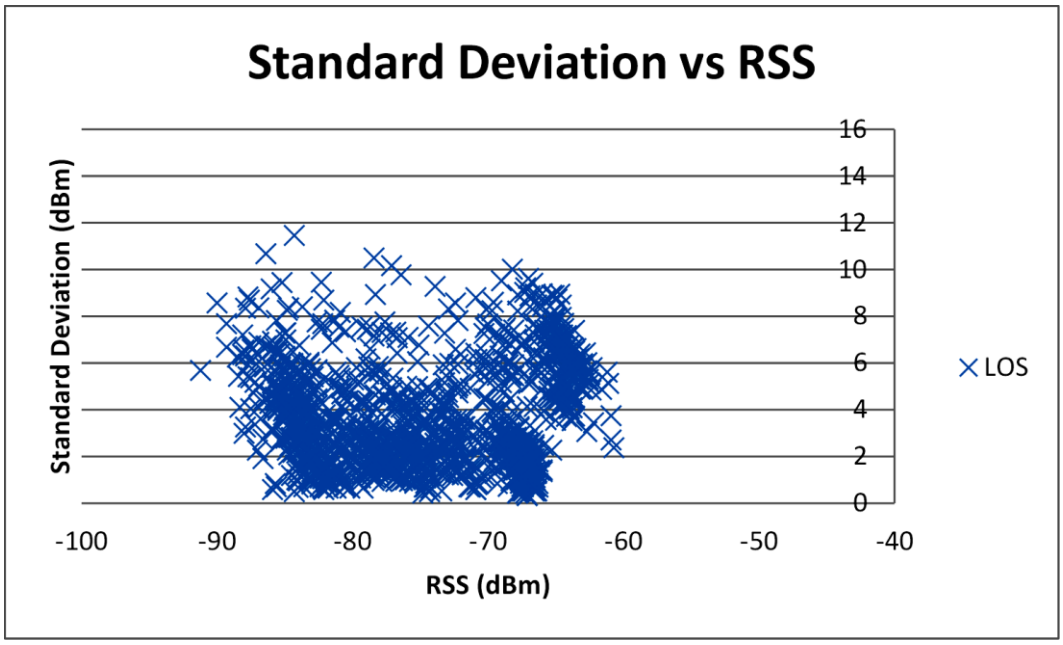

Figure 4.4: Standard deviation of LOS signals

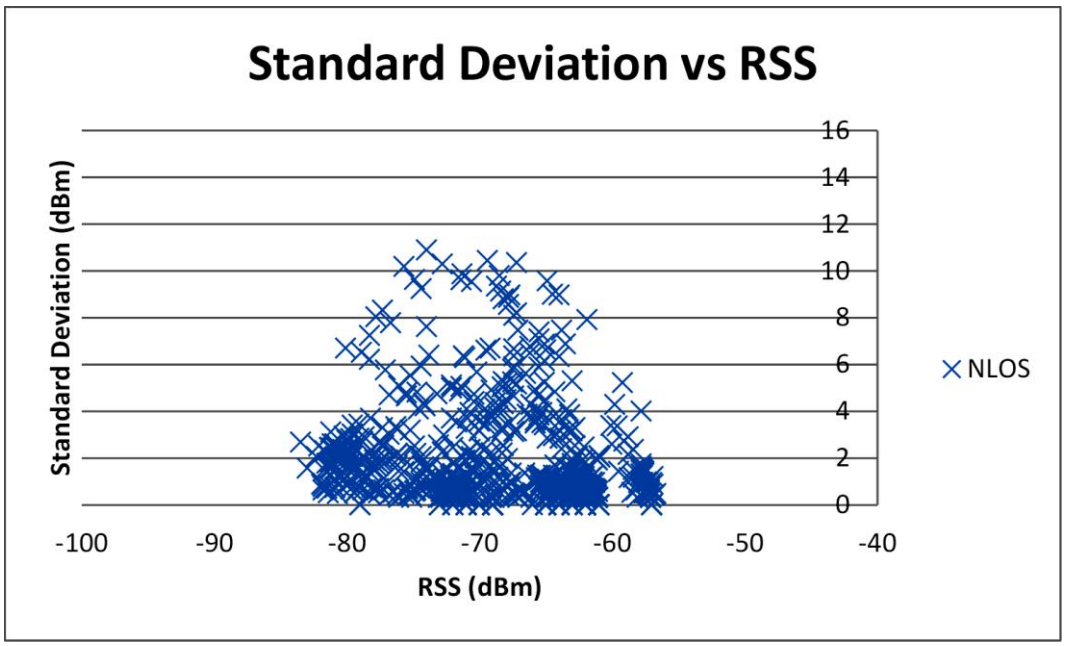

Figure 4.5: Standard deviation of NLOS signals

is available. Distance derived from the RSS might be erroneous, and using this information will only amplify the error.

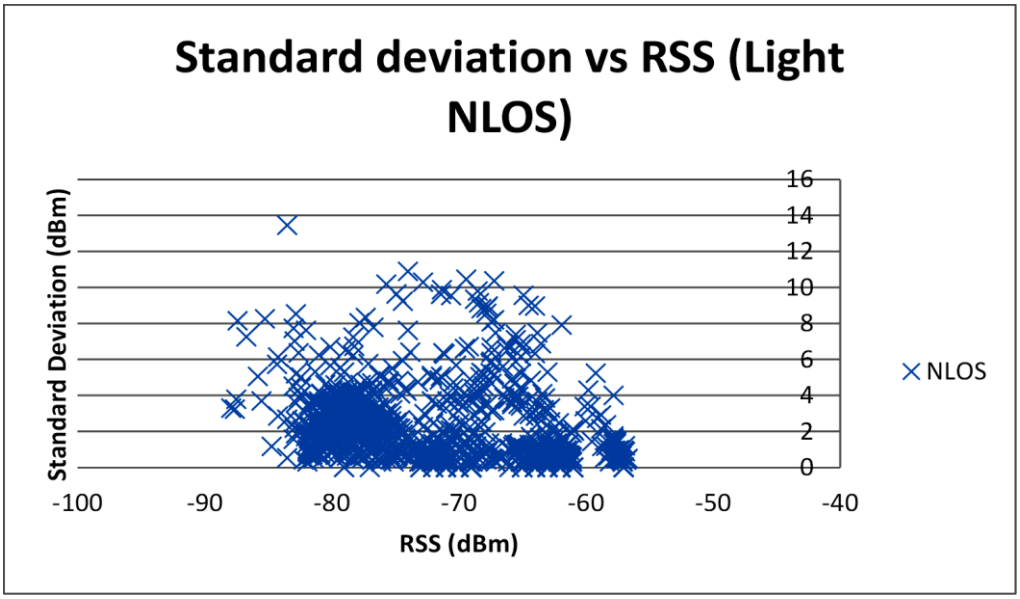

Figure 4.6: Standard deviation graph for light NLOS

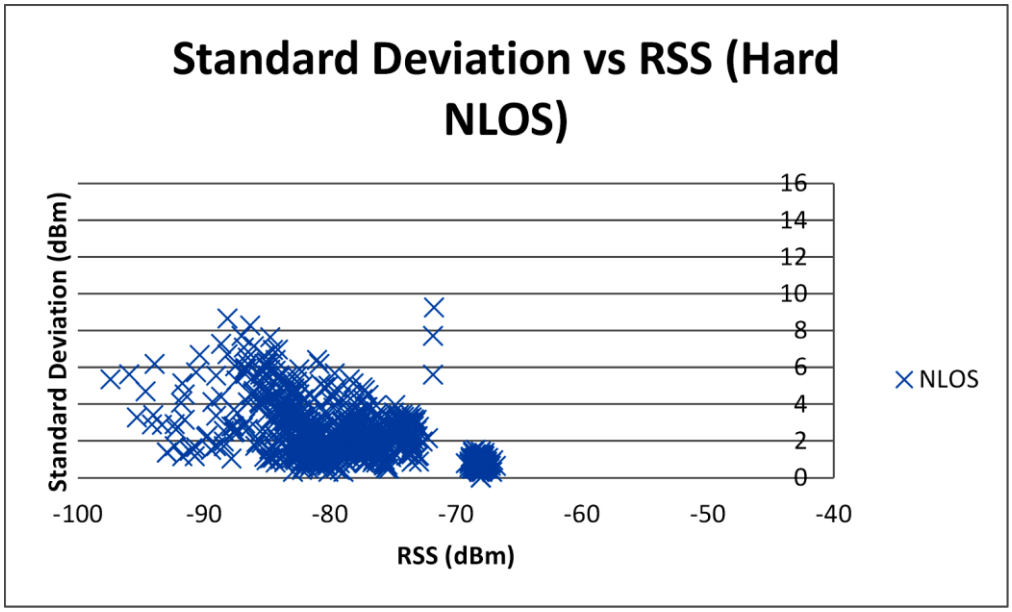

Figure 4.7: Standard deviation graph for hard NLOS

Table 4.1: Estimation result based on linear threshold line

Condition	Estimote Estimation	Texas Instrument Estimation
LOS	81%	70%
Light NLOS	32%	70%
Hard NLOS	65%	76%

The results of light NLOS obstruction and hard NLOS obstruction are illustrated in Figure 4.6 and Figure 4.7 respectively. The figures suggest that the hard NLOS obstruction displays a less random standard deviation value and follows an inverse linear line. In contrast, for light NLOS obstruction, the results are somewhat more random although with less randomness than LOS. The result's variation is because of the thickness and conductivity of the material, which are the main properties affecting attenuation through an obstruction. The differences are related to the degree to which the material affected the attenuation.

Based on the resulting linear regression line of the hard NLOS obstruction, the slope of a linear threshold line can be drawn to differentiate between NLOS and LOS. Hard NLOS was chosen because it exhibited the most significant difference in differentiating NLOS and LOS. As a regression line is meant to balance the value across the graph, the linear threshold line is instead based on the RSS calibration value at 1 m. The linear equation is shown in (4.1):

$$y = -0.1216x - C \tag{4.1}$$

where *C* is the y-axis intersect value required to have the linear line intersect the x-axis at the RSS measured at a 1 m distance minus the window size used to calculate the standard deviation, as indicated in (4.2):

$$C = -0.1216(A + N), \quad N < 40 \tag{4.2}$$

A is the value of RSS measured at a 1 m distance, and *N* is the sample number used to calculate the standard deviation. The y-axis intersect, *C*, is based on (4.2) because the standard deviation probability relates to the distance, as previously mentioned. The signals of users who are further away from the beacon are more susceptible to variations of signal interference and multipath than users who are close to the beacon. As the RSS value varies randomly because of the use of three widely spaced narrow bands, the standard deviation value is largely affected by the higher number of RSS samples.

By using the proposed linear threshold line, the NLOS identification has a 68% probability of estimating the correct condition, with a 67% probability of estimating the right soft NLOS and a 78% probability of predicting the correct hard NLOS.

Separating the results based on the beacons used, we can see the percentage of detection as listed in Table 4.1. An Estimote beacon has a high detection rate to differentiate LOS from hard NLOS obstruction; however, the soft NLOS obstruction resembles the LOS result rather than the hard NLOS obstruction. Compared to the Texas Instrument beacon, all three conditions have a high detection rate based on the proposed linear threshold line. These detection rates demonstrate that this algorithm can be used to differentiate between LOS and hard NLOS obstructions, but it has a mixed result if used against soft NLOS obstruction.

By using 25 of the standard deviation values, a further estimation to identify the NLOS can be performed by using a normal probability distribution function. From the empirical analysis, we found that the resulting standard deviation values form a normal probability distribution with an LOS that resembles the distribution function better than the hard NLOS

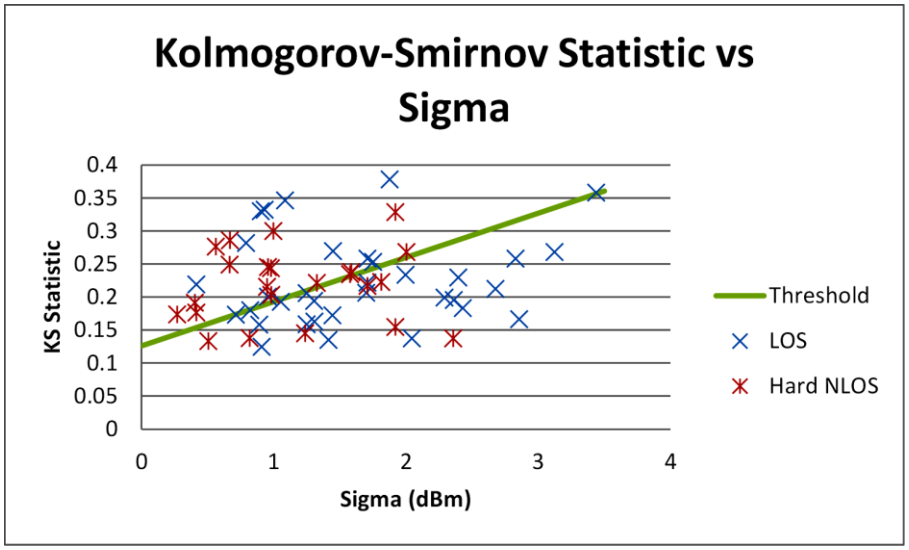

Figure 4.8: Kolmogorov-Smirnov test against normal probability function

obstruction. This similarity is measured based on a Kolmogorov-Smirnov (KS) test. The relation of similarity between both LOS and NLOS and the normal probability distribution is illustrated in Figure 4.8 against the standard deviation, σ, which was used to derive the normal probability distribution function. The blue X marks LOS, and the red star marks hard NLOS.

As the hard NLOS tends to have a lower standard deviation, the overall standard deviation of the group tends to be lower and is because of less variation in RSS. However, in general, most of the results are in the range of 0–2 dBm, where the two conditions are mixed. In this range, LOS has a lower KS statistic. A linear line can consequently be drawn to differentiate LOS and hard NLOS conditions. The linear line is drawn based on the empirical data by connecting the values that comprise the border for the hard NLOS. These results are in (4.3):

$$y = 0.067x - 0.126 \tag{4.3}$$

Based on this equation, there is a 69% detection rate to identify the hard NLOS. The soft NLOS is not included, as it generally follows the result of the LOS condition. As the soft NLOS does not heavily affect the distance estimation, the same distance estimation algorithm as in LOS can be used.

Based on the NLOS identification result, the log-distance path-loss model can be used to estimate the distance. Depending on the result from the NLOS identification, the path-loss exponent can be modified accordingly. As the standard deviation can differentiate the soft NLOS with varying accuracy, and since the KS test can differentiate the hard NLOS, using both techniques allows us to distinguish between the soft NLOS and hard NLOS. However, the detection of the soft NLOS has a limited accuracy, as it depends on the NLOS detection using the standard deviation.

4.4. Impact on Positioning

As NLOS identification is mainly used for positioning, it is important to determine the performance in terms of positioning accuracy. The positioning is performed by using trilateration with the log-distance path-loss model as the distance estimation. The equation for the log-distance path-loss model is shown in (4.4):

$$RSS(d) = RSS(d_0) + 10n\,log\left(\frac{d}{d_0}\right) + X_\sigma \tag{4.4}$$

where $RSS(d_0)$ is the RSS measure at distance d_0, n is the path-loss exponent depending on the environment where the positioning is performed, and X_σ is the zero-mean Gaussian noise with a variance of σ^2. Using 1 m as the reference distance, the equation can be simplified to the following:

$$RSS(d) = A - 10n\,log(d) \tag{4.5}$$

Since a 1 m range is used as the reference distance d_0, A is the RSS measured at a distance of 1 m. The value of the path-loss exponent n depends on the NLOS condition. For LOS, a value of 2.2 was used, while a value of 2.6 was used for NLOS, as suggested by the author in [72].

The positioning test was performed in the Mary Bruck Building at the University of Edinburgh, as illustrated in Figure 3.13. The circle indicates the area used for the experiment. The area has a dimension of 12 m × 12 m divided into several rooms, as depicted in Figure 4.9. The red crosses denote the locations of the beacons, and the blue squares represent the test points' locations. In total, five beacons and 26 test points were used for this test.

The positioning was compared against the algorithm in [77]. The positioning that implemented obstruction detection demonstrated an improvement in the RMSE from 3.77 m to 3.30 m using the proposed NLOS identification algorithm. Figure 4.10 depicts the path

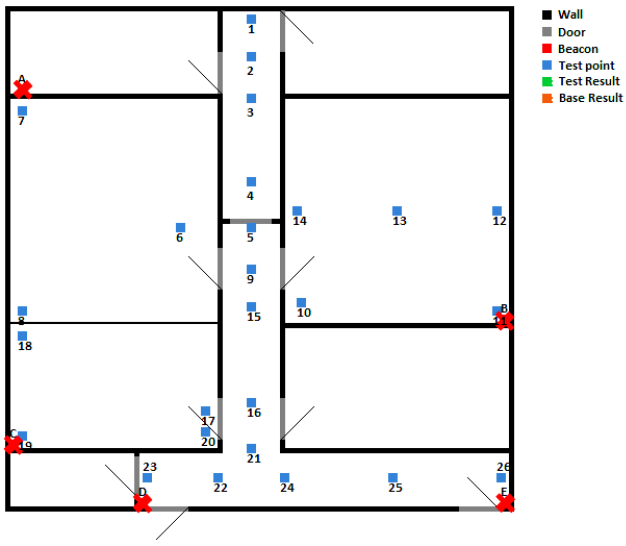

Figure 4.9: Test area floor plan and test layout

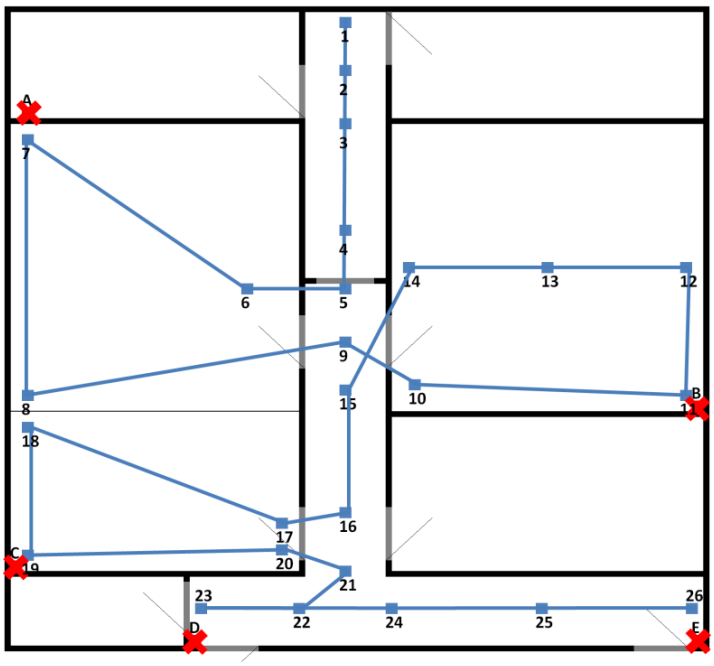

Figure 4.10: Path trajectory of the ground truth

trajectory of the ground truth, while Figure 4.13 displays the resulting trajectory from [77]. Figure 4.14 and Figure 4.15 present the results for proposed algorithm on two different devices: K Zoom and Galaxy S5.

The result reveals varied test point accuracy with a maximum error of 7 m and a minimum error of 1 m. The maximum and minimum errors are similar for the proposed algorithm. This is assumed to be because of the advertisement channel hopping discussed in Section 3.2. This can be seen in Figure 4.11, where the signal from one of the beacons is illustrated. The signal contains three groups of signals; the first group is at time 10–40, the second group is at time 40–80, and the third group is at time 80–120. The probability density function (PDF) generated by this signal is depicted in Figure 4.12. It can be seen that advertisement channel hopping affects the generated PDF, and any information derived from the PDF will also be affected. The proposed algorithm incorporates this issue into the algorithm by having a larger threshold as the RSS lowers. However, the algorithm proposed in [77] assumes a constant signal and only an external source of signal degradation such as attenuation or multipath.

Figure 4.16 illustrates the accuracy of the base and proposed algorithms on both, K Zoom and Galaxy S5 devices. In most of the cases, the proposed algorithm improves the accuracy of the positioning – on average, by 48%.

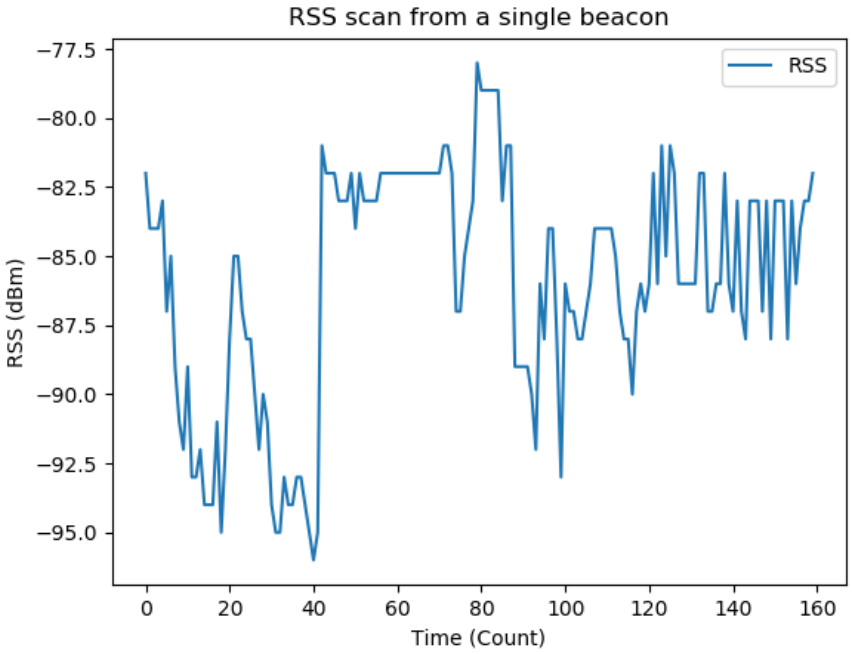

Figure 4.11: Bluetooth low-energy signal from a single beacon with three distinguishable groups

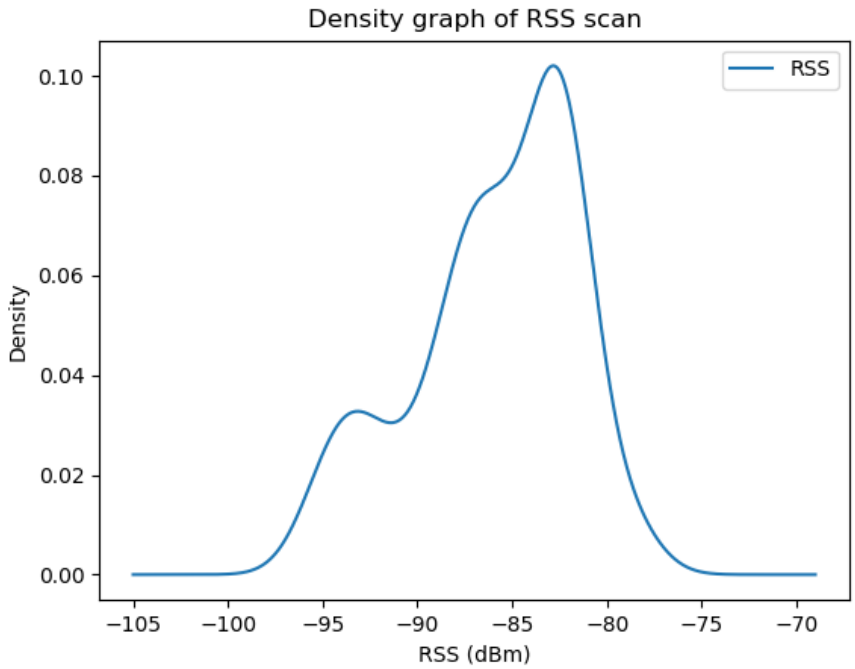

Figure 4.12: Probability density function of the beacon

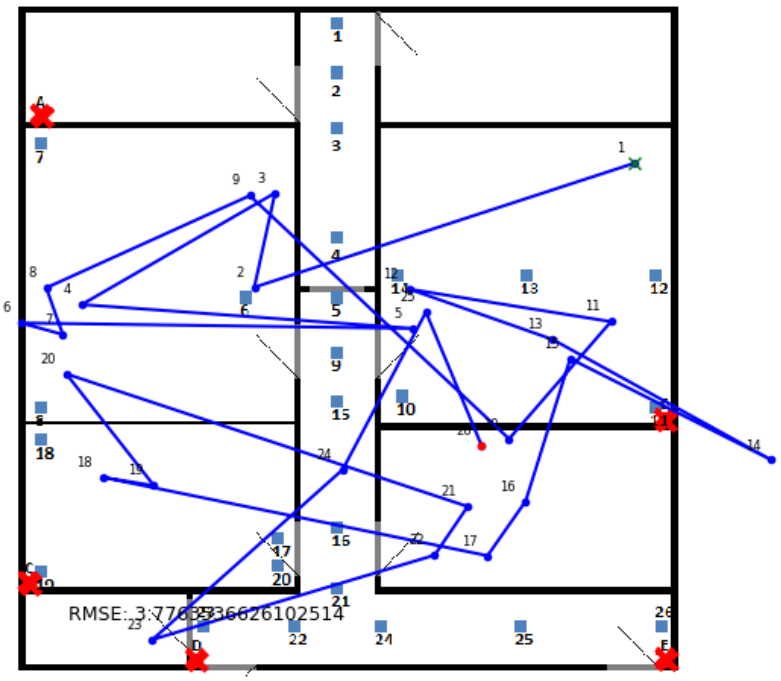

Figure 4.13: Positioning results for Ramadan [76] (3.77 m)

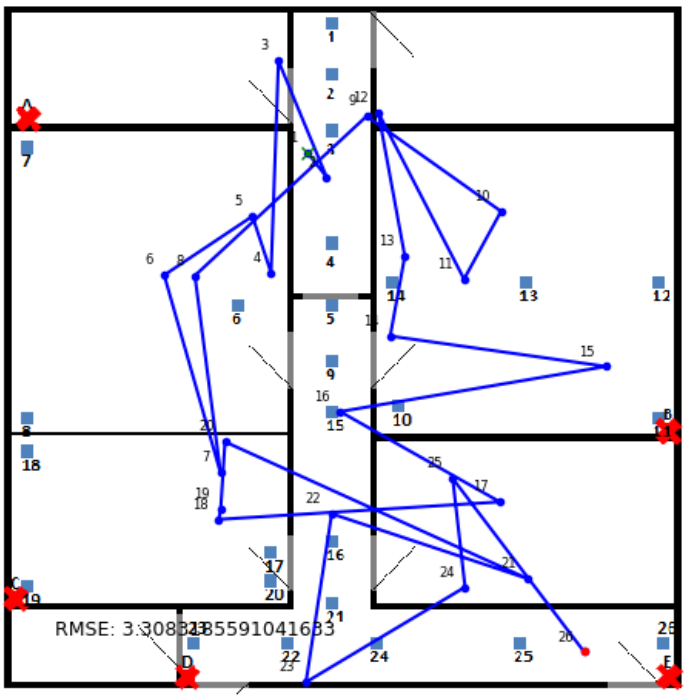

Figure 4.14: Positioning results for proposed algorithm on a K Zoom device (3.51 m)

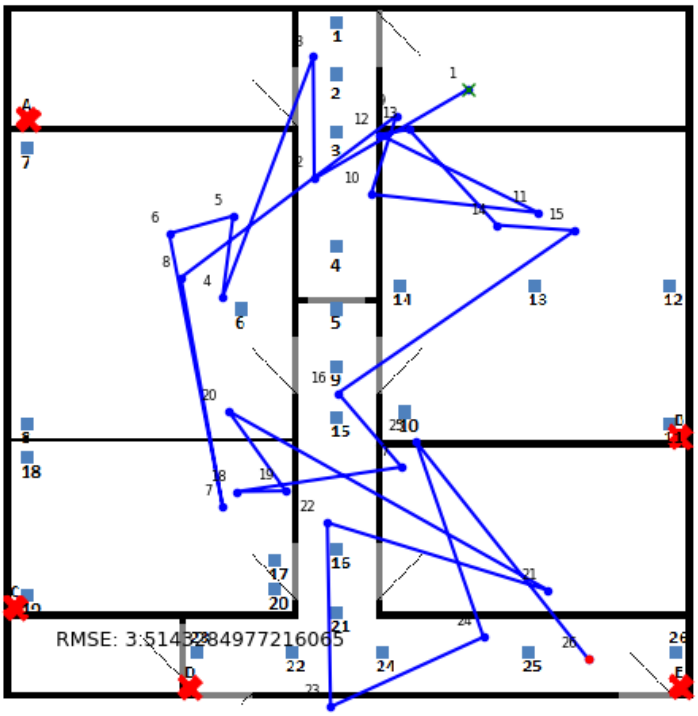

Figure 4.15: Positioning results for proposed algorithm on a Galaxy S5 device (3.30 m)

4.5. Conclusion

This chapter describes another challenge in estimating distance using RSS values caused by external sources. Any obstruction to the signal will cause an attenuation that will change the signal variation. An analysis was shown to highlight the NLOS effect on the selected feature. It was demonstrated that the relation between the selected feature and the NLOS would also consider the information regarding the distance or the RSS. An NLOS identification algorithm was proposed using a dynamic linear threshold that makes use of a beacon's reference signal, which is broadcasted alongside the advertisement signal. The proposed algorithm was tested alongside another state-of-the-art algorithm, and it demonstrates comparable performance. The proposed algorithm yielded a better result in several test points. This occurred because the algorithm in [77] did not anticipate the advertisement channel hopping, and this affected the feature used.

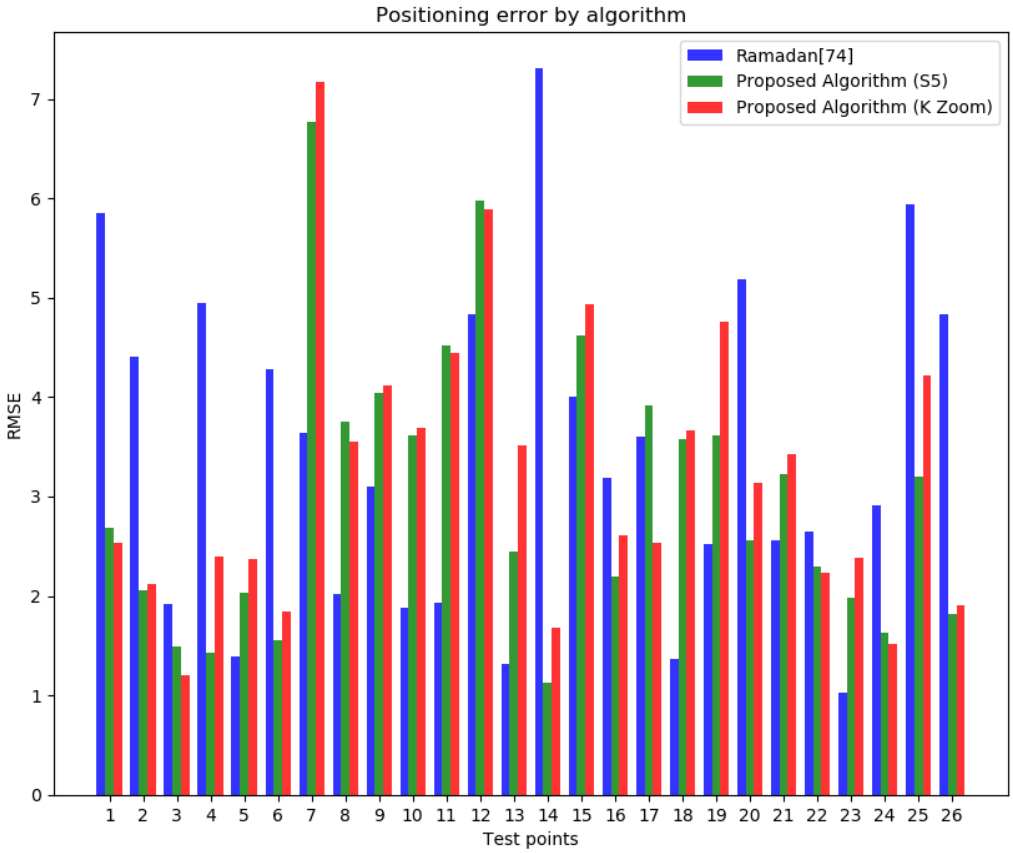

Figure 4.16: Positioning error for both algorithms

5. Directional positioning algorithm for automatic Bluetooth Low-energy beacon mapping

5.1. Introduction

The previous chapter explained the challenges in estimating distance based on RSS because of external signal disturbance, and an algorithm was proposed to detect the effect of obstruction on the RSS values. The detected signal condition allows for more accurate distance estimation, which in turn allows for a better manipulation of the estimated distance.

As one of the challenges in BLE beacon implementation is related to the beacon's deployment, this chapter proposes an algorithm to reduce the calibration for that deployment. This will increase the viability of the BLE beacon's positioning, as compared to Wi-Fi-based positioning.

5.2. Beacon Mapping

Several beacon placement strategies have been proposed, such as in [83], [84], [85], [86], and [87]. These proposed algorithms demonstrate the importance of a beacon's placement. It is even more necessary to know the exact location of each beacon if a triangulation or trilateration algorithm is to be used. This need to know the specific beacon location also translates into a demanding calibration process.

The placement of the beacons was traditionally done by determining the position of the beacons and placing them exactly at the determined position. Any discrepancy in the determined position and the placement would result in an inaccurate estimation for any algorithm that requires the position of those beacons. The other solution is based on placing

each beacon and then recording its exact position. These solutions require a high calibration, which could be costly.

A self-beacon-mapping algorithm would be able to reduce the calibration, so that only the calibration of the first few beacons would be required to establish the initial positioning, while the rest of the beacons would be calibrated automatically, such as in [88] and [89]. The algorithm in [88] focuses on the placement of beacons with the initial locations known, effectively proposing a beacon placement strategy. An initially known location is called a reference node, whereas unknown location beacons are called blindfolded nodes.

Q. Shi et al. [89] have proposed a technique to locate blindfolded nodes. The method proposed in [89] suggests obtaining the probable region from a pair of referral nodes. Based on the proximities between the blindfolded node and reference nodes 1 and 2, and the proximity between these two reference nodes, the probable region is determined. Several iterations of these steps are performed, and the position of the blindfolded node is determined by the mid-location of the overlap of all the probable regions.

The use of a trilateration algorithm is a simple, common solution for locating a beacon. A standard trilateration process to detect a mobile device's position would require the information of several beacons' locations and their RSSs. Meanwhile, a trilateration to detect each beacon's position would require the information of several users' positions and the beacons' RSSs at those locations.

Figure 5.1 displays the circles for a trilateration algorithm. For this algorithm to detect a mobile device's position, points A, B, and C will be the positions of the beacons used or the reference nodes. The circles radiating from these points are the estimated distances from the beacons, and the mobile device's position is located at the intersection of the three

circles. If the same trilateration algorithm is applied to detect a beacon's position, then points A, B, and C will be the positions of the mobile device when reading the signal from the beacon. The circles radiating from these points are the estimated distances from the beacons. As previously mentioned, the beacon's position is located at the intersection of the three circles.

This demonstrates that trilateration can be used to detect not only a mobile device's position, but also a beacon's position if the roles are reversed. However, as RSS is known to be unstable, it tends to be affected by errors. Furthermore, the erroneous result could also cause the overlapping size to be large, which can be deemed an uncertain result, as illustrated in Figure 5.2. In a standard trilateration implementation, almost the entire area of circle A is deemed to be the possible location of the beacon. However, that would make the RSS readings from B and C redundant, as none of the RSS values from B and C are taken into consideration to determine the position.

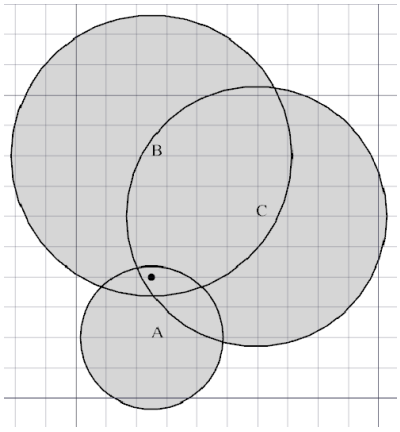

Figure 5.1. Circles for trilateration

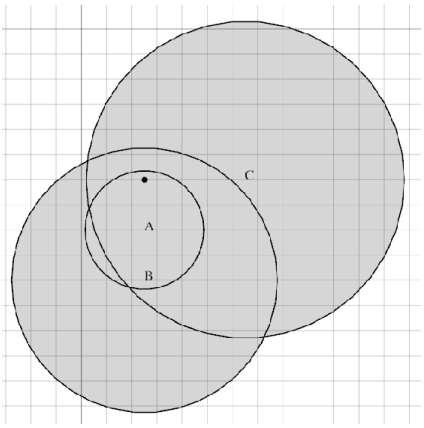

Figure 5.2. Trilateration with erroneous RSS

5.3. Automatic BLE Beacon Mapping

Automatic BLE beacon mapping consists of two parts. The first part, named non-reliable RSS detection, is used to determine the signal reliability and set an expected error based on the distance from the RSS values. The second part, called the directional detection algorithm, will use the expected error from the first part to create a directional area where the beacon is possibly located.

5.3.1. Non-reliable RSS detection

Based on the distance calculated from the RSS value, a probability weight can be assigned to the RSS signal. This probability weight is assigned based on the distance because the greater the distance from the beacon, the less reliable the RSS becomes. Further than a certain distance, the RSS is highly susceptible to interference, multipath, and obstruction, all of which would affect the RSS's reliability.

Table 5.1 lists the probability weight and its fulfilment condition, where the symbol *d* is the distance of the probability weight fulfilment. The probability weight was derived from the RSS of the measured distance. Thereafter, Table 5.2 presents the results for RSS readings at multiple distances from a beacon. The readings were taken in a large hallway in the Sanderson Building, King's Buildings, University of Edinburgh.

Table 5.1. Non-reliable RSS detection

Probability Weight	Condition
High	$d > 2.2$ m
Medium	$2.2 \text{ m} < d < 6$ m
Low	$6 \text{ m} < d < 15$ m
Unreliable	$15 \text{ m} < d < 20$ m
Error	$d > 20$ m

Table 5.3. Beacon's RSS reading in a shopping mall

Distance (m)	Mean RSS (dBm)	Est Distance (m)	Error (m)
1	-59.8	1.625965	0.625965
2	-65.2667	2.229195	0.229195
3	-71.6333	5.033289	2.033289
4	-70.8	4.524343	0.524343
5	-74.2	6.989473	1.989473
6	-78.7333	12.48235	6.482348
7	-81.0667	16.82387	9.823871
8	-79.8667	14.42977	6.429765
9	-79.3333	13.47813	4.47813
10	-79.3333	13.47813	3.47813

Table 5.3 presents the same test done in a large open space in Overgate Shopping Mall, Dundee. The estimated distances in these tests were calculated using a log-distance path-loss equation, with a path-loss exponent n of 1.8 and the RSS at a 1 m distance A of -56 dBm.

Based on Table 5.2 and Table 5.3, the high probability weight is given up to 2.2 m because at a close distance to the beacon, the RSS signal will be strong and less susceptible to anything affecting it. Even if an error exists with the RSS signal, it will tend to be small and will still be

within an acceptable range. Within this distance, the error would usually be less than one metre.

The medium probability weight is given at a distance of 2.2–6 m because within this distance, the error occurs inconsistently, and some accurate readings can still be made. This is demonstrated in Table 5.2 and Table 5.3. In both tables, for distances between 2 m and 6 m, the errors are generally small, with several cases having errors of less than one metre.

Furthermore, based on Table 5.2 and Table 5.3, for distances larger than six metres, the probability weight is set low because at this distance, the errors occur consistently with significant error values. Nevertheless, RSS readings at this distance are still useful for estimating distance because, in most cases, the error is within the usable range. The upper limit is set at 15 m, as this distance is generally the reliable distance and range limit for some manufacturers [90].

Distances between 15 m and 20 m are deemed unreliable. However, they remain in the possibility weight, as some erroneous RSSs from the upper bound of a low priority weight could reside in this distance range and still have a usable estimation.

A distance longer than 20 m is deemed to be an error because it is highly susceptible to many external factors given the large span. Furthermore, at this distance, the RSS-to-distance ratio is high, where a 1 dBm RSS would displace the distance for up to three metres. This would cause even a small RSS inconsistency to result in a large error in the distance estimation calculation.

5.3.2. Directional Positioning Algorithm

The directional positioning algorithm is designed based on the idea that the RSS is unstable, and the estimated error thus needs to be considered. This algorithm focuses on

generating possible regions instead of pinpointing them, as this will lessen the effect of erroneous RSS readings. This algorithm assumes that an initial positioning algorithm is available, using other reference nodes or other techniques and technologies altogether.

Directional beacon positioning has been done previously, such as in [91] and [92]. However, the solution provided in these papers would a require an antenna-specific beacon, which is a directional antenna. In the proposed algorithm, the focus is on making use of the RSS and its reliability to create a cone shape of a possible position in the direction of the actual point, instead of the usual circle.

In this algorithm, RSS readings of the beacon to be located are taken at two different points, known as RPs, and labelled as RP A and RP B, as in the example illustrated in Figure 5.3. Depending on the estimated distance, based on the RSS value read at RP A and RP B, a probability weight is assigned to each point according to non-reliable RSS detection. The point with the lower RSS, which is RP B, will be used as the base and directed towards RP A.

Thereafter, three additional region circles are drawn, with two additional circles for RP B called the B inner circle and the B outer circle and one additional circle for RP A called the A outer circle, as depicted in Figure 5.3. The distance gap between the main circle and the inner or outer circle is determined by the priority weight assigned earlier. The gap distance is ±0.5 m for a high priority weight, approximately one metre for a medium priority weight, and approximately two metres for a low and unreliable priority weight. If the RP priority weight is an error ($d > 20$ m), then it should not be used in this algorithm.

Two pairs of lines are then drawn from the base, which is RP B, towards the intersection of the B inner circle with the A circle and the intersection of the B outer circle with the A circle. One pair will face in one direction, and another will face the opposite direction. Figure

5.3 presents the line example of a single pair. If the angle between the paired lines is smaller than 5°, then the A outer circle will be used instead of the A circle. This is to allow for an adequately sized region to be generated. If either the B outer or the B inner circle does not touch the A circle, then the line will pass through RP A instead, as illustrated in Figure 5.4. The region within the lines pairs is considered the possible area for the beacon, as indicated by the dark region in Figure 5.3.

This algorithm can be performed iteratively with several different RSS reading points. The possible regions are then laid on top of one another, and the midpoint of the region, where all or most of the regions overlap, is considered to be the beacon's position. This algorithm can also be combined with other algorithms to further reduce the possible region size.

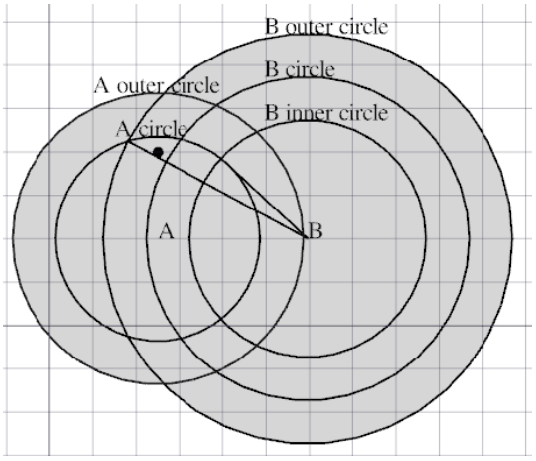

Figure 5.3. Directional positioning

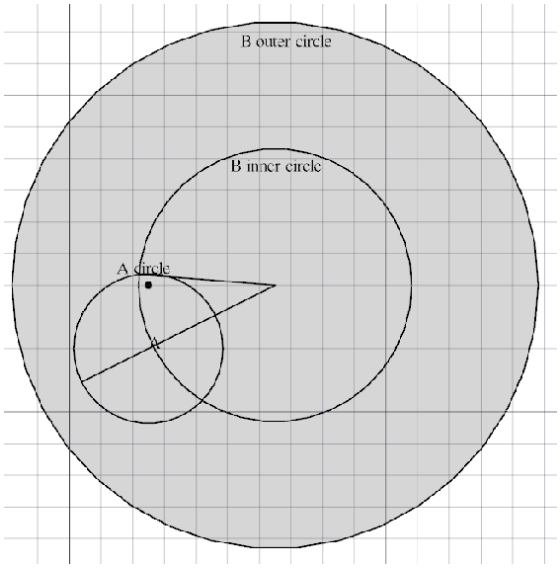

Figure 5.4. Non-overlapping B outer circle

5.4. Implementation Results

The directional positioning algorithm was implemented and tested using the Texas Instrument BLE beacon (CC2540DK-MINI) and a Samsung Galaxy S5. The beacon was placed at one location, and several RSS readings were taken in the area surrounding the beacon.

Figure 5.5 depicts the implementation of the directional positioning algorithm with six RPs: A and B1 to B5. The latter five were set so that they were at different angles to the beacon's position with A as the RP. On the one hand, B1 and B3 cast a wide direction angle that is as large as half of the circle A. On the other hand, B2, B4, and B5 cast a smaller direction angles. The result indicates that the beacon is within the possible location of all five regions. If all five regions are used to determine the beacon's position, then the error is only 0.03 m.

This algorithm can also be used in conjunction with other algorithms. Figure 5.6 presents the directional positioning algorithm used together with a trilateration algorithm. If trilateration is used on its own, then the error would be 0.55 m, whereas if it used together

with the directional positioning algorithm, then the error is only 0.26 m. This demonstrates that this algorithm can further improve the results of other algorithms.

Another implementation test was also conducted with six random RPs. These RPs were recorded, and RP A was reused from the previous implementation. One region did not manage to estimate the correct beacon's position, with another RP failing to provide a possible region owing to the distance estimation error being too large, with an approximate seven-metre error.

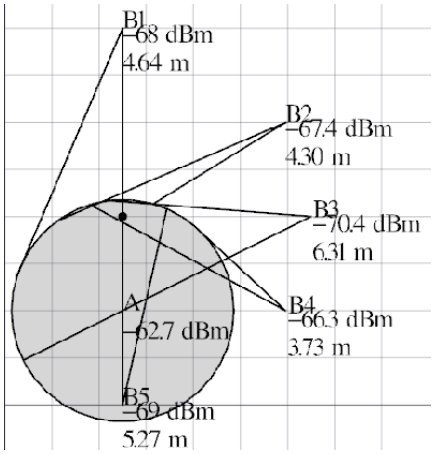

Figure 5.5. Implementation with six points

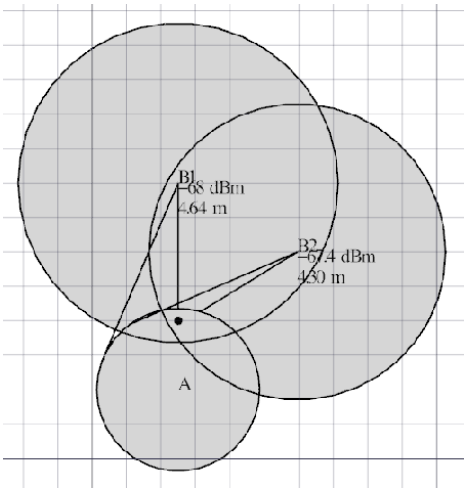

Figure 5.6. Directional positioning with trilateration

This algorithm works by encompassing the beacon's position in the possible region. It is important for this algorithm to ensure that the beacon's position is always within the possible region. In the overall result, 90% of the regions encompass the beacon's position. This further proves the algorithm's usability for the estimation of a beacon's position.

5.5. Conclusion

This chapter described the challenge of high calibration required for BLE beacon positioning. Each BLE beacon's placement needs to be precisely recorded to obtain the best result and estimation for positioning. A common solution to map the beacons and several solutions to reduce the calibration required for beacon deployment were discussed. An algorithm called non-reliable RSS detection was proposed to estimate the reliability of a signal and to subsequently use that signal to estimate the error. This has the advantage of expecting a certain error to adjust for the signal's error. An algorithm for directional positioning was propose by using the reliability of a signal. The proposed algorithm will lessen the probability area size, which will cause a lower average error. The implementation demonstrates that the proposed algorithm is able to improve the probability area of an actual position.

6. Crowdsourced BLE Beacon Mapping

6.1. Introduction

The previous chapter discussed the challenges that BLE positioning faces; they are mainly related to the laborious calibration needed. The previous chapter also proposed a mapping solution to detect the location of a beacon.

As the process of mapping an unknown beacon is a laborious task, this chapter proposes a crowdsourced BLE beacon-mapping system, which allows for the mapping of unknown beacons in an area with partially known beacons. Crowdsourcing is a low-cost and efficient way in which to collect large data through crowd participants [93]. For a number of crowdsourced indoor positioning approaches, the users are also the database constructors [70].

6.2. System Architecture

The system has three main phases: the online positioning phase, the beacon-mapping phase, and the offline positioning phase. The online positioning phase involves the attainment of an instant or real-time position, which can be returned to the user as the position. The user's position will be recorded alongside its BLE scans, and with that, a fingerprint can also be performed using this record if needed. This position will thus be named the 'fingerprint point' (FP). In this phase, the intention is to collect the fingerprint position with BLE scans to map unknown BLE in a range. In the next phase, which is the beacon-mapping phase, the beacon location is mapped using the detected positions as the RPs. In this phase, unknown beacons are mapped, and non-calibrated known beacon details are updated. The final phase, namely the offline positioning phase, involves processing the

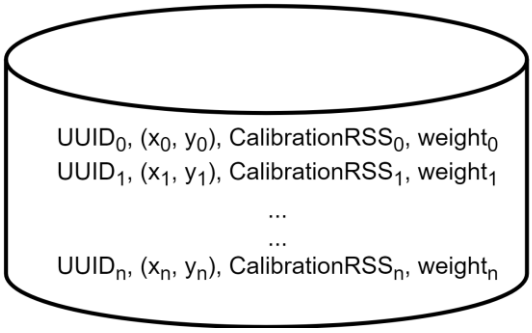

Figure 6.1. Structure of BLE beacon database

remaining BLE scans that cannot be used in the online positioning phase, because of the lack of known BLE beacons in the range to be used as RPs.

6.2.1. Online Positioning Phase

The online positioning phase is utilised to obtain a user's location by making use of any available information. In this implementation, the available information is the location of several known location beacons among a combination of known and unknown beacons.

For the online positioning phase, the user's position, which will be recorded as the FP position, is calculated using the information of the known beacons. Each of the known BLE beacons will have a position weight associated with it. This weight helps to determine the maturity and reliability of the beacon's position, and manually calibrated beacons will have a high weight value. It is also important to record the calibration value of each beacon because this value is needed to estimate the distance. The calibration value is the beacon signal recorded at a reference distance, generally at 1 m. This value is provided in the transmitted signal from BLE beacons using the iBeacons protocol. The BLE beacons using the Eddystone protocol have calibration values recorded at 0 m and need to calculate the estimated calibration value at 1 m. This can be done by subtracting 41 dBm from the calibration values recorded at 0 m, as defined by Eddystone-UID in the Eddystone Protocol

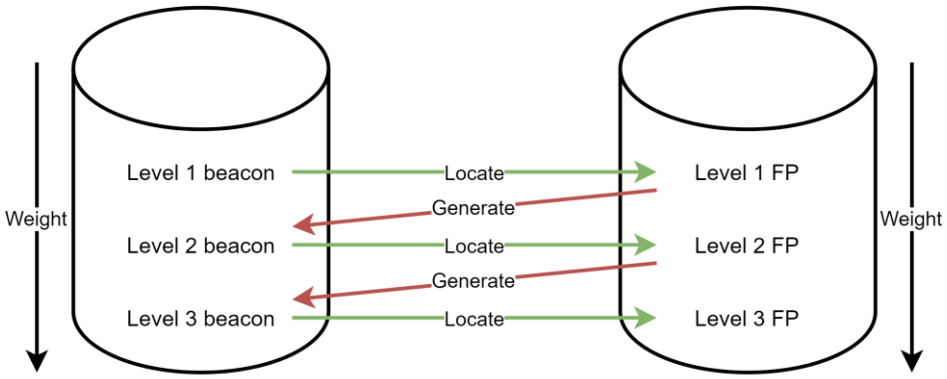

Figure 6.2. Relationship between Beacon level and FP level

Specification section [57]. The structure of the BLE beacon database is illustrated in Figure 6.1.

The scanned BLE signals are the data recorded from a user's mobile device. These signals are used to calculate the FP position using a lateration algorithm based on the list of known beacon information. To allow for reliable positioning, the scanned BLE signals needs to be filtered to minimise any error from unreliable scans. The BLE scans are first filtered using the filter proposed in Section 3.3; The filter is based on the RSS value or distance. Only beacons with RSS values higher than a predetermined threshold value will be used for positioning. The filter classifier can also be changed to use the estimated distance from the beacon given that the distance is smaller than a predetermined threshold.

It is also important to filter the known BLE to ensure that only the BLE beacon with a reliable position will be used. This is fine for the first iteration of the FP positioning when all data inside the BLE beacon database only include the calibrated beacon position; however, after a number of iterations, a number of beacons will have positions generated from the estimated FP position. The calibrated beacon is named a Level 1 beacon, and the FP position – called a Level 1 FP – is calculated using the Level 1 beacon. Based on this naming, beacons

generated from Level 1 FPs will be called Level 2 beacons. Furthermore, several other beacon positions will be generated from the level 2 position with less reliability, and they will be termed Level 3 beacons. This naming process is depicted in Figure 6.2. The more a beacon is generated using a higher-level FP, the less reliable the beacon position will be. This is captured in the weight information from the database, and with this information, the BLE beacons to be used for FP positioning can be filtered to include only beacons with a reliable position. This is done by filtering the list of known BLE beacon positions to be used for FP positioning to display only beacons that have an adequate weight value for implementation. The above-mentioned filters only filter the beacons to be used but do not remove them from the database. This is to allow for a lower-weight beacon to be improved when more data are available.

Using the filtered beacons from the database and the filtered scans, the position of the FP is then calculated if a sufficient number of remaining BLE scans are available for positioning. In the case of inadequately known BLE scans to perform the positioning, the BLE scans will be kept in a separate database referred to as the unprocessed scans database. The unprocessed scans will be used in a later phase after a sufficient number of BLE beacons are built in the databases. In this implementation, the position is calculated using the lateration technique with RSS as the distance estimator. The lateration is calculated using linear least square, as discussed in Section 2.2.3. The output FP position's weight is the adjusted mean of the BLE beacon's weight used in determining the position:

$$W_p = \frac{\sum_{i=1}^{n} w_i}{n} * C_{FP} \qquad (6.1)$$

W_p is the output FP position's weight, and w_i is the beacon's weight. Furthermore, n is the number of beacons used in determining the position. Finally, C_{FP} is the FP position weight coefficient, which is meant to define the degree to which the beacon's weight will affect the positioning weight. The value for C_{FP} is set to 0.6 to get the lowest RMSE value based on Figure 6.3. The equation demonstrates that even using less reliable BLE beacons, given a sufficient number of beacons, the returned FP position can still be used. For an FP position that is determined using only unreliable BLE beacons, a large number of beacons would be required to make the FP position usable, and based on the deployment density of the beacons, the unreliable FP position can even be filtered out. This step is important to ensure that any error amplified by the increasing number of beacons used will be limited to a certain predetermined value.

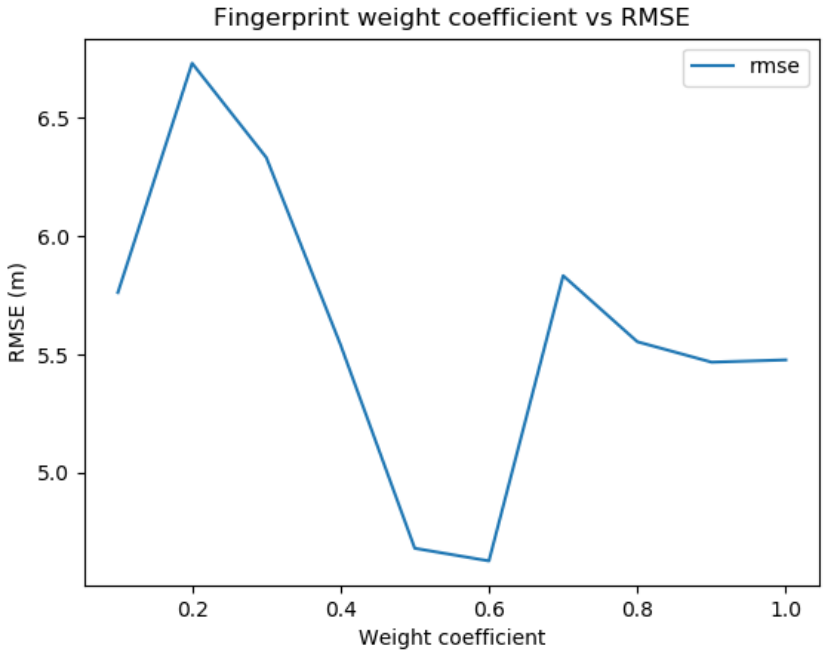

Figure 6.3. Fingerprint weight coefficient against RMSE. The best coefficient is the one with the lowest RMSE.

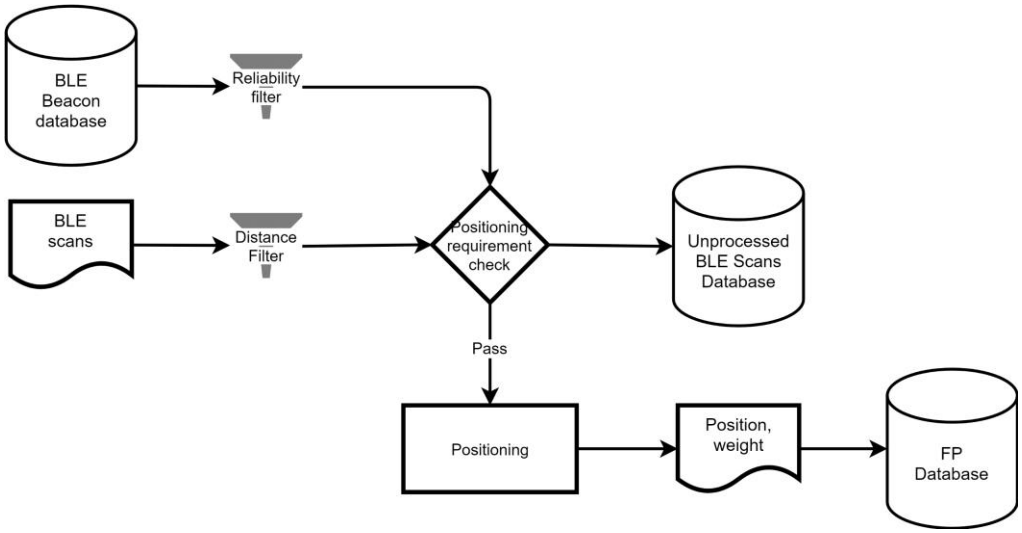

Figure 6.4. Online positioning phase

The calculated user's position will be recorded in the FP database. The built FB database will then be used in the next phase to estimate the position of the BLE beacons. The complete online positioning phase is illustrated in Figure 6.4.

6.2.2. Beacon-Mapping Phase

The beacon-mapping phase involves determining or updating the position of an unknown or low-weighted beacon. For this phase, the non-calibrated beacon's position will be estimated using a Level 1 FP or higher. The position of a Level 1 or higher FP is an estimated position, and it thus contains some errors because of the estimation process. Estimating a beacon's location using a position with some errors will cause the error to be amplified if not dealt with properly. Therefore, it is important to filter which FP position should be used for the mapping. By default, the position generated by a Level 1 FP should always pass the filter. Similarly to the online positioning phase, the filter is based on the FP position's weight and the RSS or distance of the beacon to be located.

Any FP that passes the filter will be used to estimate a beacon's position. In this phase, the mapping algorithm used will be based on the algorithm proposed in Section 5.3. In this phase, the equation to calculate the position's weight is the same as (6.1); however, it uses its own coefficient C_b, which is the beacon position weight coefficient. The beacon position's weight requires a different coefficient to further reduce the weight to avoid amplifying the estimation error. The current value of C_b is set to 0.1 to further reduce the weight, which can be introduced by the lower reliability of the beacons. Furthermore, $C_b$of 0.1 yield the lowest RMSE as shown in Figure 6.5.

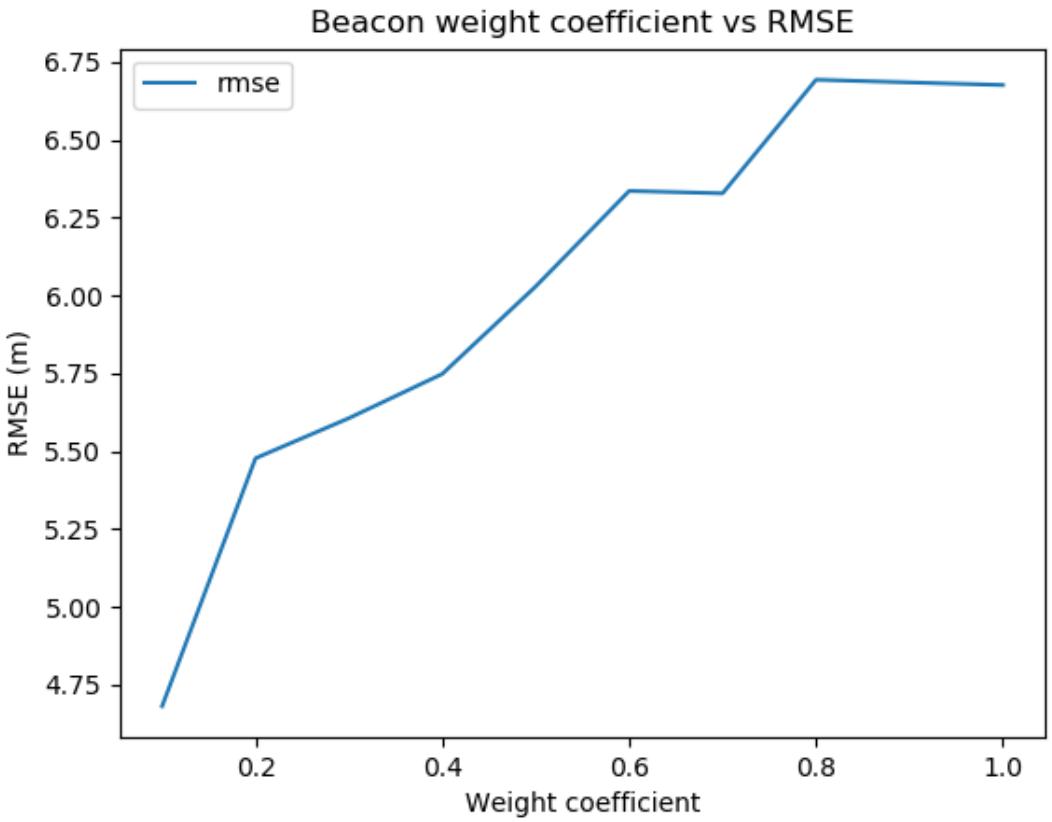

Figure 6.5. Beacon weight coefficient vs RMSE. The best coefficient value is the one with the lowest RMSE

If the beacon position is already in the BLE beacon database, then the position's value and weight will be updated. The position is updated based on the ratio of its weight in the database and the newly estimated position. This is demonstrated in (6.2):

$$P_b = \frac{(p_{db} * w_{db}) + (p_c * w_c)}{w_{db} + w_c} \quad (6.2)$$

where P_b is the updated beacon's position, p_{db} is the beacon's position recorded in the database, p_c is the calculated position, w_{db} is the beacon position's weight, and w_c is the calculated position's weight. The beacon position's weight is then updated using the sum of both weights. Furthermore, the position assigned is based on a ratio to allow the beacons in the database to be updated using an additional position and to emphasise the position to be used using the one with better reliability. The beacon-mapping phase steps are presented in Figure 6.6.

6.2.3. Offline Positioning Phase

The offline positioning phase is a phase to calculate the position of unprocessed scans. The process in this phase resembles the one in Section 6.2.1; however, it uses the BLE scans from unprocessed scans as the input. This phase is an offline phase and is thus used only for

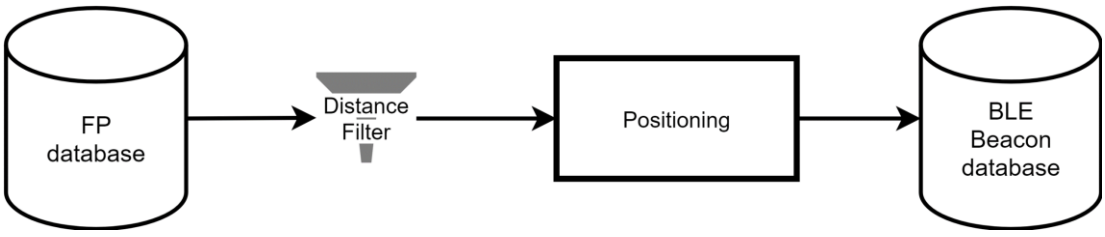

Figure 6.6. Beacon-mapping phase

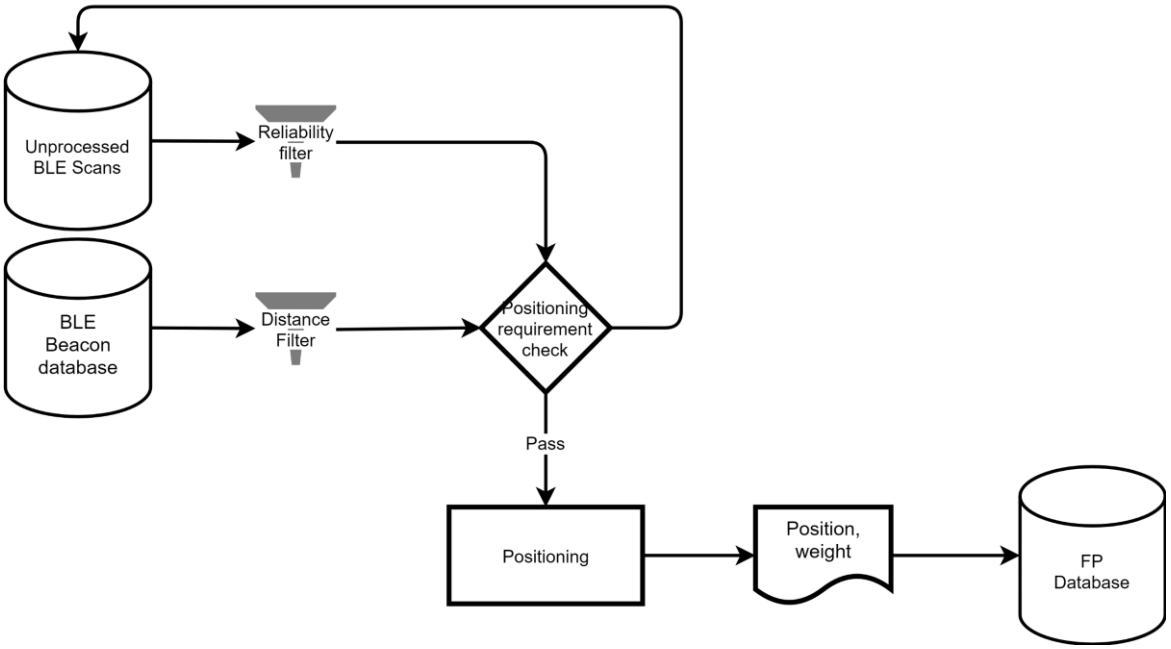

Figure 6.7. Offline positioning phase

building the BLE beacon database. This phase also uses the same parameter setting as set in Section 6.2.1. The complete steps for the offline positioning phase are depicted in Figure 6.7.

6.3. Implementation

To determine the effect of the proposed system, the complete system was implemented. The BLE scans were recorded using an Android application written for this purpose. The application records the BLE at low latency or at the fastest scan mode; however, it is not necessary for the system's implementation. Moreover, the application records the timestamp, mac address, RSS, and calibrated RSS at 1 m. For the calibrated RSS at a 1 m distance, the application will utilise the measured RSS value from beacons using the iBeacon protocol, and it will convert the value of the measured RSS at a 0 m distance for beacons using the Eddystone protocol. The device used in this implementation is a Samsung Galaxy S5 smartphone running Android Marshmallow version 6.0.1.

The system was implemented in an office space on Princess Street in Edinburgh. The floor plan of the office space with a total of 20 pre-deployed beacons is illustrated in Figure 6.8. The deployment of the beacons is not specific to this system. The 20 beacons used in this implementation are of the Estimote brand with a mix of proximity and location beacons [94], and seven of them were recorded as the initial known BLE beacons to be used to build the Level 1 FP.

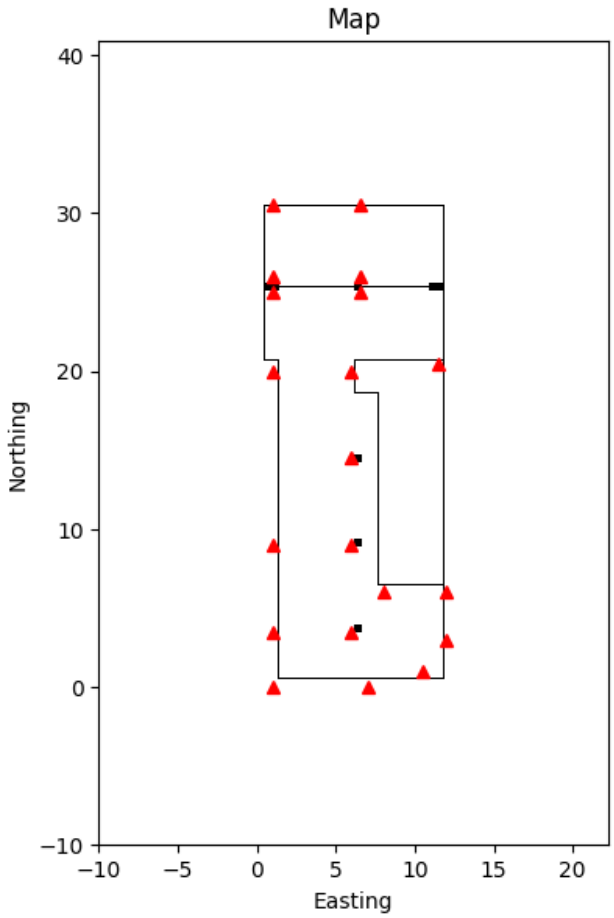

Figure 6.8. Test area floor plan and BLE beacons' placements

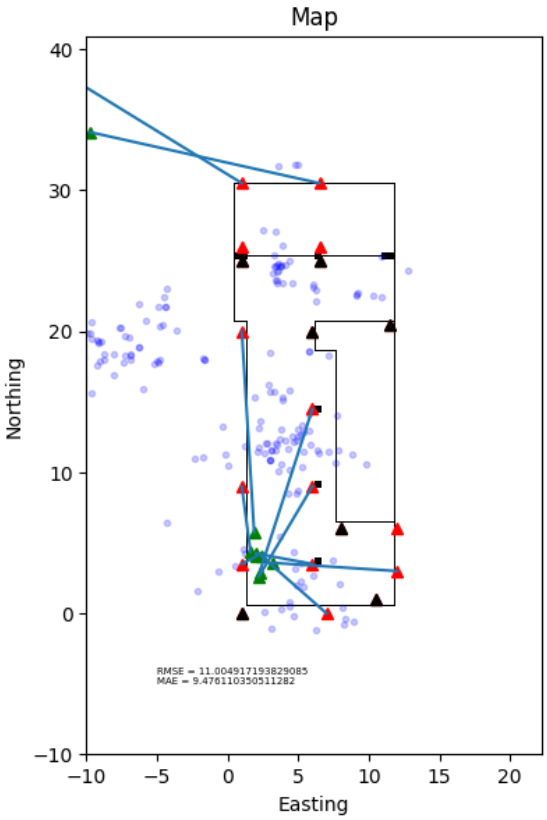

Figure 6.9. Bluetooth low-energy mapping result with base algorithm

6.4. Results

The results are compared against iterative BLE mapping based on lateration using linear least square. The linear least square algorithm displayed an RMSE of 11 m with a mean of absolute error (MAE) of 9.47 m with estimated beacon positions, as illustrated in Figure 6.9. The large difference in RMSE and MAE values indicates that there is a large difference in average error and largest error.

The proposed algorithm demonstrated more accurate performance with an RMSE of 4.64 m and an MAE of 4.28 m with estimated beacon placement, as depicted in Figure 6.10. The red triangles denote the ground truth positions of the beacons, while the black triangles mark

the positions of initially known BLE beacons, and the green triangles indicate the estimated positions of the beacons. The blue circles in Figure 6.10 show the FP positions in the database that was used to estimate the BLE beacon positions.

Iterating through the results demonstrates that the estimated BLE beacon positions improved by each iteration, as illustrated in Figure 6.13 - Figure 6.18. The initial iteration revealed BLE beacon positions with an RMSE of 8.40 m. The RMSE then improved to 6.46 m

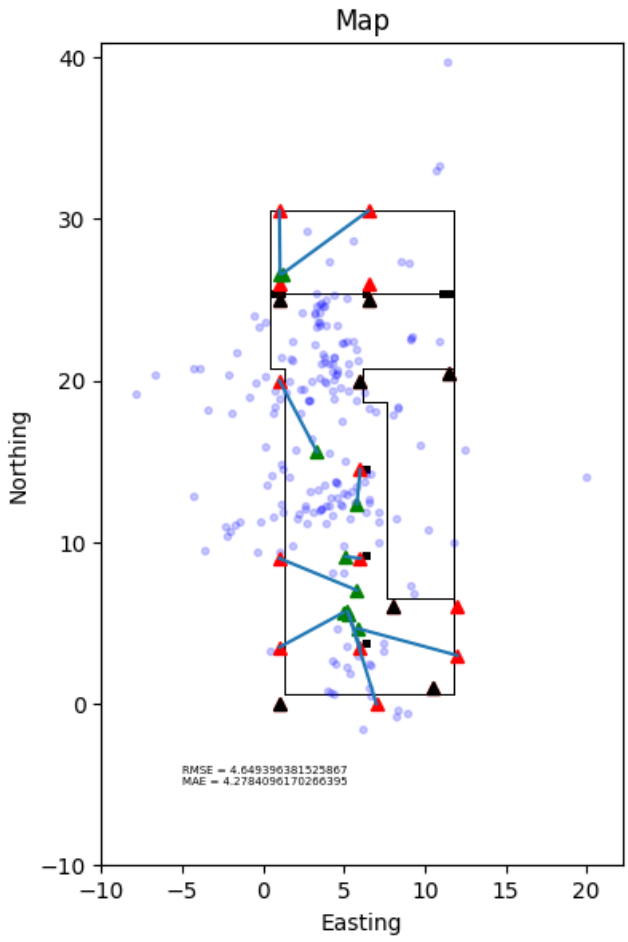

Figure 6.10. Bluetooth low-energy mapping result using proposed system

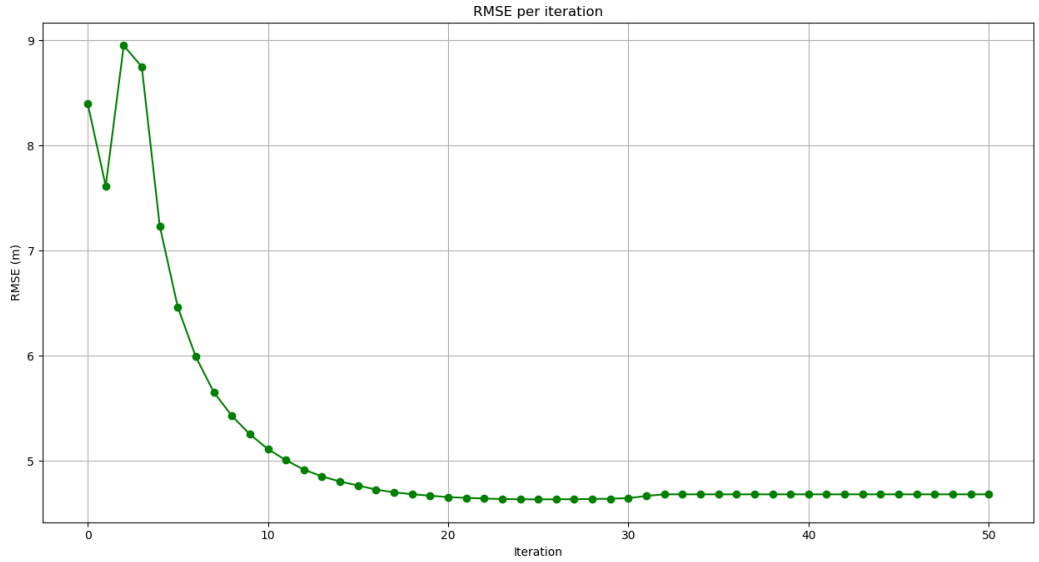

Figure 6.11. Changes in RMSE per iteration. The RMSE changes become saturated close to the 23rd iteration

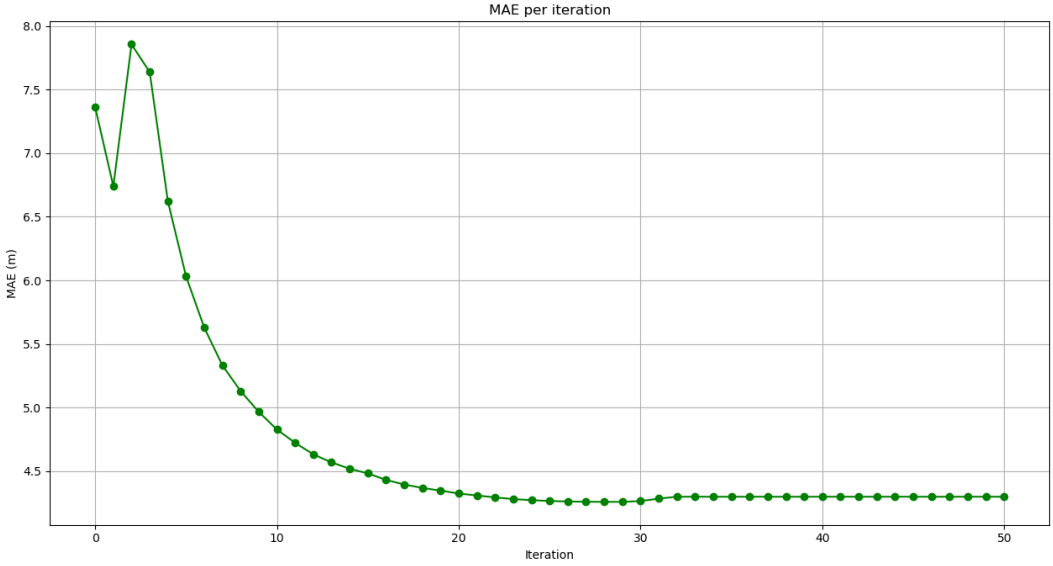

Figure 6.12. Changes in MAE per iteration. The MAE changes become saturated close to the 30th iteration

at the fifth iteration, and further to 5.11 m at the 10th iteration. Thereafter, the RMSE improvement can be seen at a slower rate, with the RMSE at the 15th iteration being 4.75 m and 4.66 m at the 20th iteration. Finally, the RMSE improvement became saturated at 4.65 m from the 23rd iteration onwards, as illustrated in Figure 6.11. Meanwhile, for the MAE, the

saturation occurred slightly later at around the 30th iteration with an MAE of 4.25 m, as depicted in Figure 6.12. This demonstrates that the proposed system is able to iteratively improve the estimated BLE beacon locations. The more scans provided to the system, the more accurately the BLE beacon positions can be estimated.

6.5. Conclusion

This chapter proposed a crowdsourced BLE beacon-mapping system that allows for the estimation of a BLE beacon based on the limited information of a few BLE beacons as the initial positioning. First, the architecture of the proposed system was introduced. The proposed system consists of three phases: online, mapping, and offline. The first phase, the online positioning phase, focuses on generating the position for the user and recording the signals to be stored in the database for mapping. The structure of the database was also presented to understand the stored data. Then, the second phase, namely the beacon-mapping phase, is triggered to map any scanned beacon, but not in the database. The beacons that are manually placed and the beacons' positions derived in the online phase will have different weights to emphasise the confidence of the position. Finally, the last phase, the offline positioning phase, is used to process the data of any unprocessed scans. This phase scans the database to ensure that all scans are and will be used. Unprocessed scans can arise because of limited information at the time of the scan.

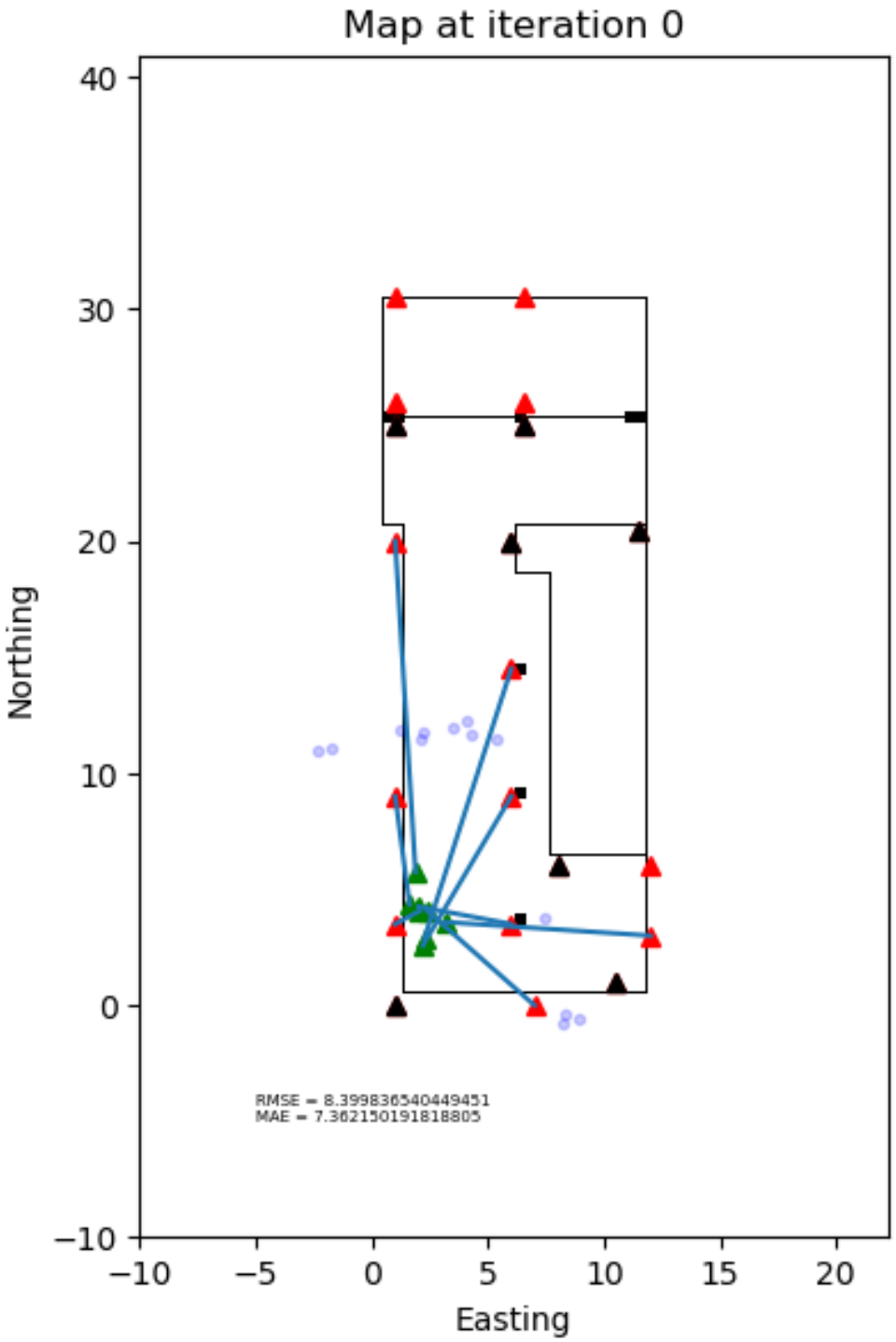

Figure 6.13. Bluetooth low-energy beacon mapping at iterations 0 and 5

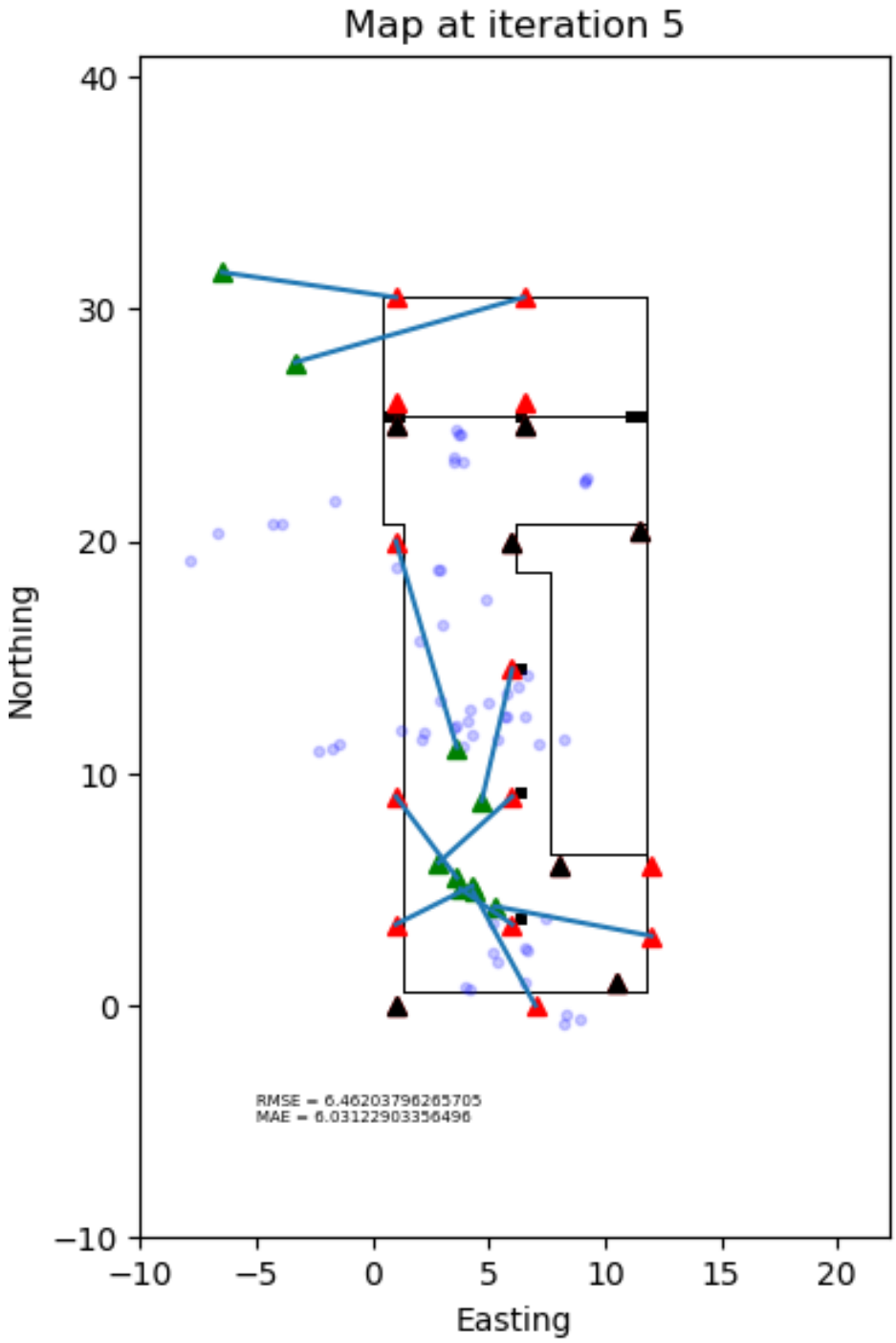

Figure 6.14. Bluetooth low-energy beacon mapping at iterations 5

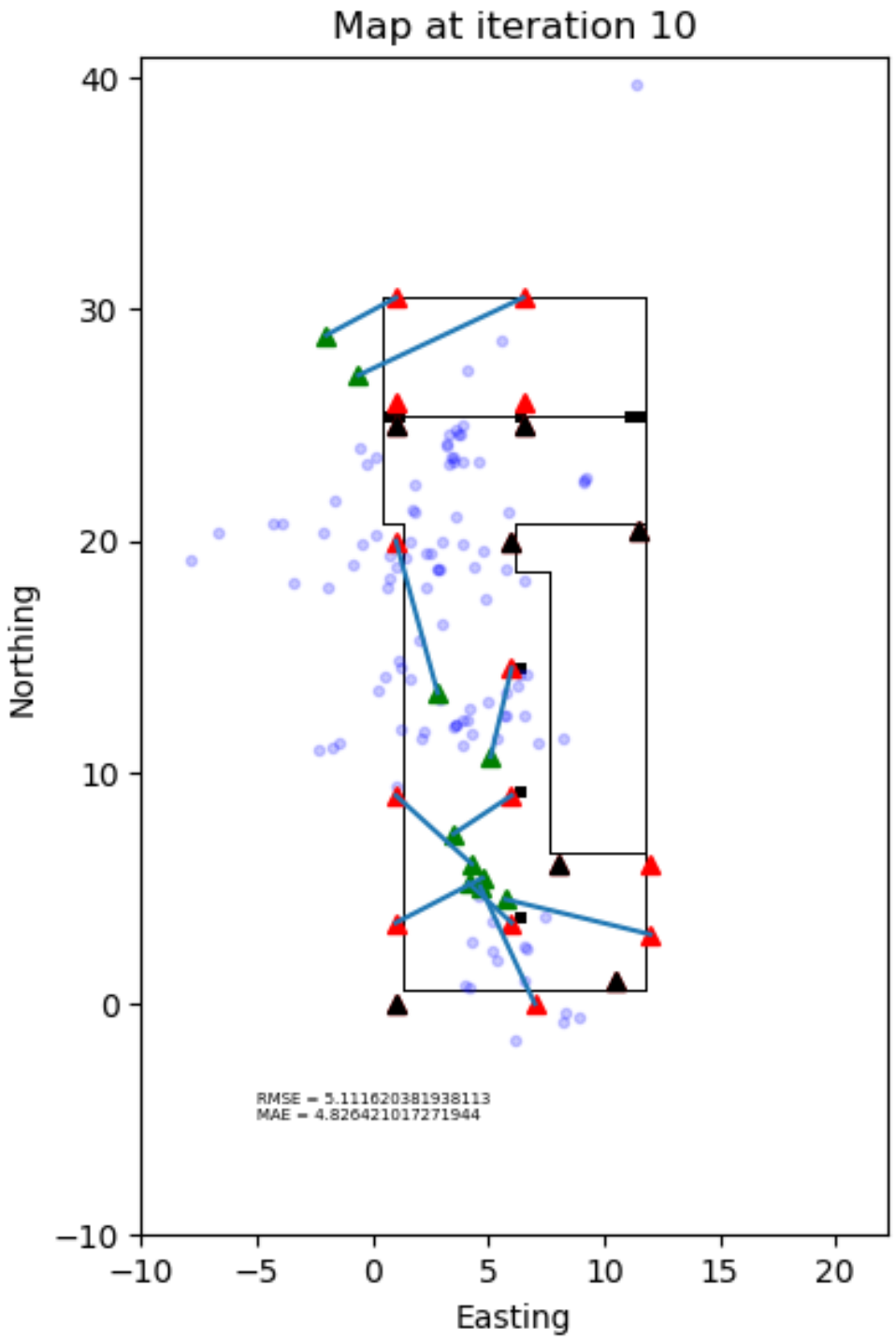

Figure 6.15. Bluetooth low-energy beacon mapping at iterations 10

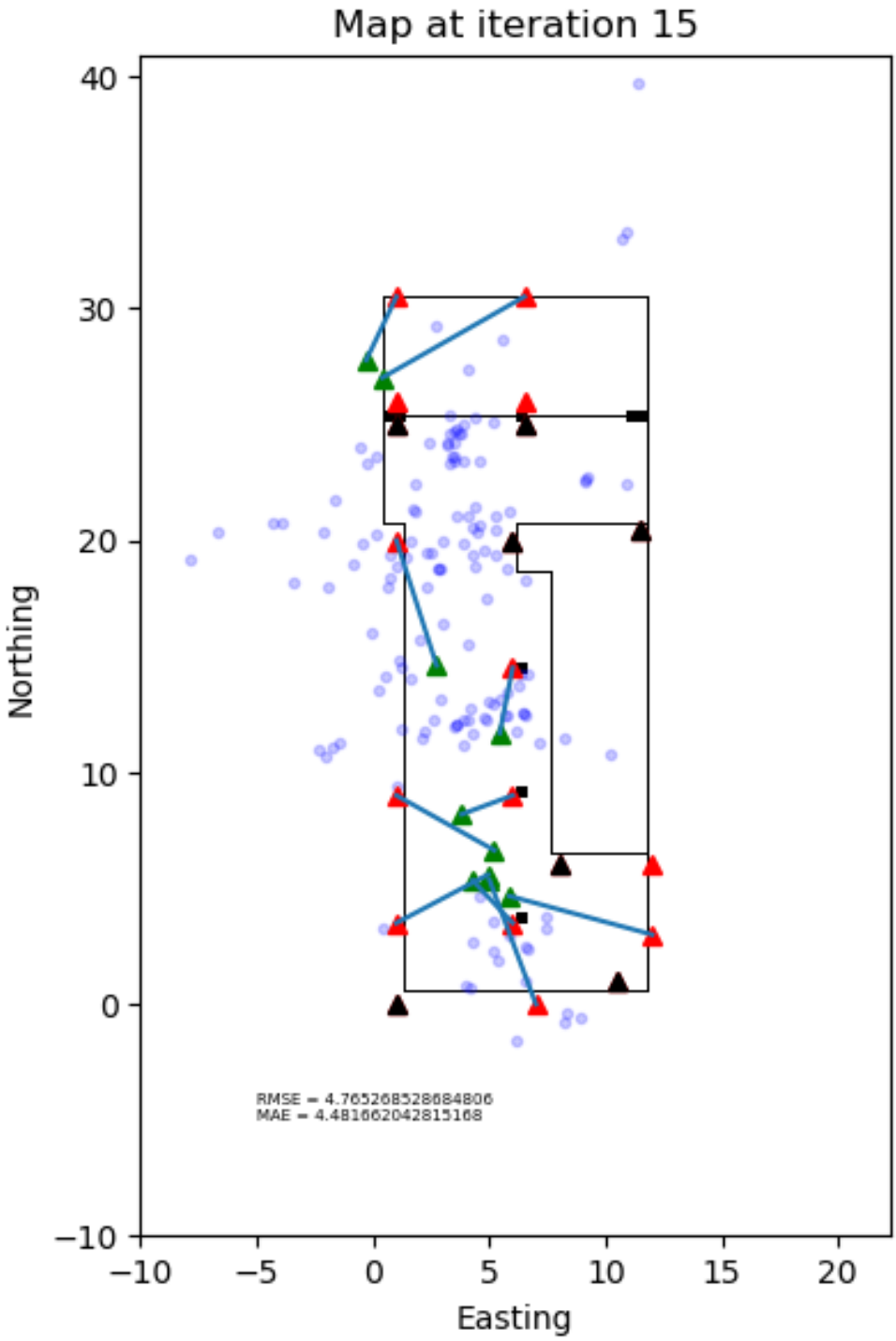

Figure 6.16. Bluetooth low-energy beacon mapping at iterations 15

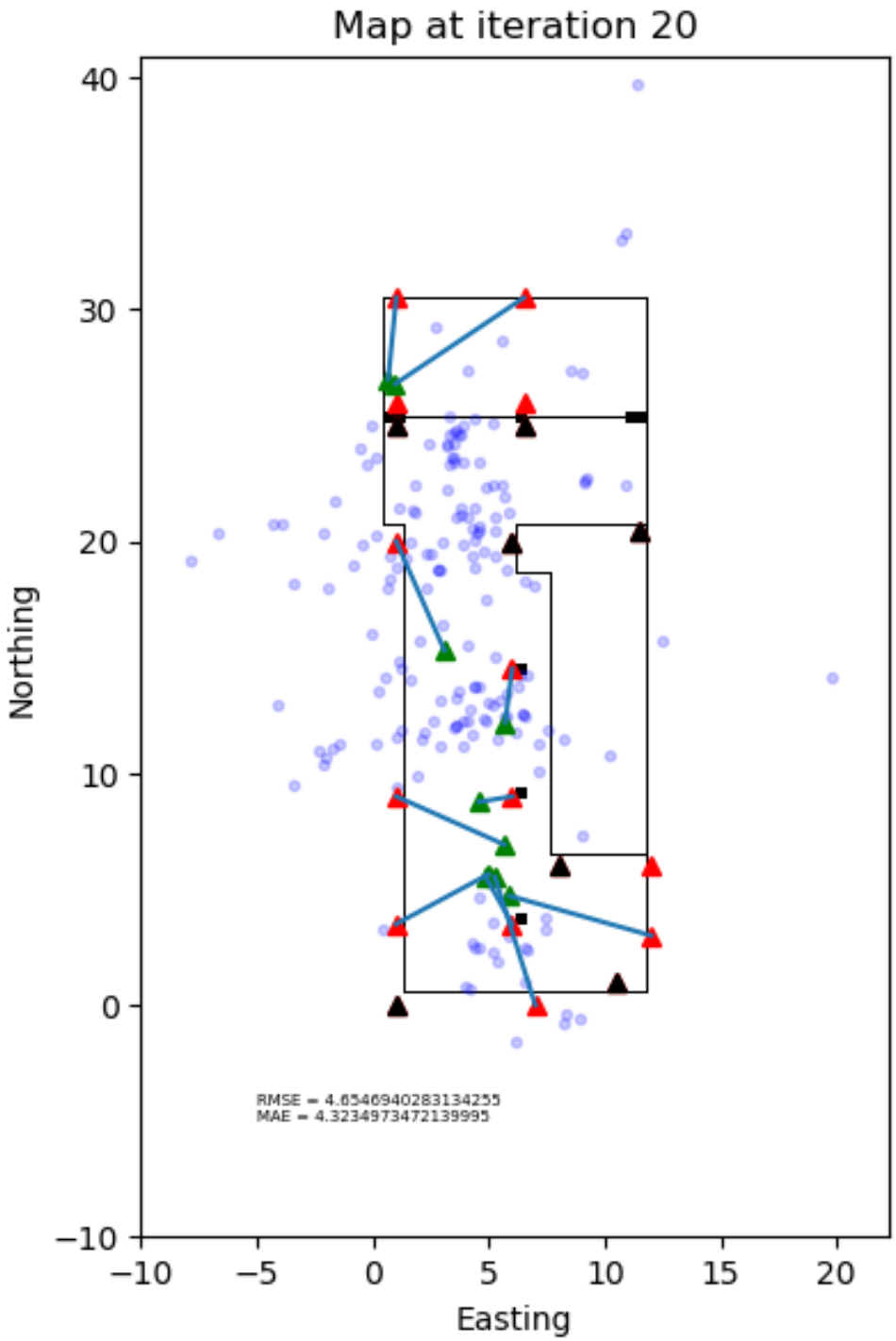

Figure 6.17. Bluetooth low-energy beacon mapping at iterations 20

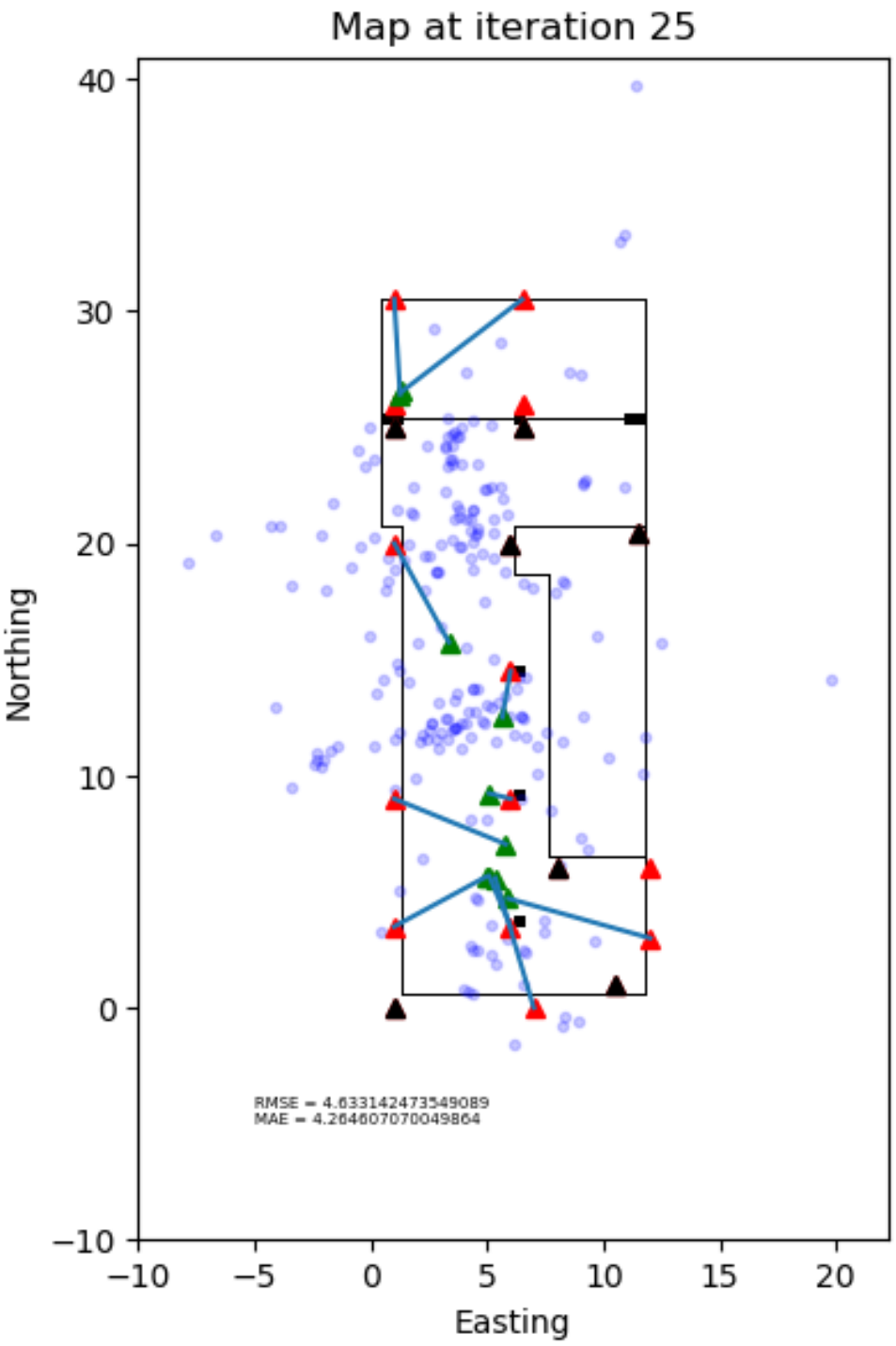

Figure 6.18. Bluetooth low-energy beacon mapping at iterations 25

7. Conclusion

7.1. Achievement

The main objective of this work is to develop a mapping system to determine the location of BLE beacons whose position is unknown. A positioning system using BLE beacons tends to have a laborious calibration process, which would require a precise fingerprint calibration or details of each BLE beacon recorded manually. A self-mapping algorithm would allow this laborious task to be reduced by integrating an iterated approach. The objective is achieved by developing a beacon-mapping system to detect the location of unknown beacons.

It starts with the development of an algorithm to filter the BLE signal to be less affected by advertisement channel hopping. This allows a more stable and reliable RSS value to be captured from a BLE beacon, which in turn would enable more consistent fingerprint map and a more stable distance estimation. This is important because distance estimation is the data required for a lateration process, and errors in data provided will translate to errors in estimated position. Several researchers have proposed a solution by using only a certain channel; however, this solution is not applicable to all devices. This research consequently proposes a solution that can be applied to all devices. The filter is proposed based on a Fourier transform high pass filter. The proposed filter demonstrates an improvement in 88% of the test points when implemented, with a maximum improvement of 1.33 m.

As the previous proposal targeted a signal instability caused by an internal effect, another algorithm is proposed to detect the cause that originated from the environment. To achieve this, an isolated beacon detection algorithm is proposed. The isolated beacon is proposed using a detection threshold based on the regression line of the BLE signal's standard

deviation. This deviation is then further analysed using a KS test to detect whether the beacon is isolated. A positioning performed with the proposed filter demonstrates a comparable result to a state-of-the-art algorithm used for comparison. The advantage of the proposed solution is that it is not affected by advertisement channel hopping, which changes the statistical values of a sequence of BLE scans. It also able to differentiate various levels of NLOS with limited accuracy.

The previously proposed algorithm aims at improving the signal to allow for a more accurate distance detection. Another algorithm is proposed to detect a beacon location using several positions with the beacon signal scanned. The proposed algorithm adds a direction term, which allows for a possible deviation resulting from the distance estimation error to be reduced. Unlike other directional positioning solutions, the proposed algorithm attempts to make use of the reliability of the signal to estimate the direction.

The crowdsourced beacon-mapping system is proposed using the suggested algorithm used to tackle different problems. The crowdsourced beacon-mapping system enables one to use a limited set of beacons to obtain the position of other beacons within the surrounding area. This heavily reduces the need to calibrate all beacons in the system. Using a crowdsourced approach, it enables the database to be built overtime, and it allows for wider coverage. The proposed beacon-mapping system consists of three phases: online positioning, beacon mapping, and offline positioning. Each of the phases is used to determine the FP, map a beacon using the determined FP, and determine the positions of BLE scans that were unable to be located because of inadequate information. The proposed system yields a beacon-mapping RMSE of 4.65 m.

7.2. Future Work

The current work described and implemented crowdsourced beacon mapping with isolated signal-aware BLE positioning. The proposed system has the advantage of being able to locate the position of unknown beacons; however, it also has several drawbacks that can be improved to further enhance the usability and scalability of the system.

The proposed system can be further improved by implementing a hybrid approach in the online positioning phase to allow for more accurate detection of FPs and to improve the iteration required to locate unknown beacons. The hybrid positioning approach can utilise a Wi-Fi position, GNSS, PDR, other positioning techniques, or a different positioning system altogether. The position obtained by another positioning technique would need to be weighted based on reliability for it to be usable in the proposed system.

Furthermore, as the system records three different databases, it is best to implement an algorithm that can reduce the size of the database to improve the scalability of the system. The improvement can be in terms of database management or a reduction in recorded data. One suggestion is to cluster the FPs; this would allow any similar FP to be combined. However, it is important to ensure that the clustering of the FPs will not lead to any changes or missing information.

Another phase could also be added to process the FP database using its own data. One of the processes that can be performed here is the previously suggested clustering of the FP database. In addition, a filter could be implemented here to remove any FPs that are conflicting with one another. This will be beneficial in terms of a smaller database size and a more reliable radio map when the FP database is to be used with the fingerprint algorithm.

Running all three phases in all iterations could be an exhaustive process that would increase the load of the system and could further reduce the scalability. This can be improved by implementing a system check that can flag the mapping phase to run rather than running all three phases in all iterations. However, it also important to note that the longer the delays in running the mapping phase, the more the database will be built up, which would cause a traffic issue.

Bibliography

[1] Federal Communications Commission, “A Short History of Radio,” *Federal Communications Commission*, no. 1899, 2004.

[2] L. S. Howeth, *History of communications electronics in the United States Navy*. Washington: Bureau of Ships and Office of Naval History, 1963.

[3] J. & BAILEY, “The Loran-C System of Navigation,” 1962.

[4] N. Samama, “A Brief History of Navigation and Positioning,” in *Global Positioning*, Hoboken, NJ, USA: John Wiley & Sons, Inc., 2007, pp. 1–27.

[5] E. Deretey, M. T. Ahmed, J. A. Marshall, and M. Greenspan, “Visual Indoor Positioning with a Single Camera Using PnP,” in *2015 International Conference on Indoor Positioning and Indoor Navigation, IPIN*, 2015.

[6] M. a. Al-Ammar *et al.*, “Comparative Survey of Indoor Positioning Technologies, Techniques, and Algorithms,” in *2014 International Conference on Cyberworlds*, 2014.

[7] Y. Gu, A. Lo, and I. Niemegeers, “A survey of indoor positioning systems for wireless personal networks,” *IEEE Communications Surveys & Tutorials*, vol. 11, no. 1, pp. 13–32, 2009.

[8] R. Mautz and S. Tilch, “Survey of optical indoor positioning systems,” in *2011 International Conference on Indoor Positioning and Indoor Navigation, IPIN 2011*, 2011.

[9] M. Hazas and A. Hopper, “Broadband ultrasonic location systems for improved indoor positioning,” *IEEE Transactions on Mobile Computing*, vol. 5, no. 5, pp. 536–547, May 2006.

[10] F. Palumbo, P. Barsocchi, S. Chessa, and J. C. Augusto, “A stigmergic approach to indoor localization using Bluetooth Low Energy beacons,” in *Advanced Video and Signal Based Surveillance (AVSS), 2015 12th IEEE International Conference on*, 2015.

[11] Apple Inc., “iOS: Understanding iBeacon - Apple Support.” [Online]. Available: https://support.apple.com/en-gb/HT202880. [Accessed: 09-May-2016].

[12] S. S. Chawathe, “Low-latency indoor localization using bluetooth beacons,” in *2009 12th International IEEE Conference on Intelligent Transportation Systems*, 2009.

[13] K. Bouchard, R. Ramezani, and A. Naeim, “Features based proximity localization with Bluetooth emitters,” in *2016 IEEE 7th Annual Ubiquitous Computing, Electronics Mobile Communication Conference (UEMCON)*, 2016.

[14] J. Hightower and G. Borriello, “Location systems for ubiquitous computing,” *Computer*, vol. 34, no. 8, pp. 57–66, Aug. 2001.

[15] P. Brida, J. Machaj, and J. Benikovsky, “A modular localization system as a positioning service for road transport,” *Sensors (Switzerland)*, vol. 14, no. 11, pp. 20274–20296,

2014.

[16] M. Pelka, “Position Calculation with Least Squares based on Distance Measurements,” 2015.

[17] T. K. Sarkar, Z. Ji, K. Kim, A. Medouri, and M. Salazar-Palma, “A survey of various propagation models for mobile communication,” *IEEE Antennas and Propagation Magazine*, vol. 45, no. 3, pp. 51–82, Jun. 2003.

[18] E. Greenberg and E. Klodzh, “Comparison of deterministic, empirical and physical propagation models in urban environments,” in *2015 IEEE International Conference on Microwaves, Communications, Antennas and Electronic Systems (COMCAS)*, 2015.

[19] V. S. Abhayawardhana, I. J. Wassell, D. Crosby, M. P. Sellars, and M. G. Brown, “Comparison of empirical propagation path loss models for fixed wireless access systems,” in *2005 IEEE 61st Vehicular Technology Conference*, 2005.

[20] G. E. Athanasiadou, A. R. Nix, and J. P. McGeehan, “A microcellular ray-tracing propagation model and evaluation of its narrow-band and wide-band predictions,” *IEEE Journal on Selected Areas in Communications*, vol. 18, no. 3, pp. 322–335, Mar. 2000.

[21] R. V. Akhpashev and A. V. Andreev, “COST 231 Hata adaptation model for urban conditions in LTE networks,” 2016, pp. 64–66.

[22] L. Bruno, M. Khider, and P. Robertson, “On-line training of the path-loss model in Bayesian WLAN indoor positioning,” in *2013 International Conference on Indoor Positioning and Indoor Navigation, IPIN 2013*, 2013.

[23] S. R. Saunders, *Antennas and Propagation for Wireless Communication Systems*, 1st ed. New York, NY, USA: John Wiley & Sons, Inc., 1999.

[24] Y. J. Kim, J. J. J. Y. Lee, M. S. Aldosari, M. S. Altokhais, and J. J. J. Y. Lee, “Vision-Based Corridor Path Search of a Mobile Robot,” in *2011 11th International Conference on Control, Automation and Systems*, 2011.

[25] H. Hile and G. Borriello, “Positioning and orientation in indoor environments using camera phones,” *IEEE Computer Graphics and Applications*, vol. 28, no. 4, pp. 32–39, Aug. 2008.

[26] N. Ravi, P. Shankar, A. Frankel, A. Elgammal, and L. Iftode, “Indoor Localization Using Camera Phones,” in *Seventh IEEE Workshop on Mobile Computing Systems & Applications (WMCSA’06 Supplement)*, 2006.

[27] M. Nozawa, Y. Hagiwara, and Y. Choi, “Indoor human navigation system on smartphones using view-based navigation,” in *Control, Automation and Systems (ICCAS), 2012 12th International Conference on*, 2012.

[28] A. Xiao, R. Chen, D. Li, Y. Chen, and D. Wu, “An indoor positioning system based on static objects in large indoor scenes by using smartphone cameras,” *Sensors (Switzerland)*, vol. 18, no. 7, 2018.

[29] H. Morimitsu, M. Hashimoto, R. B. Pimentel, R. M. Cesar, and R. Hirata, “Keygraphs

for sign detection in indoor environments by mobile phones," in *Lecture Notes in Computer Science (including subseries Lecture Notes in Artificial Intelligence and Lecture Notes in Bioinformatics)*, 2011, vol. 6658 LNCS, pp. 315–324.

[30] W.-T. T. Huang, C.-L. L. Tsai, and H.-Y. Y. Lin, "Mobile robot localization using ceiling landmarks and images captured from an RGB-D camera," in *IEEE/ASME International Conference on Advanced Intelligent Mechatronics, AIM*, 2012.

[31] X. Li, J. Wang, A. Olesk, N. Knight, and W. Ding, "Indoor positioning within a single camera and 3D maps," in *2010 Ubiquitous Positioning Indoor Navigation and Location Based Service, UPINLBS 2010*, 2010.

[32] W. Winterhalter, F. Fleckenstein, B. Steder, L. Spinello, and W. Burgard, "Accurate indoor localization for RGB-D smartphones and tablets given 2D floor plans," in *2015 IEEE/RSJ International Conference on Intelligent Robots and Systems (IROS)*, 2015.

[33] W. Dai, Y. Zhang, P. Li, and Z. Fang, "RGB-D SLAM in Dynamic Environments Using Points Correlations," *ArXiv*, vol. abs/1811.0, 2018.

[34] Y. Li, Z. Ghassemlooy, X. Tang, B. Lin, and Y. Zhang, "A VLC Smartphone Camera Based Indoor Positioning System," *IEEE Photonics Technology Letters*, vol. 30, no. 13, pp. 1171–1174, 2018.

[35] J. Rabadan, V. Guerra, C. Guerra, J. Rufo, and R. Perez-Jimenez, "A Novel Ranging Technique Based on Optical Camera Communications and Time Difference of Arrival," *Applied Sciences*, vol. 9, no. 11, p. 2382, 2019.

[36] Y. Chae, D. T. Nguyen, S. Park, and Y. Park, "Indoor Localization Using Digital Auto Zoom of a Smart-Phone Camera and Integrated Sensors," in *International Conference on Ubiquitous and Future Networks, ICUFN*, 2018.

[37] J. Haverinen and A. Kemppainen, "Global indoor self-localization based on the ambient magnetic field," *Robotics and Autonomous Systems*, vol. 57, no. 10, pp. 1028–1035, Oct. 2009.

[38] T. H. Riehle, S. M. Anderson, P. A. Lichter, J. P. Condon, S. I. Sheikh, and D. S. Hedin, "Indoor waypoint navigation via magnetic anomalies," in *Proceedings of the Annual International Conference of the IEEE Engineering in Medicine and Biology Society, EMBS*, 2011.

[39] S. E. Kim, Y. Kim, J. Yoon, and E. S. Kim, "Indoor positioning system using geomagnetic anomalies for smartphones," in *2012 International Conference on Indoor Positioning and Indoor Navigation, IPIN 2012 - Conference Proceedings*, 2012.

[40] B. Li, T. Gallagher, A. G. Dempster, and C. Rizos, "How feasible is the use of magnetic field alone for indoor positioning?," in *2012 International Conference on Indoor Positioning and Indoor Navigation (IPIN)*, 2012.

[41] N. Aloui, K. Raoof, A. Bouallegue, S. Letourneur, and S. Zaibi, "Performance evaluation of an acoustic indoor localization system based on a fingerprinting technique," *EURASIP Journal on Advances in Signal Processing*, vol. 2014, no. 1, p. 13, 2014.

[42] I. Rishabh, D. Kimber, and J. Adcock, “Indoor localization using controlled ambient sounds,” in *2012 International Conference on Indoor Positioning and Indoor Navigation (IPIN)*, 2012, no. November.

[43] K. Liu, X. Liu, L. Xie, and X. Li, “Towards accurate acoustic localization on a smartphone,” in *2013 IEEE INFOCOM*, 2013.

[44] K. Liu, X. Liu, and X. Li, “Guoguo: Enabling Fine-Grained Smartphone Localization via Acoustic Anchors,” *IEEE Transactions on Mobile Computing*, vol. 15, no. 5, pp. 1144–1156, May 2016.

[45] V. Moghtadaiee, A. G. Dempster, and S. Lim, “Indoor localization using FM radio signals: A fingerprinting approach,” in *2011 International Conference on Indoor Positioning and Indoor Navigation, IPIN 2011*, 2011.

[46] H. Zou, L. Xie, Q. Jia, and H. Wang, “An Integrative Weighted Path Loss and Extreme Learning Machine Approach to RFID based Indoor Positioning,” in *International Conference on Indoor Positioning and Indoor Navigation*, 2013.

[47] L. M. Ni, Yunhao Liu, Yiu Cho Lau, and A. P. Patil, “LANDMARC: indoor location sensing using active RFID,” in *Proceedings of the First IEEE International Conference on Pervasive Computing and Communications, 2003. (PerCom 2003).*

[48] F. Poad and W. Ismail, “Automated switching mechanism for indoor and outdoor propagation with embedded RFID and GPS in wireless sensor network platform,” *Proceedings of the World Congress on Engineering*, vol. I, 2014.

[49] L. Vu-Hoang *et al.*, “A new technique to enhance accuracy of WLAN fingerprinting based indoor positioning system,” in *2014 IEEE 5th International Conference on Communications and Electronics, IEEE ICCE 2014*, 2014.

[50] S. Eisa, J. Peixoto, F. Meneses, and A. Moreira, “Removing useless APs and fingerprints from WiFi indoor positioning radio maps,” in *2013 International Conference on Indoor Positioning and Indoor Navigation, IPIN 2013*, 2013.

[51] V. Moghtadaiee and A. G. Dempster, “WiFi fingerprinting signal strength error modeling for short distances,” in *2012 International Conference on Indoor Positioning and Indoor Navigation, IPIN 2012 - Conference Proceedings*, 2012.

[52] O. S. Oguejiofor, V. N. Okorogu, A. Adewale, and B. O. Osuesu, “Outdoor Localization System Using RSSI Measurement of Wireless Sensor Network,” *International Journal of Innovative Technology and Exploring Engineering*, vol. 2, no. 2, pp. 1–6, 2013.

[53] L. Schauer, F. Dorfmeister, and M. Maier, “Potentials and limitations of WIFI-positioning using time-of-flight,” in *2013 International Conference on Indoor Positioning and Indoor Navigation, IPIN 2013*, 2013.

[54] A. Bose and H. F. Chuan, “A practical path loss model for indoor WiFi positioning enhancement,” in *2007 6th International Conference on Information, Communications and Signal Processing, ICICS*, 2007.

[55] X. Zhao, Z. Xiao, A. Markham, N. Trigoni, and Y. Ren, “Does BTLE measure up against

WiFi? A comparison of indoor location performance," in *20th European Wireless Conference*, 2014.

[56] Google Inc., "Beacons | Google Developers." [Online]. Available: https://developers.google.com/beacons/. [Accessed: 21-Mar-2017].

[57] Google Inc., "Specification for Eddystone, an open beacon format from Google." [Online]. Available: https://github.com/google/eddystone. [Accessed: 21-Mar-2017].

[58] R. Faragher and R. Harle, "Location Fingerprinting with Bluetooth Low Energy Beacons," *IEEE Journal on Selected Areas in Communications*, vol. PP, no. 99, pp. 1–1, 2015.

[59] T. King, H. Lemelson, A. Färber, and W. Effelsberg, "BluePos: Positioning with bluetooth," in *WISP 2009 - 6th IEEE International Symposium on Intelligent Signal Processing - Proceedings*, 2009.

[60] F. Zaid, D. Costantini, S. M. Parag, A. Reinhardt, J. Schmitt, and R. Steinmetz, "WBroximity: Mobile participatory sensing for WLAN- and bluetooth-based positioning," in *Proceedings - Conference on Local Computer Networks, LCN*, 2010.

[61] A. Baniukevic, C. S. Jensen, and H. Lu, "Hybrid indoor positioning with Wi-Fi and Bluetooth: Architecture and performance," in *Proceedings - IEEE International Conference on Mobile Data Management*, 2013, vol. 1.

[62] J. Zhu, K. Zeng, K. H. Kim, and P. Mohapatra, "Improving crowd-sourced Wi-Fi localization systems using Bluetooth beacons," in *Annual IEEE Communications Society Conference on Sensor, Mesh and Ad Hoc Communications and Networks workshops*, 2012.

[63] Z. Jianyong, L. Haiyong, C. Zili, and L. L. Zhaohui, "RSSI based Bluetooth low energy indoor positioning," in *IPIN 2014 - 2014 International Conference on Indoor Positioning and Indoor Navigation*, 2014.

[64] L. Pei, R. Chen, J. Liu, T. Tenhunen, H. Kuusniemi, and Y. Chen, "Inquiry-based bluetooth indoor positioning via RSSI probability distributions," in *2nd International Conference on Advances in Satellite and Space Communications, SPACOMM 2010*, 2010.

[65] M. E. E. Rida, F. Liu, Y. Jadi, A. A. A. Algawhari, and A. Askourih, "Indoor Location Position Based on Bluetooth Signal Strength," in *2015 2nd International Conference on Information Science and Control Engineering*, 2015.

[66] J. L. Carrera, "LOCALISATION SYSTEMS AND LOS/NLOS IDENTIFICATION IN INDOOR SCENARIOS," University of Bern, 2015.

[67] Z. Xiao, H. Wen, A. Markham, N. Trigoni, P. Blunsom, and J. Frolik, "Non-Line-of-Sight Identification and Mitigation Using Received Signal Strength," *IEEE Transactions on Wireless Communications*, vol. 14, no. 3, pp. 1689–1702, 2015.

[68] R. Faragher and R. Harle, "An Analysis of the Accuracy of Bluetooth Low Energy for Indoor Positioning Applications," in *27th International Technical Meeting of The*

Satellite Division of the Institute of Navigation, 2014, pp. 201–210.

[69] D. Čabarkapa, I. Grujić, P. Pavlović, D. Čabarkapa, I. Gruji, and P. Pavlovic, "Comparative Analysis of the Bluetooth Low-Energy Indoor Positioning Systems," in *Telecommunication in Modern Satellite, Cable and Broadcasting Services*, 2015, pp. 76–79.

[70] Q. Chang, Q. Li, Z. Shi, W. Chen, and W. Wang, "Scalable indoor localization via mobile crowdsourcing and Gaussian process," *Sensors (Switzerland)*, vol. 16, no. 3, pp. 1–19, 2016.

[71] X. Hou and T. Arslan, "Indoor Localization for Bluetooth Low Energy Devices Using Wavelet and Smoothing Filters," in *7th International Conference on Localisation and GNSS (ICL-GNSS)*, 2017.

[72] T. Rappaport, *Wireless Communications: Principles and Practice*. Upper Saddle River, NJ: Prentice Hall, 2001.

[73] W. Xu, "Multi-antenna non-line-of-sight identification techniques for target localization in mobile ad-hoc networks," Michigan Technological University, 2011.

[74] R. Divya, "Non-Line-Of-Sight Environment based Localization in Wireless Sensor Networks," *International Journal of Computer Applications*, vol. 96, no. 6, pp. 38–43, 2014.

[75] Z. Zhou, Z. Yang, C. Wu, W. Sun, and Y. Liu, "LiFi: Line-Of-Sight identification with WiFi," in *Proceedings - IEEE INFOCOM*, 2014.

[76] Z. Xiao, H. Wen, A. Markham, N. Trigoni, P. Blunsom, and J. Frolik, "Identification and mitigation of non-line-of-sight conditions using received signal strength," in *International Conference on Wireless and Mobile Computing, Networking and Communications*, 2013.

[77] M. Ramadan, V. Sark, J. Gutiérrez, and E. Grass, "NLOS Identification for Indoor Localization using Random Forest Algorithm," in *WSA 2018; 22nd International ITG Workshop on Smart Antennas*, 2018.

[78] H. J. Jo and S. Kim, "Indoor Smartphone Localization Based on LOS and NLOS Identification," *Sensors (Basel, Switzerland)*, vol. 18, no. 11, 2018.

[79] K. Han, H. Xing, Z. Deng, and Y. Du, "A RSSI/PDR-Based Probabilistic Position Selection Algorithm with NLOS Identification for Indoor Localisation," *ISPRS International Journal of Geo-Information*, vol. 7, no. 6, p. 232, 2018.

[80] C. Wu, H. Hou, W. Wang, Q. Huang, and X. Gao, "TDOA Based Indoor Positioning with NLOS Identification by Machine Learning," in *2018 10th International Conference on Wireless Communications and Signal Processing, WCSP 2018*, 2018.

[81] K. Kaemarungsi and P. Krishnamurthy, "Analysis of WLAN's received signal strength indication for indoor location fingerprinting," *Pervasive and Mobile Computing*, vol. 8, no. 2, pp. 292–316, Apr. 2012.

[82] R. Mehra and A. Singh, "Real time RSSI error reduction in distance estimation using

RLS algorithm," in *Proceedings of the 2013 3rd IEEE International Advance Computing Conference, IACC 2013*, 2013.

[83] S. S. Chawathe, "Beacon Placement for Indoor Localization using Bluetooth," in *2008 11th International IEEE Conference on Intelligent Transportation Systems*, 2008.

[84] V. S. S. Rani and S. V. V. Raghavan, "A greedy approach to beacon placement for localization," in *2008 1st IFIP Wireless Days, WD 2008*, 2008.

[85] Z. Yuan, W. Li, J. Zhu, and W. Zhao, "A cost-efficiency method on beacon nodes placement for wireless localization," in *2015 International Conference on Computing, Networking and Communications (ICNC)*, 2015.

[86] S. Roy and N. Mukherjee, "Integer linear programming formulation of optimal beacon placement problem in WSN," in *2014 Applications and Innovations in Mobile Computing (AIMoC)*, 2014, pp. 111–117.

[87] S. Kammoun, J.-B. J.-B. J.-B. Pothin, and J.-C. J.-C. Cousin, "Beacon placement using simulated annealing for RSS-based localization systems," in *2014 11th International Symposium on Wireless Communications Systems (ISWCS)*, 2014.

[88] Y. Zheng *et al.*, "A placement strategy for accurate TOA localization algorithm," in *Proceedings of the 7th Annual Communication Networks and Services Research Conference, CNSR 2009*, 2009.

[89] Q. Shi, N. S. Correal, J. Huang, and S. Kyperountas, "Method for estimating the location of a wireless device in a communication network," US20060281470 A1, 14-Dec-2006.

[90] Nordic Semiconductor, "nRF51822 Reference Beacon Kit," 2014. [Online]. Available: https://www.nordicsemi.com/eng/Products/Bluetooth-Smart-Bluetooth-low-energy/nRF51822-Bluetooth-Smart-Beacon-Kit. [Accessed: 10-May-2016].

[91] S. Srirangarajan, S. F. A. Shah, and A. H. Tewfik, "Directional beacon based positioning system using RF signals," in *European Signal Processing Conference*, 2008.

[92] S. F. a Shah, S. Srirangarajan, and a. Tewfik, "Implementation of a directional beacon-based position location algorithm in a signal processing framework," *IEEE Transactions on Wireless Communications*, vol. 9, no. 3, pp. 1044–1053, Mar. 2010.

[93] B. Zhou, Q. Li, Q. Mao, and W. Tu, "A robust crowdsourcing-based indoor localization system," *Sensors (Switzerland)*, vol. 17, no. 4, pp. 1–16, 2017.

[94] Estimore Inc, "Estimote products." [Online]. Available: https://estimote.com/products/. [Accessed: 30-Dec-2017].

[95] R. Nilsson, "Shaping the Wireless Future with Low Energy Applications and Systems," 2013. [Online]. Available: https://www.digikey.co.uk/en/articles/techzone/2013/jun/shaping-the-wireless-future-with-low-energy-applications-and-systems.

List of publication

A. Juri, T. Arslan, and F. Wang, “Obstruction-aware Bluetooth Low Energy Indoor Positioning,” in ION GNSS+, Portland, 2016.

A. Juri and T. Arslan, “Bluetooth Low Energy Positioning with NLOS Correction Using Statistical Techniques,” in 2016 International Navigation Conference (INC), Glasgow, 2016.

A. Juri and T. Arslan, “Isolated Beacon Identification Using a Statistical Approach,” in 8th International Conference on Indoor Positioning and Indoor Navigation (IPIN), Sapporo, 2017.

X. Hou, T. Arslan, A. Juri, and F. Wang, “Indoor Localization for Bluetooth Low Energy Devices Using Weighted Off-set Triangulation Algorithm,” in ION GNSS+, Portland, 2016.

X. Hou, T. Arslan and A. Juri, “A Received Signal Strength based Self-adaptive Algorithm Targeting for Indoor Positioning,” in 2016 International Navigation Conference (INC), Glasgow, 2016.